

**Hox-C9 activates the intrinsic pathway of apoptosis  
and is associated with spontaneous regression in  
neuroblastoma**

**Inaugural Dissertation**

zur  
Erlangung des Doktorgrades  
Dr. nat. med.  
der Medizinischen Fakultät  
und  
der Mathematisch Naturwissenschaftlichen Fakultät  
der Universität zu Köln

vorgelegt von

Dipl. Biol. Hayriye Kocak  
aus Lauf a. d. Pegnitz

Köln, 2013

Berichterstatter:

Prof. Dr. Roman Thomas

Prof. Dr. Matthias Hammerschmidt

Tag der letzten mündlichen Prüfung:

19. 12. 2013

<b>Zusammenfassung</b>	<b>I</b>
<b>Summary</b>	<b>III</b>
<b>1. Introduction</b>	<b>1</b>
<b>1.1 Neuroblastoma</b>	<b>1</b>
1.1.1 International Neuroblastoma Staging System (INSS)	2
1.1.2 Neuroblastoma risk stratification	3
1.1.3 Molecular biology of neuroblastoma	5
1.1.3.1 <i>MYCN</i> amplification	5
1.1.3.2 <i>ALK</i> amplification and activating mutations	6
1.1.3.3 Chromosome 1p deletion	6
1.1.3.4 Chromosome 11q deletion	7
1.1.3.5 Chromosome 17q gain	7
1.1.3.6 DNA index	7
1.1.3.7 Aberrant gene expression	8
1.1.4 Hereditary neuroblastoma	9
1.1.5 Origin of neuroblastoma	9
1.1.6 Spontaneous regression and differentiation in neuroblastoma	12
<b>1.2 Homeobox genes</b>	<b>13</b>
1.2.1 <i>HOX</i> gene expression	14
1.2.2 Hox cofactors	15
1.2.3 <i>HOX</i> genes in human diseases	16
1.2.3.1 <i>HOX</i> genes in cancer	16
1.2.3.2 <i>HOX</i> genes in neuroblastoma	19
1.2.4 <i>HOXC9</i> gene expression in development and tumorigenesis	20
<b>2 Aim of the study</b>	<b>22</b>
<b>3 Materials and Methods</b>	<b>23</b>
<b>3.1 Microarrays and data analysis</b>	<b>23</b>
3.1.1 Neuroblastoma patient characteristics	23
3.1.2 Gene expression arrays	24
3.1.2.1 Analysis of gene expression data	25
3.1.2.2 <i>HOX</i> gene expression-based classification	25
3.1.2.3 Gene Ontology enrichment analyses	26
3.1.3 Array-based Comparative Genomic Hybridization	26
<b>3.2 Statistics</b>	<b>27</b>
<b>3.3 Cell Culture</b>	<b>27</b>
3.3.1 Neuroblastoma cell line characteristics	28
3.3.2 Stable inducible neuroblastoma cell lines	29
3.3.3 <i>In vitro</i> growth properties	29
3.3.3.1 Trypan blue dye exclusion	29
3.3.3.2 Cell cycle distribution	29
3.3.3.3 Anchorage independent growth	30
3.3.4 Cell viability analyses	31
3.3.4.1 TUNEL assay	31
3.3.4.2 Annexin-V binding assay	32
3.3.4.3 Hypoploidy assay	33
3.3.5 <i>In vivo</i> growth properties	33
<b>3.4 Molecular Biology</b>	<b>34</b>
3.4.1 RNA isolation	34
3.4.2 DNA isolation	35
3.4.3 cDNA synthesis	35
3.4.4 Whole Genome Amplification	36
3.4.5 Quantitative real-time reverse transcriptase-polymerase chain reaction	36
3.4.6 Methylation analysis	38
3.4.7 Sequencing	39

3.4.7.1 Sequencing of the <i>HOXC9</i> locus in neuroblastoma tumors and cell lines	39
3.4.7.2 Sequencing of Plasmid DNA	40
3.4.8 Retroviral plasmids and cloning procedure	41
3.4.9 Immunoblotting	42
3.4.10 Immunofluorescence	44
3.4.10.1 Hox-C9 immunofluorescence	44
3.4.10.2 F-Actin cytoskeleton staining	45
<b>4. Results</b>	<b>47</b>
<b>4.1 <i>HOX</i> gene expression in neuroblastoma</b>	<b>47</b>
4.1.1 Prediction of neuroblastoma outcome based on a <i>HOX</i> gene expression-based classifier	51
<b>4.2 Elevated <i>HOXC9</i> expression is associated with favorable prognostic markers, beneficial patient outcome and spontaneous regression in neuroblastoma</b>	<b>54</b>
4.2.1 Elevated <i>HOXC9</i> expression is associated with abdominal neuroblastoma	57
<b>4.3 Molecular basis for differential expression of <i>HOXC9</i> in neuroblastoma</b>	<b>60</b>
4.3.1 Numerical gain of chromosome 12 correlates with elevated expression of <i>HOXC9</i>	60
4.3.2 Sequencing of <i>HOXC9</i>	61
4.3.3 Methylation pattern of the promoter region of <i>HOXC9</i>	62
<b>4.4 Functional investigation of <i>HOXC9</i> in neuroblastoma</b>	<b>64</b>
4.4.1 Doxycycline-inducible expression of <i>HOXC9</i> in neuroblastoma cell lines	64
4.4.2 <i>HOXC9</i> expression inhibits neuroblastoma cell growth	66
4.4.2.1 <i>HOXC9</i> expression inhibits growth of neuroblastoma cells <i>in vitro</i>	66
4.4.2.2 <i>HOXC9</i> expression abrogates neuroblastoma tumor growth <i>in vivo</i>	68
4.4.3 Hox-C9 induces neuronal differentiation in neuroblastoma	70
4.4.3.1 Hox-C9-induced neuronal differentiation of IMR-32 cells is accompanied by down-regulation of <i>REST</i>	70
4.4.4 <i>HOXC9</i> re-expression induces apoptosis in neuroblastoma cell lines	72
4.4.4.1 Hox-C9 activates the intrinsic pathway of apoptosis	74
4.4.5 <i>HOXC9</i> expression affects transcriptional pathways regulating differentiation and cell death	76
<b>5 Discussion</b>	<b>82</b>
<b>5.1 Expression patterns of <i>HOX</i> genes in neuroblastoma</b>	<b>82</b>
<b>5.2 Expression patterns of <i>HOXC9</i> in neuroblastoma</b>	<b>84</b>
<b>5.3 The functional relevance of <i>HOXC9</i> expression in neuroblastoma</b>	<b>85</b>
5.3.1 <i>HOXC9</i> leads to neuronal differentiation in IMR-32 cells	85
5.3.2 <i>HOXC9</i> suppresses growth of neuroblastoma cells <i>in vitro</i> and <i>in vivo</i>	87
5.3.3 <i>HOXC9</i> induces apoptosis in neuroblastoma cells	87
<b>5.4 <i>HOXC9</i> expression and the association with spontaneous tumor regression in neuroblastoma</b>	<b>88</b>
<b>6 Conclusion</b>	<b>90</b>
<b>7 References</b>	<b>91</b>
<b>8 Appendix</b>	<b>105</b>
<b>8.1 Abbreviations</b>	<b>105</b>
<b>8.2 List of Figures</b>	<b>108</b>
<b>8.3 List of Tables</b>	<b>109</b>
<b>9 Erklärung</b>	<b>110</b>
<b>10 Danksagung</b>	<b><u>112</u></b>

## Zusammenfassung

Das Neuroblastom ist eine maligne Erkrankung des sympathischen Nervensystems und im Kindesalter der häufigste extrakranielle solide Tumor. Die klinischen Verläufe sind vielfältig und reichen von spontaner Regression oder Differenzierung des Tumors bis zu aggressiven, fatalen Verlaufsformen. Unter Berücksichtigung der embryonalen Entwicklung des sympathischen Nervensystems wird eine verzögerte Aktivierung apoptotischer Prozesse als Grundlage der spontanen Regression im Neuroblastom diskutiert. *HOX* Gene spielen eine entscheidende Rolle bei der embryonalen Entwicklung und sind maßgeblich an den Prozessen der Zelldifferenzierung und Apoptose beteiligt.

In dieser Arbeit wurde anhand eines umfangreichen Datensatzes von 649 Genexpressionsprofilen primärer Neuroblastome gezeigt, dass die Expression einer Mehrzahl der Klasse I *HOX* Gene signifikant mit klinischen Markern beim Neuroblastom assoziiert ist. Die prognostische Bedeutung der *HOX* Gen Expressionsmuster wurde darüber hinaus durch die Beobachtung verdeutlicht, dass eine *HOX* Gen Expressions-Signatur, unabhängig von den derzeit angewandten Prognosemarkern Alter, Stadium und *MYCN*-Amplifikationsstatus eine zuverlässige Vorhersage der Krankheitsverläufe im Neuroblastom ermöglicht.

In prognostisch günstigen Neuroblastomen, bei denen es regelhaft zu einer spontanen Regression kommt, wurde eine auffallend hohe *HOXC9* Expression detektiert. Um die Bedeutung des Transkriptionsfaktors Hox-C9 für die Pathogenese der unterschiedlichen Krankheitsverläufe des Neuroblastoms zu untersuchen, wurden Tetrazyklin-induzierbare *HOXC9*-transgene Neuroblastom-Zelllinien generiert.

Die Re-expression von *HOXC9* führte zu einer verminderten Zellviabilität und inhibierte das Tumorwachstum in einem Xenograft-Maus-Modell nahezu vollständig. Eine signifikante Zunahme der Sub-G<sub>1</sub> Zellfraktion und die Translokation von Phosphatidylserin

auf die Außenseite der Zellmembran deuten auf apoptotische Vorgänge hin. In diesem Zusammenhang wurde nach Hox-C9 Induktion ein erhöhter *BAX/BCL-2* Quotient, eine erhöhte Ausschüttung von Cytochrom c aus den Mitochondrien und eine Aktivierung der intrinsischen Caspase Kaskade nachgewiesen. Des Weiteren zeigte sich, dass die Expression von *HOXC9* zu einer signifikanten Abnahme der Proliferation in den untersuchten Zelllinien führte, was durch einen Zellzyklusarrest in der G<sub>0</sub>/G<sub>1</sub> Phase erklärt wurde. Soft-Agar Analysen zeigten außerdem eine Einschränkung des kontaktunabhängigen Wachstums nach Hox-C9 Induktion. In einer von drei untersuchten Zelllinien wurde nach Hox-C9 Induktion eine zunehmende morphologische Differenzierung der Neuroblastomazellen detektiert.

Zusammenfassend zeigt diese Arbeit einen starken prognostischen Einfluss von *HOX* Genen im Neuroblastom im Allgemeinen, und weist auf eine Bedeutung des Transkriptionsfaktors Hox-C9 bei den Prozessen der spontanen Regression des Neuroblastoms hin.

## Summary

Neuroblastoma is an embryonal malignancy of the sympathetic nervous system. Spontaneous regression and differentiation of neuroblastoma is observed in a subset of patients, and has been suggested to represent delayed activation of physiologic molecular programs of fetal neuroblasts. Homeobox genes constitute an important family of transcription factors which play a fundamental role in morphogenesis and cell differentiation during embryogenesis.

In this study, I demonstrate that expression of the majority of the human *HOX* class I homeobox genes is significantly associated with clinical covariates in neuroblastoma using microarray expression data of 649 primary tumors. Moreover, a *HOX* gene expression-based classifier predicted neuroblastoma patient outcome independently from age, stage and *MYCN* amplification status. Among all *HOX* genes, *HOXC9* expression was most prominently associated with favorable prognostic markers. Notably, elevated *HOXC9* expression was significantly associated with spontaneous regression in infant neuroblastoma.

Re-expression of *HOXC9* in three neuroblastoma cell lines led to a significant reduction in cell viability, and abrogated tumor growth almost completely in neuroblastoma xenografts. Neuroblastoma growth arrest was related to induction of programmed cell death, as indicated by an increase in the sub-G<sub>1</sub> fraction and translocation of phosphatidylserine to the outer membrane. Programmed cell death was associated with a shifted *BCL-2/BAX* ratio, the release of cytochrome c from the mitochondria into the cytosol, and activation of the intrinsic cascade of caspases, indicating that *HOXC9* re-expression triggers the intrinsic apoptotic pathway. Furthermore, re-expression of *HOXC9* resulted in a significant reduction of proliferation accompanied by cell cycle arrest in the G<sub>0</sub>/G<sub>1</sub> phase, and decreased colony formation in soft agar. Neuronal differentiation was observed in one out of three cell lines upon *HOXC9* re-expression.

Collectively, the results of my thesis demonstrate a strong prognostic impact of *HOX* gene expression in neuroblastoma, and point towards a critical role of Hox-C9 in neuroblastoma spontaneous regression.

# 1. Introduction

## 1.1 Neuroblastoma

Neuroblastoma, one of the most common malignant solid tumors occurring in infancy and childhood, accounts for 8% of all pediatric cancers (1-3). With a median age of 22 months at diagnosis, neuroblastoma is responsible for 15% of all childhood cancer deaths (4). Neuroblastoma represents a neuro-ectodermal malignancy derived from fetal precursors of the sympathetic nervous system (5, 6). In the developing embryo, neuroblasts migrate along the neural crest, and populate primarily the sympathetic ganglia and adrenal medulla. The distribution pattern of these cells correlates highly with the sites of primary neuroblastomas and consequently neuroblastomas are most often located in the adrenal medulla or along the sympathetic nervous system chain ganglia. Multiple genetic abnormalities, like chromosomal gains and losses, aneuploidy, and amplification of chromosomal material, are found in neuroblastoma. Age at diagnosis, tumor stage and biological features encountered in neuroblastoma tumor cells are important prognostic factors and in use for risk estimation and treatment stratification. Neuroblastoma shows remarkable variations in clinical presentation ranging from aggressive, therapy-resistant progression to spontaneous regression, which regularly occurs in younger infants with both localized and metastasized disease. Furthermore, neuroblastoma cells show the potential to differentiate towards a sympathetic ganglion cell phenotype (9). The arrested differentiation of neuroblasts is proposed to be an early event in the pathogenesis of neuroblastoma caused by a disruption of the normal developmental genetic program (7). It has been suggested that in spontaneously regressing neuroblastomas this disruption results in a reversible phenotype, with initial proliferation of immature neural-crest cells followed by a delayed activation of naturally occurring processes of programmed cell death and differentiation (10-12).

### 1.1.1 International Neuroblastoma Staging System (INSS)

Staging of neuroblastoma is performed according to the International Neuroblastoma Staging System (INSS, Table 1) (8). The INSS is based on clinical, radiographic and surgical criteria and is now widely accepted as the standard neuroblastoma staging system.

<b>INSS</b>	
<b>Stage</b>	<b>Definition</b>
1	Localized tumor with complete gross excision, with or without microscopic residual diseases; representative ipsilateral lymph nodes negative for tumor microscopically (nodes attached to and removed with the primary tumor may be positive).
2A	Localized tumor with incomplete gross excision; representative ipsilateral nonadherent lymph nodes negative for tumor microscopically.
2B	Localized tumor with or without complete gross excision, with ipsilateral nonadherent lymph nodes positive for tumor. Enlarged contralateral lymph nodes must be negative microscopically.
3	Unresectable unilateral tumor infiltrating across the midline, with or without regional lymph node involvement; or localized unilateral tumor with contralateral regional lymph node involvement; or midline tumor with bilateral extension by infiltration (unresectable) or by lymph node involvement. The midline is defined as the vertebral column. Tumors originating on one side and acrossing the midline must infiltrate to or beyond the opposite side of the vertebral column.
4	Any primary tumor with dissemination to distant lymph nodes, bone, bone marrow, liver, skin and/or other organs (except as defined as 4S).
4S	Localized primary tumor (as defined for stage 1, 2A or 2B), with dissemination limited to skin, liver, and/or bone marrow (limited to infants < 1 year of age). Marrow involvement in stage 4S should be minimal, i.e., < 10% of total nucleated cells indentified as malignant on bone marrow biopsy or on marrow aspirate. More extensive marrow involvement would be considered to be stage 4. The MIBG scan (if performed) should be negative in marrow.

**Table 1:** INSS (8).

The INSS distinguishes three localized stages (stage 1-3, collectively approximately 50% of cases) from an unfavorable, disseminated stage (stage 4, approximately 40% of cases). The remaining approximately 10% of patients present with a special form of disseminated disease categorized as stage 4S (“S”, special). Stage 4S diseases were first described by D’Angio *et al.* (9) and are clinically defined by patients younger than 12 months of age and a restrict pattern of distant metastases to skin, liver and bone marrow. A high percentage of stage 4S patients regress spontaneously or differentiate into benign ganglioneuroma (9).

### **1.1.2 Neuroblastoma risk stratification**

Neuroblastoma risk assessment depends on several clinical and biological features. The main goal of neuroblastoma risk stratification is to predict each patients individual risk to die from the disease at diagnosis. To choose the most appropriate form of treatment, the German Neuroblastoma Trial NB2004 categorizes patients into three risk-based groups: low-, intermediate- and high-risk. The NB2004 risk stratification criteria (Figure 1, (10)) include clinical parameters such as tumor stage defined by INSS (8) and patient age at diagnosis, since younger age at diagnosis is significantly associated with better outcome (11, 12). Furthermore, genetic characteristics like *MYCN* amplification status (13) and loss of the short arm of chromosome 1 (14) are included as markers of poor outcome in the NB2004 risk stratification criteria. Further markers used in international clinical trials for neuroblastoma risk stratification (15) are histopathologic classification according to the Shimada system (16), allelic loss of chromosomal regions at 11q (14, 17) and DNA ploidy (18, 19).

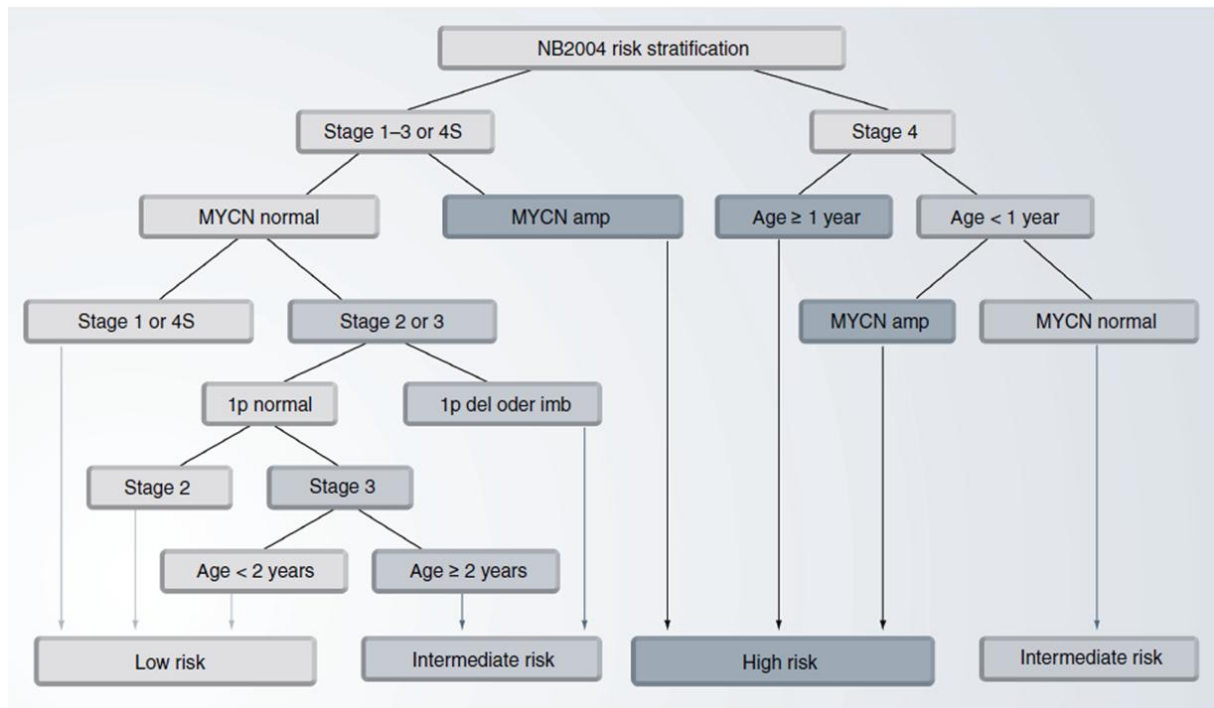


**Figure 1:** Risk stratification according to the German Neuroblastoma Trial, NB2004 (10).

It has been demonstrated that risk stratification according to NB2004 criteria significantly discriminates neuroblastoma patients with different event-free survival (EFS) and overall survival (OS) (Figure 2, (20)).

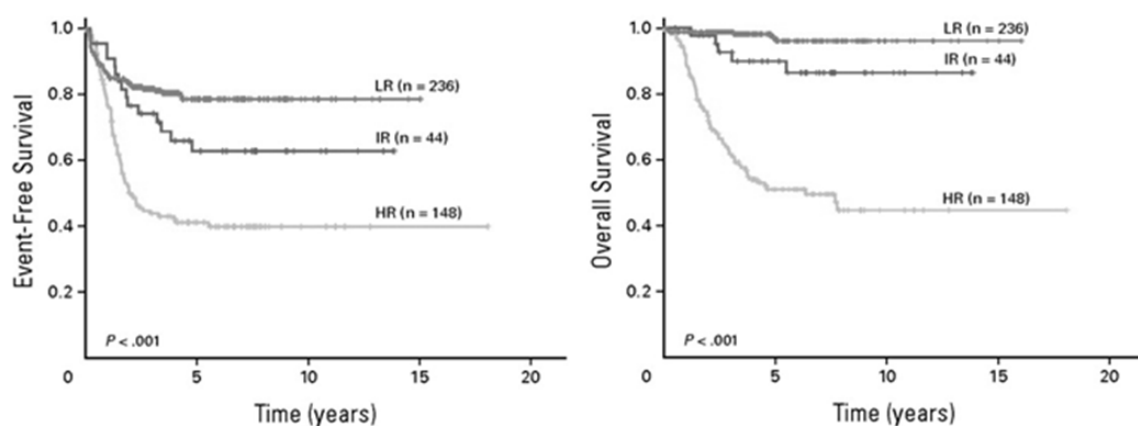


**Figure 2:** Kaplan-Meier estimates for EFS and OS for 428 neuroblastoma patients stratified according to the German neuroblastoma trial NB2004 (10). Abbreviations: LR, low-risk; IR, intermediate-risk; HR, high-risk.

Despite such complex risk stratification systems, there are some neuroblastoma cases where the individual tumor behavior is not precisely predictable on initial presentation. It has been thus suggested to implement global genetic aberration patterns or gene-expression signatures in risk estimation systems to more accurately predict neuroblastoma patient outcome (20-26).

### **1.1.3 Molecular biology of neuroblastoma**

Clinical heterogeneity is a hallmark of neuroblastoma which is reflected by specific patterns of genetic and transcriptomic abnormalities. The best characterized biological parameters associated with clinical phenotypes are *MYCN* amplification, *ALK* amplification and activating mutations, 1p and 11q deletion, unbalanced 17q gain and aberrant gene expression patterns.

#### **1.1.3.1 *MYCN* amplification**

The genetic aberration most consistently associated with advanced disease stage, rapid tumor progression and poor outcome in neuroblastoma, is genomic amplification of the proto-oncogene *MYCN* (27-29). Amplification of *MYCN* in neuroblastoma was first described by Schwab *et al.* in 1983 (30). *MYCN* is located at chromosome 2p24, and amplification occurs in about 20% of all neuroblastoma cases. *MYCN* amplification values range between 5- to more than 500-fold, which lead to its overexpression at mRNA and protein level (31-35). High expression of *MYCN* in neuroblastoma results in activation of genes associated with aggressive tumor behavior. The exact mechanisms by which *MYCN* amplification contributes to aggressive tumor biology are still not clarified. The transcription factor N-myc regulates a huge amount of target genes, including transcriptional regulators (36). Many of these genes are involved in development and neuronal differentiation (36), cell proliferation (37), cell cycle (38) and apoptosis (36). However, even though *MYCN* amplification is strongly

associated with high-risk neuroblastomas, more than 60% of patients with aggressive disease do not harbor this amplification.

### **1.1.3.2 *ALK* amplification and activating mutations**

Anaplastic lymphoma kinase (*ALK*) is a transmembrane receptor tyrosine kinase preferentially expressed in the central and peripheral nervous system (39). Activating mutations in the tyrosine kinase domain of *ALK* encode for single base substitutions in key regions of the enzymatic domain and result in constitutive activation of the kinase and a premalignant state. These mutations appear to be responsible for most of the rare cases of hereditary neuroblastomas, and might also be relevant for a smaller fraction of sporadic neuroblastomas (6-9%). A substantial number of primary neuroblastomas (20-25%) present low-level copy number gains at the *ALK* locus on 2p23 (40-42). High-level genomic amplification of *ALK* occurs in about 1% of neuroblastoma, and is highly associated with *MYCN* amplification (43-46).

### **1.1.3.3 Chromosome 1p deletion**

Chromosome 1p36 deletion is a common structural aberration occurring in about 30% of all neuroblastomas. The deletion is variable but consistently encompasses 1p36.1 to 1pter, including a 261 kb region at 1p36.3, which is highly correlated with the amplification of *MYCN* and advanced disease stage (47-51). Further, 1p36 deletion is an independent predictor of neuroblastoma progression, and evidence suggests that 1p36 deletion predicts an increased risk of relapse in patients with localized tumors (47-51). Several lines of evidence have led to the hypothesis that this region harbors tumor suppressor genes involved in the development of neuroblastoma. Consequently, several candidate genes were found to be

decreased in expression levels. However, none of these have been proven to be crucial for the pathogenesis of aggressive neuroblastoma (52-55).

#### **1.1.3.4 Chromosome 11q deletion**

Allelic loss of 11q occurs in a subgroup of high-risk neuroblastomas accounting for approximately 15-22% of all patients (56-58). The majority of 11q deletions are distal losses encompassing a large portion of the long arm of chromosome 11. Aberrations at 11q are rarely seen in tumors with *MYCN* amplification, but they remain highly associated with other high-risk features like stage 4 disease, increased age at diagnosis and poor EFS and OS (17, 59). Consequently, the presence of 11q deletions and *MYCN* amplifications appear to delineate two molecularly distinct subgroups of unfavorable neuroblastoma.

#### **1.1.3.5 Chromosome 17q gain**

Unbalanced gain of a long segment at chromosome 17q is found in 54-68% of neuroblastoma patients, thus representing the most frequent structural genomic aberration in neuroblastoma (60-62). Although 17q gains are associated with poor outcome and hence with unfavorable prognostic markers such as stage 4 disease, increased age at diagnosis and other chromosomal aberrations such as *MYCN* amplification, 1p and 11q loss, the pertinence of 17q gain as an independent prognostic marker for neuroblastoma patient outcome has remained controversial (60, 62).

#### **1.1.3.6 DNA index**

DNA ploidy is a well established prognostic marker in several human malignancies, and an aneuploid (hyperdiploid or near-triploid) DNA content is usually an indicator for disease

progression and poor outcome. In 1984, Look *et al.* (19) showed that neuroblastoma represents an exception since aneuploid neuroblastomas are correlated with favorable outcome and a better response to chemotherapy, particular in younger patients (< 12 months). For neuroblastoma patients older than 1-2 years of age, DNA ploidy loses its prognostic significance (63).

### **1.1.3.7 Aberrant gene expression**

In addition to genomic aberrations, alterations in gene expression have been studied extensively in neuroblastoma (10, 20, 25, 64). Of particular interest are members of the neurotrophin receptor pathways, since the neurotrophin receptors TrkA, TrkB and TrkC together with their ligands NGF, BDNF and NT3 are important regulators of survival, growth, and differentiation of neuronal cells (7). The first report showing elevated TrkA expression in favorable neuroblastomas was presented by Nakagawara and colleagues in 1993 (7). High TrkA expression is associated with favorable prognostic markers and favorable outcome, whereas decreased expression correlates strongly with poor prognosis and *MYCN* amplification (7, 65). Another candidate gene in neuroblastoma is caspase 8, an apoptosis-related cysteine peptidase. Loss of caspase 8 expression is estimated to occur in 25-35% of neuroblastoma patients, predominantly high-risk tumors. Absence of caspase 8 expression appears to be strongly correlated with *MYCN* amplification (66, 67). Caspase 8 is homozygously deleted in a small subset of neuroblastomas (67), but more importantly, it is inactivated by hypermethylation in nearly all neuroblastoma patients with *MYCN* amplification (67). Loss of caspase 8 expression may represent a critical event for impaired activation of the extrinsic apoptotic pathway in high-risk neuroblastoma.

### **1.1.4 Hereditary neuroblastoma**

Familial neuroblastoma accounts for 1-2% of all neuroblastomas (68) and are associated with younger age at diagnosis and multiple sites of primary tumors. Apart from that, hereditary neuroblastoma shows the same diverse clinical behavior as sporadic neuroblastomas, ranging from aggressive progression to spontaneous regression (69). Germline mutations in two genes, *PHOX2B* and *ALK*, account for around 90% of hereditary neuroblastomas. *PHOX2B* belongs to the homeobox gene family and is involved in the development of the normal autonomic nervous system (70, 71). Loss of function mutations in *PHOX2B* have been found in a small subset of hereditary neuroblastomas and rarely in sporadic neuroblastomas (72). *ALK* mutations (see also section 1.1.3.2) are known to be the most common cause of hereditary neuroblastoma so far (42).

### **1.1.5 Origin of neuroblastoma**

The neural crest develops early in embryogenesis (73) and consists of pluripotent cells that migrate from the neural tube to the dorsal aorta. At this early stage of neural crest cell migration and differentiation, bone morphogenetic protein (BMP) signaling plays an important role for cell fate determination and specification (74). From the dorsal aorta, pluripotent cells migrate further to sites where they differentiate into several lineages, including the sympathoadrenal lineage. The oncogenic events responsible for neuroblastoma development appear to be strictly lineage-dependent, because neuroblastomas never arise from other neural precursors than sympathoadrenal lineage cells (75). The cell fate specification is then regulated by multiple transcription factors and their target genes which includes several growth factors and growth factor receptors (76, 77). Homeodomain containing genes such as *ASCL1* (78, 79), *PHOX2A* (80, 81), *PHOX2B* (82) and *HAND2* (83, 84) appear to be of high importance for cell fate determination and sympathetic differentiation.

For example, *ASCL1* expression usually decreases after transient expression during the development of neural crest cells, which in turn promotes differentiation to mature sympathetic neurons (85), whereas high expression of *ASCL1* is still detectable in neuroblastomas (86, 87). The transcription factors Phox2a and Phox2b are essential for the differentiation of noradrenergic neurons (88). *PHOX2A* and *PHOX2B* encode two highly related homeobox transcription factors with similar expression patterns throughout the peripheral autonomic nervous system development (89). Although rare, *PHOX2B* mutations were found in hereditary and sporadic neuroblastomas as indicated in section 1.1.4. *PHOX2B* was identified as the major disease causing gene of congenital central hypoventilation syndrome (CCHS) (70), and CCHS patients are predisposed to develop tumors of the sympathetic nervous system, such as neuroblastoma (90). *PHOX2B* also regulates, among other factors, the expression of *HAND2* (83), another candidate tumor suppressor gene, which is de-regulated in neuroblastoma (84). Together with *MYCN*, these factors control neural crest cell fate and are necessary for sympathetic neuronal differentiation. As *MYCN* is frequently amplified in neuroblastoma, it has been suggested that its de-regulation may play a major role in the cellular transformation process and thus the initiation of neuroblastoma at this stage of cell maturation (83). Finally, the terminal differentiation of sympathetic progenitor neurons depends on TrkC and TrkA receptor stimulation by the neurotrophins NT3 and NGF. Increased expression of *TRKC* and activation by NT3 induces up-regulation of *TRKA*. Activation of the TrkA receptor by NGF's then leads to the terminal differentiation of sympathetic nerve cells. Consistent with these regulatory functions, a higher expression of *TRKA* and *TRKC* was found to be strongly correlated with favorable neuroblastomas (7, 91).

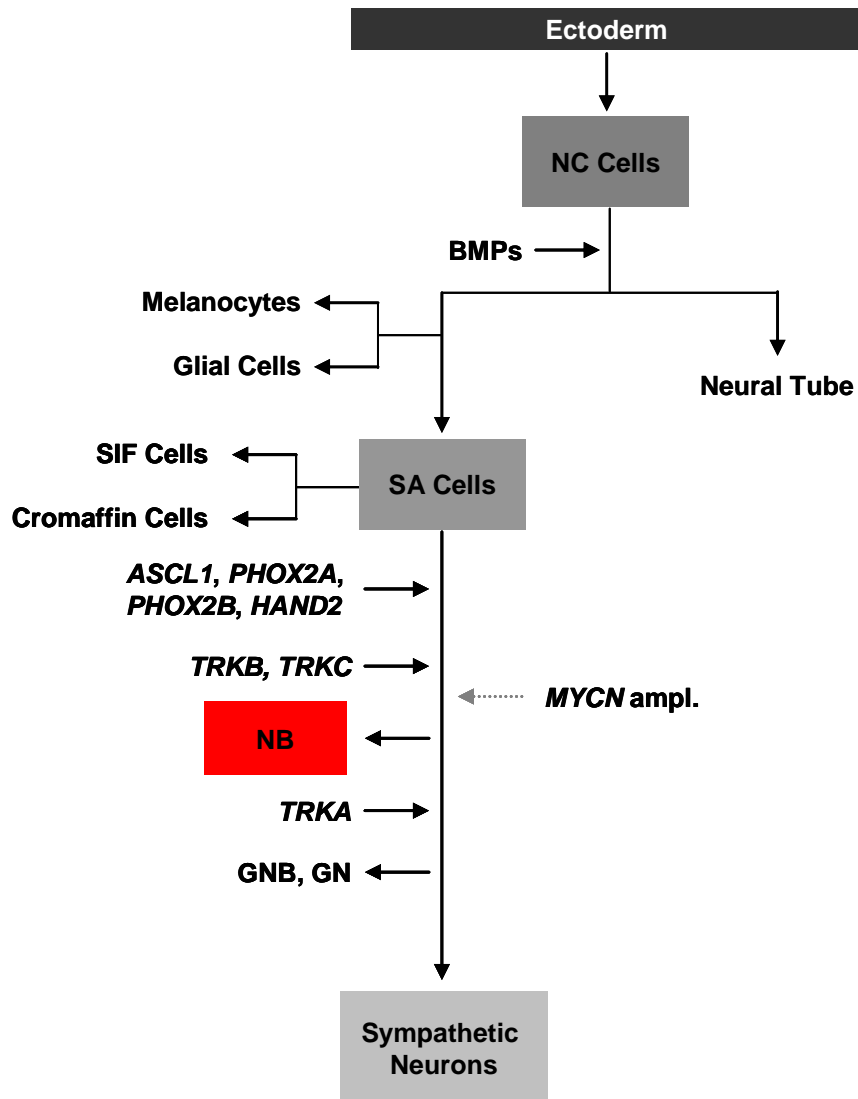


**Figure 3:** Regulators of the sympathetic nervous system cell lineage (Figure modified from Mohlin et al. (83)). BMP signaling initiates the migration of neural crest (NC) cells and commits precursor cells to melanocytic, glial and sympathetic neuronal lineages. The main cell types of the sympathetic nervous system (SNS) are proposed to originate from sympathoadrenal (SA) progenitor cells. Cell fate restriction is induced and controlled by a set of transcription factors (Ascl1, Phox2a Phox2b and Hand2) expressed at various stages of development. *MYCN* gene expression is first detectable after cell fate restriction has been induced, and it is suggested that *MYCN* amplified tumors arise at this developmental stage. Based on a strong correlation of high *TRKA* expression levels with more favorable neuroblastomas (NB), ganglioneuroblastomas (GNB) and ganglioneuromas (GN), it is supposed that high *TRKA* expression is sufficient to induce further differentiation even if the cells are already neoplastic.

### **1.1.6 Spontaneous regression and differentiation in neuroblastoma**

Spontaneous regression of neuroblastoma was first reported by Beckwith and Perrin in 1963 (92). In infants, the vast majority of neuroblastomas may disappear before becoming clinically apparent, as suggested by several mass screening studies on infants, in which a significant increase of neuroblastoma cases was detected, while a decrease in the frequency of advanced disease stages in older children was not observed (93-96). These investigations have led to the assumption that a large number of neuroblastomas detected by mass screening are favorable tumors that regress spontaneously.

In general, spontaneous regression and differentiation of neuroblastomas are observed less frequently in older patients (21, 97). It has been suggested that the physiologic genetic program of neuroblast differentiation and growth control (Figure 3) is disrupted in neuroblastoma (7), and that this developmental arrest may be reversible and activated delayed in spontaneously regressing neuroblastomas. In this context, a delayed activation of naturally occurring processes of programmed cell death and neuronal differentiation has been suspected (98-100). Consistent with its embryonic nature, many genes de-regulated in neuroblastoma are involved in developmental processes (75). Among these, several transcription factors involved in the development of autonomic neural crest derivatives (Figure 3) are implicated in the pathogenesis of neuroblastoma (30, 71, 82, 83, 101), and various *HOX* genes have been described to be aberrantly expressed in neuroblastoma cell lines and primary tumors (Table 2, (36, 102)).

## 1.2 Homeobox genes

*HOX* genes are master regulators of embryonic development and stem cell differentiation. They encode for highly conserved transcription factors that organize the anterior-posterior (AP) body axis during embryogenesis (103). Beside this, they act as critical regulators of growth and differentiation. They control cell identity, cellular communication, cell cycle progression, hematopoiesis, and apoptosis (104) by activating or repressing their target genes (105-109). *HOX* genes are separated in 2 classes; class I clustered *HOX* genes and class II dispersed *HOX* genes (110). The mammalian class I *HOX* gene cluster comprises 39 *HOX* genes, which are arranged within 4 different clusters (A – D) on 4 different chromosomes (chromosome 2, 7, 12, and 17) and organized into 13 paralogous groups.

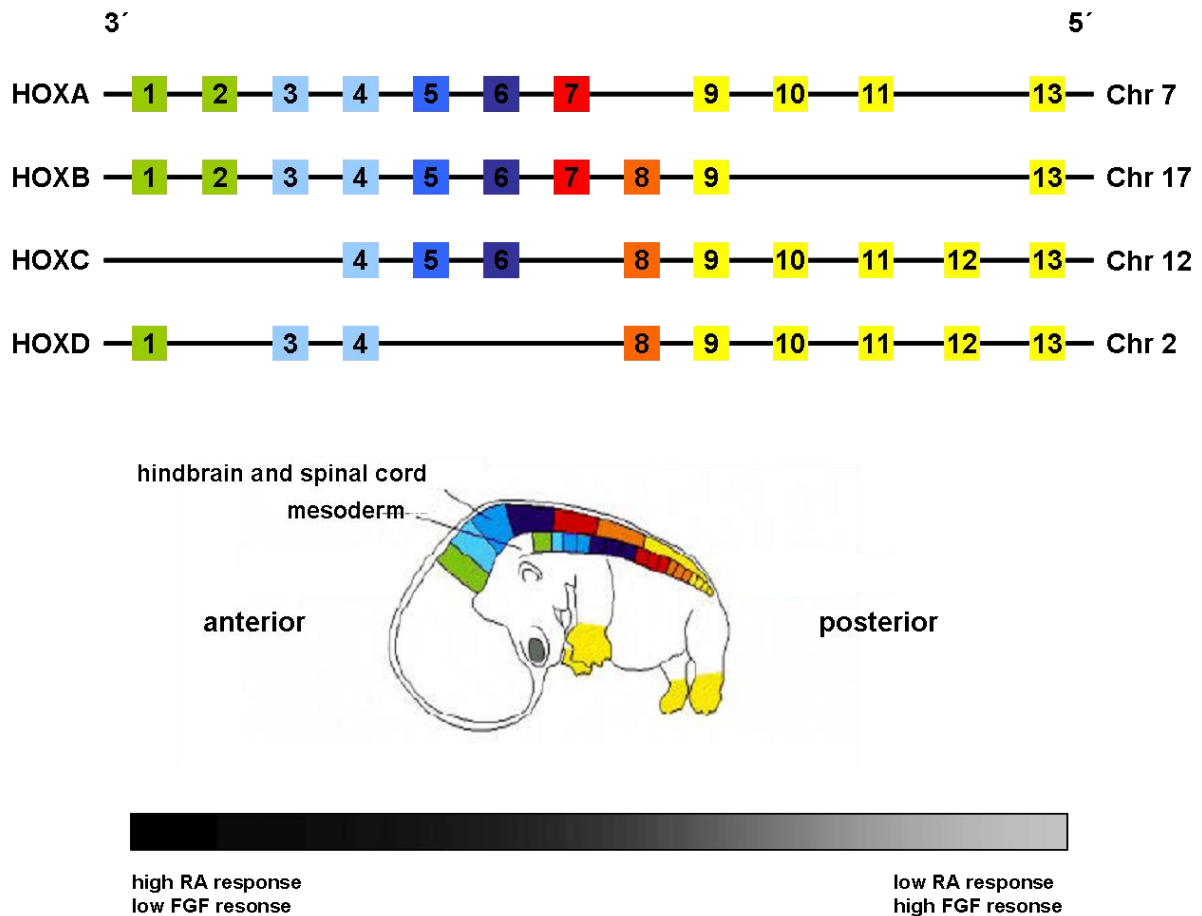


**Figure 4:** Homeotic gene organization and transcriptional expression (Figure modified from Nolte and Krumlauf (111)). In humans, there are 4 clusters on 4 chromosomes with 39 *HOX* genes in total. Genes located closer to the 3' end of the cluster are stronger expressed in anterior tissues whereas 5' located genes show a stronger expression pattern in posterior tissues (spatial colinearity). *HOX* genes that are positioned more 5' in the cluster (yellow) will have a dominant phenotype compared with those more 3' (green), which is described as posterior prevalence. *HOX* genes are expressed temporally in an order corresponding to their positions from 3' to 5' within each cluster, known as temporal colinearity. Early 3' located *HOX* genes display the highest level of retinoic acid (RA) responsiveness, whereas the 5' members show stronger response to fibroblast growth factors (FGF's).

### 1.2.1 *HOX* gene expression

*HOX* gene expression is well controlled during embryonic development. The position of a *HOX* gene from 3' to 5' within a *HOX* cluster corresponds to its expression along the AP axis of the body and to its temporally order of expression (spatial and temporal colinearity). *HOX* genes located at the 3' region of each *HOX* cluster are activated earlier and more anteriorly compared to the more 5' genes which are expressed later and more posterior (112, 113).

Furthermore, *HOX* genes which are located in the 5' region of the *HOX* cluster lead to a more dominant phenotype than those located more 3' (posterior prevalence). This precisely organized expression pattern is modulated by complex regulative mechanisms.

It has been suggested that a unidirectional chromatin opening process plays a role in the spatial and temporal expression pattern of *HOX* genes (114). Two classes of chromatin-modifying proteins epigenetically regulate *HOX* gene expression. The Polycomb group (PcG) proteins and trithorax group (TrxG) proteins form multiprotein chromatin remodeling complexes that either repress (PcG) or activate (TrxG) the transcription of *HOX* genes.

Furthermore, *HOX* gene expression is controlled by a dose dependent response to retinoic acid (RA) and fibroblast growth factors (FGF's) (115-117). *HOX* genes located more 3' in the *HOX* cluster show a stronger response to RA as compared to 5' located *HOX* genes, which are more sensitive to FGF's (118, 119). Although RA and FGF's are the best described and analyzed global regulators of *HOX* gene expression, there are several other factors that can influence *HOX* gene expression such as regulative RNA's (miRNA's (120), lincRNA's (121, 122) or *HOTAIR*'s (123)). Finally, *HOX* gene expression is also regulated by auto- and cross-regulative processes (124-126), in which Hox transcription factors bind to *HOX* responsive elements (HRE's) together with one or more cofactors. HRE mediated *HOX* regulation functions in three different ways: Hox transcription factors can regulate their own expression (auto-regulation), they can activate the expression of other *HOX* genes within the same segment (cross-activation), or they can have antagonistic interactions in which one Hox transcription factor represses the expression of another *HOX* gene (cross-repression).

### **1.2.2 Hox cofactors**

Hox cofactors are important for modifying Hox DNA binding sensitivity and specificity (127). Although Hox proteins can bind sequence-specific to a 4-base pair target site (TAAT)

as single molecule, their affinity to this site is low in general due to the very short sequence, which allows only restricted specificity in target selection. HRE's are essential for Hox target regulation. In addition to Hox binding sites, they also contain specific binding sites for Hox cofactors. Therefore, the transcriptional regulation by Hox and cofactor complexes is more specific and allows a precisely defined transcriptional regulation of target genes. Pbx (128-131) and Meis (132, 133) are the two best studied cofactors of Hox proteins, both belonging to the TALE (three-amino acid-loop-extension) family of homeodomain proteins, which are known to be involved in various forms of leukemia (134). Interestingly, both *MEIS* and *PBX* have been described to be involved in the pathogenesis of neuroblastoma (135).

### **1.2.3 *HOX* genes in human diseases**

De-regulated expression of *HOX* genes leads to various forms of human disease (114). *HOX* genes are involved in several disorders of limb development. Muragaki and colleagues showed that mutation of *HOXD13* cause synpolydactyly in humans (136). *HOXA13*, another member of the class I *HOX* gene family, was identified to play a potential role in the pathogenesis of hand/foot/genital syndrome (137, 138). A malformation of the foot, congenital vertical talus, has been associated to a *HOXD10* mutation (139), and it has been hypothesized that *HOX* genes may be involved in clubfoot and other limb malformations (140, 141). In the central nervous system, homozygous *HOXA1* mutations disrupt human brainstem, inner ear, cardiovascular and cognitive development (142).

#### **1.2.3.1 *HOX* genes in cancer**

De-regulated expression of *HOX* genes is reported in several tumor entities (Table 2). Precise mechanisms by which *HOX* genes mediate tumor formation or tumor suppression are still not defined. They may influence tumorigenity through proliferative, apoptotic or angiogenic

effects, but the activity is dependent on the availability of their cofactors (143, 144). Aberrant expression of a single *HOX* gene can lead to tumor formation in one type of tissue by blocking cell differentiation or apoptosis and increasing proliferation, whereas the same *HOX* gene can exert tumor suppressive functions in a different tissue type. *HOXB13*, for example, represents a tumor suppressor gene (145) and is necessary for normal prostate development (146) while it is associated with tumorigenesis and aggressive disease course in breast cancer (147). This tissue specificity is also reflected in the broad variation of signaling pathways by which *HOX* genes exert their effects. In neuroblastoma, the expression of a single *HOX* gene (*HOXC6*) induces differentiation and prevents tumorigenesis (148), while in other diseases such as acute myeloid leukemia (AML), overexpression of *HOXC6* promotes clonal expansion (149). An example for a fusion protein-mediated malignant transformation is given by *HOXA9*, which is overexpressed and fused to *NUP98* and represents the gene most highly correlated with poor prognosis (150, 151) and treatment failure in AML (152).

Tumor Entity	HOX Gene	Expression	Effect
Esophageal squamous cell carcinoma	5' HOX genes	Increased	Associated with primary tumors (153)
Lung Carcinoma	5' HOXA and HOXD genes, A1, C5	Increased	Associated with primary tumors (154)
	A7, A9	Decreased (promoter methylation)	Associated with primary tumors (155)
Neuroblastoma	D1, D8, C6	Decreased	Expressed in differentiated cell lines (156)
	C6, C11	Decreased	Expression leads to cell differentiation (148)
Ovarian Carcinoma	B13	Increased	Promotes cancer progression (157)
	B4	Increased	Associated with primary tumors and cell lines (158)
Cervical Carcinoma	C Cluster	Increased	Associated with primary tumors (159)
	C10	Increased	Increased invasion (160)
Prostate Carcinoma	B13	Decreased	Loss of differentiation, transactivation of androgen receptors and proliferation (145, 146, 161)
	C8	Increased	Associated with primary tumors, loss of differentiation, androgen receptor - independent growth (162)
Breast Carcinoma	A5	Decreased (promoter methylation)	Down-regulation of p53, decreased apoptosis (163-165)
	A10	Decreased	Down-regulation of p53 (166)
	B7	Increased	Up-regulation of <i>FGF2</i> , associated with bone metastases, increased invasion and vascularization, Associated with <i>HER2</i> amplification (167-169)
	B13	Increased	Associated with tamoxifen resistance in tumors, increased migration and invasion <i>in vitro</i> (147, 170, 171)
Leukemia	A9, A10, C6	Increased	Associated with aggressive ALL (172)
	A9	Increased	Increased proliferation by NUP98-HOXA9 fusion, <i>MEIS1</i> and <i>FLT3</i> up-regulation (152, 173-175)
Astrocytoma	A6, A7, A9, A13, B13, D4, D9, D10, D13	Increased	Associated with primary tumors and cell lines (110)
Colorectal Cancer	B13	Decreased	Associated with primary tumors and cell lines, down-regulates the $\beta$ -catenin-TCF pathway $\rightarrow$ Inhibition of cell proliferation (176)
Renal Carcinoma	B5, B9	Decreased	Associated with primary tumors (177)
	C11	Increased	Associated with primary tumors (177)
Pediatric low-grade gliomas	D1, D12	Increased	Associated with primary tumors (178)
	D3	Decreased	Associated with primary tumors (178)

**Table 2:** HOX genes in tumorigenesis (Table modified from Abate-Shen (104), Shah and Sukum (179)). Abbreviation: ALL, acute lymphocytic leukaemia.

### 1.2.3.2 *HOX* genes in neuroblastoma

Differentiation of neuroblastoma cell lines and primary tumors can be induced by various agents (180) including RA (181). Spontaneous differentiation in infant neuroblastoma into less aggressive ganglioneuroblastoma or benign ganglioneuroma was first described by Cushing in 1927 (182), and occurs regularly (183). In 1990, Peverali and colleagues showed that morphological maturation of neuroblastoma cell lines toward a neuronal differentiation phenotype is associated with increased *HOX* gene expression (184). Manohar and colleagues (102, 156) further demonstrated that *HOX* genes, such as *HOXC6*, *HOXD1* and *HOXD8*, are expressed at a low level in neuroblastoma cell lines, which can be increased by RA treatment. Zhang *et al.* (148) showed that neuroblastoma GOTO cells differentiate into schwannian cell types when exposed to 5-bromo-2'-deoxyuridine (BrdU) (148), which is accompanied with increased expression of *HOXC6*, *HOXC11* and *S100B*, a schwannian cell marker gene. They further demonstrated that these *HOX* genes directly bind to the *S100B* promoter and hence lead to its up-regulation.

Genes involved in development or neural differentiation have been described to be down-regulated in *MYCN* amplified neuroblastomas, indicating that overexpression of *MYCN* is associated with altered maturation of neuroblastoma progenitor cells. As an example, Alaminos *et al.* showed that, among other developmental regulators, the expression of *HOXC10* is decreased in *MYCN* amplified primary neuroblastoma tumors (36). In a recent publication, Zha and coworkers demonstrated that increased expression of *HOXD8*, *HOXD9* and *HOXD10* results in growth arrest and neuronal differentiation in SK-N-BE(2)-C neuroblastoma cells (185).

### 1.2.4 *HOXC9* gene expression in development and tumorigenesis

The molecular mechanisms by which *HOXC9* regulates the transcription of its target genes as well as the direct targets themselves are widely unknown. A role for *HOXC9* as a master regulator of motor neuron organization and development was proposed recently by Jung and colleagues who demonstrated that *HOXC9* exerts its regulative function through global cross-repressive activities (186). In fetal human smooth muscle cells (SMC), *HOXC9* was found to be expressed at higher levels as compared to adult SMC's, which indicates its role in specifying the fetal SMC phenotype (187). Furthermore, it has been hypothesized that *HOXC9* is involved in the process of cell differentiation of bone marrow derived stem cells to endothelial cells (188). *HOXC9* expression was detected in hind limb blood vessels of mice (189) and the axial vasculature of zebrafish (190). Moreover, strong *HOXC9* expression was found in human umbilical vein endothelial cell (HUVEC) spheroids which are characterized by tight cell contacts and resting proliferation (191). Enhanced expression of *HOXC9* leads to the inhibition of major angiogenic processes like tube formation, migration and proliferation in human vascular endothelial cells as demonstrated by Stoll *et al.* (192). They further showed that *HOXC9* exerts its anti-angiogenic function by repressing the transcription of interleukin 8, and independent of the VEGF pathway.

Evidence for Hox-C9 acting as a “tumor suppressor” is given by Kikuyama and co-workers (193) who showed that the *HOXC9* promoter is frequently methylated in primary breast cancers. *HOXC9* promoter methylation was also observed in stage I non-small-cell lung carcinoma samples, whereas it was absent in the lung tissue of non-cancerous lesions (194). Recently, high *HOXC9* expression was found to be associated with neuroblastoma cell differentiation and decreased cell proliferation (195). In contrast to its tumor suppressive functions, *HOXC9* may also stimulate tumor formation and malignancy and thus act as a potential “oncogene”. In cervical cancer, for example, *HOXC9* was reported to be expressed

in tumors but not in non-neoplastic tissue (196). It has been hypothesized that the expression of *HOXC9* is not implicated in the physiology of normal cervix, but it is necessary for carcinogenesis in this tumor entity. Likewise, normal brain tissues lack *HOXC9* expression, while its expression is detectable in astrocytomas of different grades, and *HOXC9* expression levels are strongly associated with the grade of malignancy (197). A transgenic mouse model lacking *HOXC9* was established and described in 1995 by Suemori and colleagues (198). The *HOXC9* knock-out mouse displayed anterior transformation of the vertebrae and malformation of the sternum and ribs (198), however, this model has not yet been used for investigating the role of *HOXC9* in cancer biology.

## 2 Aim of the study

Neuroblastoma is an embryonal tumor derived from fetal precursors of the sympathetic nervous system, and has the highest frequency of spontaneous regression observed in human malignancies. It has been suggested that spontaneous regression may represent a delayed activation of developmental apoptotic pathways. However, the molecular mechanisms of this peculiar phenomenon have remained enigmatic. Understanding the molecular processes underlying spontaneous regression is therefore a major challenge in neuroblastoma research.

Since expression of *HOX* transcription factor genes is tightly regulated during embryogenesis and fundamental for a normal embryonic development, I suggested a role of these genes in neuroblastoma pathogenesis in general and in spontaneous regression in particular. Using microarray-based expression data of a large cohort (n= 649) of primary neuroblastomas, I aimed at determining the gene expression patterns of class I *HOX* genes and their association with clinical phenotypes. *HOXC9* was found to be strongly associated with favorable prognostic markers, beneficial outcome and spontaneous regression in primary neuroblastoma. I therefore aimed to determine the functional role of Hox-C9 in neuroblastoma pathogenesis and spontaneous regression by generating and analyzing *HOXC9*-transgenic neuroblastoma cell lines.

## 3 Materials and Methods

### 3.1 Microarrays and data analysis

#### 3.1.1 Neuroblastoma patient characteristics

Tumors of 649 neuroblastoma patients were analyzed. Neuroblastoma tumor stage was classified according to the International Neuroblastoma Staging System (8): stage 1, n= 153; stage 2, n= 113; stage 3, n= 91; stage 4, n= 214; stage 4S, n= 78. Patients age at diagnosis ranged from 0 to 25.4 years (median age, 1.1 years). *MYCN* amplification was observed in 93 tumors, while it was absent in 550 tumors (not determined, n= 6). Loss of chromosome 1p were observed in 140 tumors, while the group of patients with normal chromosome 1p status comprised 407 (not determined, n= 102). Neuroblastoma tumors were further classified according to a prognostic gene expression-based classifier (25): favorable, n= 231; unfavorable n= 184; unclassified, n= 234. Primary tumors were localized in the abdomen (n= 135), at the neck/chest (n= 69) or the adrenal glands (n= 276). The primary tumor localization for the remaining 169 patients was unknown. Median follow-up for patients without fatal events was 6.4 years (range, 0.2-18.1 years). The subgroup of patients showing regression of neuroblastoma consisted of 43 infants (localized, n= 14; stage 4S, n= 29), in which the tumor manifestations showed unambiguous regression without any cytotoxic treatment (199). The neuroblastoma subgroups used for methylation and array-based Comparative Genomic Hybridization (aCGH) analysis consisted of 46 and 209 tumors, respectively. Risk group assignment of corresponding patients was performed according to the International Neuroblastoma Risk Group (INRG) classification system (15) (methylation, high-risk, n= 21; intermediate- and low-risk, n= 24; unclassified, n= 1; aCGH, high-risk, n= 56; intermediate- and low-risk, n= 153).

### 3.1.2 Gene expression arrays

Single-color gene expression profiles from 649 neuroblastoma tumors were generated previously in the laboratory of Prof. Dr. Matthias Fischer using customized 4 x 44K 60-mer oligonucleotide microarrays produced by Agilent Technologies (Palo Alto, CA, USA). These microarrays included all probes represented by Agilent's Whole Human Genome Oligo Microarray and all probes of the version V2.0 of the 2 x 11K customized microarray that were not present in the former probe set (25). Annotation files are available through the Gene Expression Omnibus database (Accession ID: GSE45480). Single-color gene expression profiles of neuroblastoma cell lines were generated using the same array platform. Total RNA of *HOXC9* and *GFP*-expressing SK-N-AS and IMR-32 neuroblastoma cells were isolated at 0, 6, 12, 24, 48 and 96 h using TRIZOL reagent (Invitrogen, Karlsruhe, Germany). Integrity of the isolated RNA was assessed using the 2100 Bioanalyzer (Agilent Technologies), and only samples with an RNA integrity number (RIN) of at least 7.5 were considered for further processing. For labeling and hybridization, 1 µg of RNA was linearly amplified and labeled with Cy3 using Agilent's one-color Quick Amp Labeling Kit (Agilent Technologies) following the instructions of the manufacturer's protocol. Then, 1650 ng of Cy3-labeled cRNA was hybridized to the 4 x 44K arrays using Agilent's High-RPM Gene Expression Hyb Kit (Agilent Technologies) according to the manufacturer's protocol. Hybridization was performed for 17 h at 65 °C in a rotating hybridization oven (Robbins Scientific, CA, USA) at 10 rpm according to the company's recommendations. After washing and scanning, resulting TIFF images were processed using Agilent's Feature Extraction software Version 9.5.1 (Agilent Technologies). The quantile normalization method (200) was applied on gene expression raw data. All raw and normalized microarray data are available through the Gene Expression Omnibus database (Accession: GSE45480).

### 3.1.2.1 Analysis of gene expression data

Associations between class I *HOX* mRNA expression levels and neuroblastoma subgroups, prognostic markers and patient outcome were analyzed using single-color gene expression profiles from 649 neuroblastoma tumors. All *HOX* genes were first tested in a univariable Cox regression model based on OS and EFS. For all *HOX* genes with p-values  $\leq 0.05$  the whole cohort (n= 649) was divided into quartiles based on *HOX* gene expression levels. Kaplan-Meier estimates for OS (n= 649) and EFS (n= 628) were compared by log-rank test. In addition, *HOXC9* was investigated separately. The entire set was divided into a training (n= 244) and validation cohort (n=405). The training cohort was divided into quartiles based on *HOXC9* expression levels and these values were applied on the validation cohort as a cut-off for high, intermediate-high, intermediate-low and low *HOXC9* expression. Kaplan-Meier estimates for OS (n= 405) and EFS (n= 384) were compared by log-rank test. Recurrence, progression and death from disease were considered as events. Multivariate Cox proportional hazard models based on EFS and OS were used to analyze the prognostic impact of *HOXC9* expression in neuroblastoma. The factors age (> 18 months vs. < 18 months), tumor stage (stage 4 vs. stage 1-3 and 4S), *MYCN* amplification status (amplified vs. normal) and *HOXC9* expression were fitted into a stepwise-backward selection model.

### 3.1.2.2 *HOX* gene expression-based classification

To develop a *HOX* gene expression-based classifier (*HOX* classifier), the nearest shrunken centroids method (PAM) (201) was applied on *HOX* gene expression data from 75 neuroblastoma patients with maximal divergent clinical outcome (patients who had died of disease despite cytotoxic treatment (n= 22) or survived event free more than 1000 days after diagnosis without cytotoxic treatment (n= 53) (25)). The classification performance in the training set was evaluated by a 10 times repeated 5-fold cross-validation. Probes that were

included in at least 65% of all cross-validation models were selected as classifier probes as recommended by Li *et al.* (202). Classification accuracy of the final *HOX* classifier was assessed in an independent validation set of 574 neuroblastoma patients using the Support Vector Machine (SVM) (203) algorithm. Multivariate Cox proportional hazard models based on EFS and OS were used to analyze the prognostic impact of this classifier. The factors age (< 18 months *vs.* > 18 months), tumor stage (stage 1-3 and 4S *vs.* stage 4), *MYCN* amplification status (normal *vs.* amplified) and *HOX* classifier were fitted into a stepwise-backward selection model.

### **3.1.2.3 Gene Ontology enrichment analyses**

To determine global differences in the expression profiles of *HOXC9* and *GFP*-induced SK-N-AS and IMR-32 cells, mean expression levels of each gene between *HOXC9* induced and control cells were compared. Differentially expressed genes, either up- or down-regulated after *HOXC9* re-expression, were determined by applying a fold-change cut off and unpaired, two-tailed Students t-test. Genes with a fold-change of  $\geq 2$  and p-values  $\leq 0.05$  were considered as significantly differentially regulated in these groups. Gene Ontology Tree Machine (GOTM) (204) was used to identify functional categories associated with the characteristics of the respective cell line. The p-value assigned to the overrepresentation of a specific category was calculated by a hypergeometric test, and results were corrected for multiple testing (Benjamini-Hochberg).

### **3.1.3 Array-based Comparative Genomic Hybridization**

High-resolution oligonucleotide aCGH profiles of 209 neuroblastoma tumors were generated previously (205, 206) using 44 K, 105 K or 1 M microarrays (Agilent Technologies). Array-CGH analysis was performed as described previously (206). The circular binary segmentation

algorithm (207) was applied to allow visualization of the resulting aCGH data by the Integrative Genomics Viewer (IGV) (208). Due to technical reasons, 9 out of 209 aCGH profiles could not be visualized. To evaluate whether chromosomal aberrations on chromosome 12 are associated with de-regulated *HOXC9* expression, I compared the results with corresponding microarray gene expression data of the same tumors using two-tailed nonparametric tests (Kruskal-Wallis).

### 3.2 Statistics

Statistical analysis of associations between *HOX* mRNA expression levels and neuroblastoma subgroups, prognostic markers and outcome was performed using SPSS version 20.0 (IBM). Two-tailed nonparametric tests (Mann-Whitney U, and Kruskal-Wallis test) were used where appropriate. Kaplan-Meier estimates for OS and EFS were compared by log-rank test. Multivariate Cox proportional hazard models based on EFS and OS were used to analyze the prognostic impact of *HOXC9* expression in neuroblastoma. The likelihood ratio test p for inclusion was  $\leq 0.05$  and for exclusion was  $> 0.05$ . Quantitative data for functional analyses were shown as means  $\pm$  SD. Unpaired two-tailed Students t-tests were used where appropriate.

### 3.3 Cell Culture

SK-N-AS and CHP-212 cells were obtained from the American Tissue Culture Collection (ATCC, Manassas, VA, USA), IMR-32 cells were purchased from the German Collection of Microorganisms and Cell Cultures (DSMZ, Braunschweig, Germany). Neuroblastoma cell lines were authenticated at the DSMZ. Neuroblastoma cell lines were maintained in RPMI-1640 (PAA, Coelbe, Germany) supplemented with 10% fetal calf serum (FCS, PAA).

Inducible cell lines were maintained in RPMI-1640 supplemented with 10% Tet-free FCS (PAA), 50 µg/ml G418 (PAA) and 30 µg/ml Hygromycin B (PAA). PT67 packaging cells were obtained from Clontech Laboratories (Clontech Laboratories, Inc., Heidelberg, Germany) and grown in DMEM (PAA) supplemented with 10% FCS. Cells were maintained in a humidified incubator at 37 °C with 5% CO<sub>2</sub> and passaged at 90% confluence using Trypsin-EDTA (PAA). Doxycycline (Sigma-Aldrich, Taufkirchen, Germany) was used to induce transgene expression (2 µg/ml). Neuroblastoma cell lines were shown to be free of mycoplasma by using the Venor® GeM Mycoplasma Detection Kit (Minerva Biolabs, Berlin, Germany) according to the manufacturer's protocol.

### 3.3.1 Neuroblastoma cell line characteristics

To mirror the broad spectrum of neuroblastoma disease, I selected a heterogeneous set of neuroblastoma cell lines for functional studies. Only cell lines which showed loss of *HOXC9* expression were considered for re-expression analyses.

Cell Line	Primary Site	1p Status	<i>MYCN</i> Status	Tumorigenic	AIG Potential	Diff Potential
SK-N-AS (209)	adrenal	del	non amplified	yes	yes	no
IMR-32 (210)	abdomen	del	amplified	yes	yes	yes
CHP-212 (211)	kidney	norm	amplified	no	no	no

**Table 3:** Neuroblastoma cell line characteristics. Abbreviations: del., deletion; norm, normal; AIG, anchorage independent growth; Diff, differentiation.

### **3.3.2 Stable inducible neuroblastoma cell lines**

Polyclonal neuroblastoma cell lines stably expressing either *HOXC9* or *GFP* under the control of the reverse tetracycline-controlled transactivator (rtTA) were generated using the RevTet™ System (Clontech) according to the manufacturer's instructions with marginal modifications. Transduction was carried out using 4 µg/ml Polybrene (Sigma-Aldrich). Transduced cells were selected with Hygromycin B (100 µg/ml) and Geneticin sulfate G418 (150 mg/ml) for 7 days, expanded and assayed for *HOXC9* and *GFP* expression upon doxycycline treatment using western blotting and fluorescence microscopy.

### **3.3.3 *In vitro* growth properties**

#### **3.3.3.1 Trypan blue dye exclusion**

The effect of *HOXC9* expression on cell proliferation was assessed using the trypan blue dye exclusion test. Neuroblastoma cells were seeded in 6-well plates at a density of  $2 \times 10^4$  cells/well in 2 ml RPMI-1640 (10% Tet-free FCS, 2 µg/ml doxycycline). To assure continuous supply of nutrients throughout the measurement interval, 1 ml fresh RPMI-1640 (2 µg/ml doxycycline) per well were added on day 4. Cells were harvested at days 2, 4, 6 and 8 and evaluated for number and viability by trypan blue exclusion using a hemocytometer (C-Chip DHC-N01; Digital Bio Technology Co., LTD, Korea).

#### **3.3.3.2 Cell cycle distribution**

The influence of *HOXC9* expression on cell cycle distribution was investigated by fluorescence-activated cell sorting (FACS) analysis. Flow cytometric analyses were performed using a PAS II flow cytometer (Partec, Muenster, Germany) equipped with a mercury vapor lamp 100 W and a filter combination for 2,4-diamidino-2-phenylindole

(DAPI) stained single cells. Neuroblastoma cells were seeded in 10 cm cell culture dishes at a density of  $1 \times 10^6$  cells/dish in 8 ml RPMI-1640 (10% Tet-free FCS, 2  $\mu\text{g/ml}$  doxycycline). To ensure continuous supply of nutrients throughout the measurement interval, 4 ml fresh RPMI-1640 (2  $\mu\text{g/ml}$  doxycycline) per well were added on day 4. Cells were harvested at days 2 and 7 using Versene and were treated with citric acid/Tween 20 solution according to the method of Otto (212). A phosphate buffer containing DAPI for staining the cell suspension ( $0.25 \times 10^6$  cells/ml) was used. Each histogram, depicting the DNA index and cell cycle distribution, represents  $3 \times 10^4$  -  $9 \times 10^4$  cells. The Multicycle program (Phoenix Flow Systems, CA, USA) was used for histogram analyses.

Solutions	Compounds	
Versene	EDTA in PBS (pH 7.2)	10 mM
Citric Acid Solution	Citric Acid Tween 20 in ddH <sub>2</sub> O	1 mM 0.5%
DAPI Staining Solution	Na <sub>2</sub> HPO <sub>4</sub> x 2H <sub>2</sub> O (pH 8) DAPI in H <sub>2</sub> O	250 mM 1 mM

**Table 4:** Solutions for cell cycle analyses.

### 3.3.3.3 Anchorage independent growth

Soft agar assays were used to assess the effect of Hox-C9 on colony formation ability of neuroblastoma cells. Transgene-induced cells ( $1 \times 10^4$  cells/well) were mixed with culture medium containing 0.8% ultra-low gelling temperature agarose (Sigma-Aldrich) with doxycycline (2  $\mu\text{g/ml}$ ) and plated on a pre-solidified layer of the same media containing 1% agarose in 12-well plates. One additional ml of culture media containing doxycycline

(2 µg/ml) was added after solidification to the top layer, and cells were incubated for 2-3 weeks at 37 °C. Media covering the agar was refreshed every 2-3 days with fresh doxycycline-containing media. Colonies were stained using 0.005% crystal violet (Invitrogen). Images were obtained with a JVC KY-F75U 3-colour CCD camera-equipped Leica DM IL LED microscope (Leica Biosystems, Wetzlar, Germany) using DISKUS Imaging software (Hilgers, Koenigswinter, Germany) and a standard digital camera.

<b>Soft Agar Media</b>	<b>Compounds</b>	
Base Agar	Ultra-low gelling temp. agarose	1%
	Tet-free FCS in RPMI-1640	10%
	Doxycycline	2 µg/ml
Top Agar	Ultra-low gelling temp. agarose	0.8%
	Tet-free FCS in RPMI-1640	10%
	Doxycycline	2 µg/ml
Media covering Agar	Tet-free FCS in RPMI-1640	10%
	Doxycycline	2 µg/ml

**Table 5:** Solutions for anchorage-independent growth analyses. Abbreviation: temp., temperature.

### 3.3.4 Cell viability analyses

#### 3.3.4.1 TUNEL assay

The terminal deoxynucleotidyl transferase (TdT)-mediated dUTP Nick End Labeling (TUNEL) analysis was performed using the In Situ Cell Death Detection Kit according to the manufacturer's protocol (Roche, Mannheim, Germany). Cells were plated, induced for transgene expression (2 µg/ml) and were harvested at days 2 and 7 using Trypsin-EDTA. Cells were spotted on cytospin slides ( $3 \times 10^4$  cells/slide), fixed with 4% paraformaldehyde for 1 h at room temperature, washed with PBS (pH 7.2) and permeabilized on ice for 2 min using Triton X-100/sodium citrate. After washing with PBS, fragmented DNA was detected

in apoptotic cells by adding TMR red dUTP to nicked ends of DNA (In Situ Cell Death Detection Kit, Roche). Slides were incubated for 1 h at 37 °C in the dark and washed with PBS three times. The slides were sealed with fluorescent mounting medium (Dako, Hamburg, Germany). Red-fluorescent, TUNEL-positive cells were counted manually using a fluorescence microscope (Leica DMRA). Total cell numbers in each field were determined by DAPI staining.

<b>Solutions</b>	<b>Compounds</b>	
Washing Buffer	PBS (pH 7.4)	
Fixation Solution	Paraformaldehyde in PBS (pH 7.4)	4%
Permeabilization Solution	Triton X-100	0.1%
	Sodium Citrate in ddH <sub>2</sub> O	0.1%
DAPI Staining Solution	DAPI in PBS (pH 7.4)	1 mM

**Table 6:** Solutions for TUNEL analyses.

### 3.3.4.2 Annexin-V binding assay

Surface exposure of phosphatidylserine by apoptotic cells was measured using APC-coupled Annexin-V and 7-AAD (BD Biosciences, Heidelberg, Germany). Cells were seeded in 10 cm cell culture dishes at a density of  $1 \times 10^6$  cells/dish in 8 ml RPMI-1640 (10% Tet-free FCS, 2 µg/ml doxycycline) and were harvested at days 2 and 7 using Trypsin-EDTA. Cells were washed twice with cold PBS (4 °C), dissolved in Annexin-V binding buffer (BD) at a concentration of  $1 \times 10^5$  cells/ml and stained with APC-coupled Annexin-V and 7-AAD for 15 min at RT according to the manufacturer's protocol. Apoptotic cells were detected by FACS (FACS Canto, BD) using DIVA software (BD).

### 3.3.4.3 Hypoploidy assay

The extent of DNA fragmentation was evaluated in a hypoploidy assay as described elsewhere (213). In brief, cells were seeded in 10 cm cell culture dishes at a density of  $1 \times 10^6$  cells/dish in 8 ml RPMI-1640 (10% Tet-free FCS, 2  $\mu\text{g/ml}$  doxycycline), harvested at days 2 and 7 using Trypsin-EDTA and dissolved in PBS at a density of  $2.5 \times 10^4$  cells/ml. Cells were stained by adding 500  $\mu\text{l}$  Nicoletti-Buffer to 200  $\mu\text{l}$  of this cell suspension. The propidium iodide (PI) fluorescence of individual nuclei was measured by FACS (FACS Canto, BD) using DIVA software (BD).

Solution	Compounds	
Nicoletti Staining Solution	Sodium-Citrate	0.1%
	Triton X-100	0.1%
	PI	50 $\mu\text{g/ml}$

**Table 7:** Nicoletti staining solution for hypoploidy analyses.

### 3.3.5 *In vivo* growth properties

A total of 32 six-week-old female athymic nude-Foxn1<sup>nu</sup> mice (Harlan Laboratories, An Venray, Netherlands) were used for the establishment of neuroblastoma xenograft tumors (Permission ID: 8.87-50.10.37.09.300; LANUV NRW, Germany). Neuroblastoma cells were induced for transgene expression by applying 2  $\mu\text{g/ml}$  doxycycline to the culture media, harvested 48 h post induction at 90% confluence using Trypsin-EDTA, and suspended in matrigel (BD). Eight mice per group were inoculated subcutaneously in the flank with either  $2.5 \times 10^7$  IMR-32 cells or  $1.7 \times 10^7$  SK-N-AS cells in 200  $\mu\text{l}$  matrigel. All mice were fed doxycycline-containing food (SSNIFF, Soest, Germany) throughout the experiment, starting 7 days before inoculation. Tumor volume (V) was calculated by using the formula  $V = (\text{length} \times \text{width} \times \text{depth}) / 2$ . Mice were sacrificed when the tumor reached a volume of about  $1 \text{ cm}^3$  or

after 35 days post inoculation. Tumors were weighed and analyzed by western blotting for Hox-C9 expression and by pathological evaluation after staining with Meyer's hematoxylin and eosin using the Leica ST4040 linear staining system (Leica Biosystems). In addition, the impact of Hox-C9 on already established neuroblastoma tumors was investigated using SK-N-AS cells. Either  $1.7 \times 10^7$  SK-N-AS *HOXC9*-Off or SK-N-AS *GFP*-Off cells were suspended in 200  $\mu$ l matrigel respectively and inoculated subcutaneously in the flank of athymic Nude-Foxn1<sup>nu</sup> mice (6/group). *HOXC9* or *GFP* gene expression was induced after the tumor had reached a mean tumor volume of  $144 \pm 41 \text{ mm}^3$  ( $120 \pm 25 \text{ mm}^3$  in SK-N-AS *GFP* tumors and  $174 \pm 36 \text{ mm}^3$  in SK-N-AS *HOXC9* tumors) by switching from standard diet to doxycycline containing diet. Mice were sacrificed when the tumor reached a volume of  $1 \text{ cm}^3$  or after 35 days post inoculation. Tumors were weighed and analyzed by western blotting for Hox-C9 expression and by pathological evaluation after staining with Meyer's hematoxylin and eosin using the Leica ST4040 linear staining system (Leica Biosystems).

## 3.4 Molecular Biology

### 3.4.1 RNA isolation

Total RNA was isolated using the TRIZOL reagent following the instructions of the supplier (Invitrogen). Either 30 mg tumor material or  $1 \times 10^6$  cells were suspended in 1 ml TRIZOL. After samples were homogenized in homogenization tubes prefilled with ceramic beads (Precellys Ceramic Kit 1.4 mm, Peqlab, Erlangen, Germany) using the FastPrep FP120 cell disrupter (Qbiogene Inc., Carlsbad, CA, USA), 200  $\mu$ l chloroform were added and the suspension was thoroughly mixed. The reaction tubes were centrifuged (12000 g, 10 min, 4 °C), the upper phase was removed, mixed with 500  $\mu$ l isopropanol (100%) and 3  $\mu$ l Glycogen, incubated for 10 min at RT and centrifuged again (12000 g, 10 min, 4 °C) to

precipitate the RNA. The pellet was washed with 500  $\mu$ l ethanol (70%), centrifuged (7500 g, 5 min, 4 °C) and dried at RT for 5 minutes. After dissolving the pellet in 10-50  $\mu$ l of nuclease-free water (USB, High Wycombe, UK), RNA concentrations were quantified by using the NanoDrop ND-1000 spectrophotometer (NanoDrop Technologies, North Carolina, USA). RNA integrity was assessed using the RNA 6000 Nano Kit (Agilent Technologies) according to the manufacturer's protocol by using the 2100 Bioanalyzer (Agilent Technologies).

### **3.4.2 DNA isolation**

Genomic DNA was isolated using the Genra Puregene Tissue Kit following the instructions of the supplier (Qiagen, Hilden, Germany). DNA concentrations were quantified by using the NanoDrop ND-1000 spectrophotometer (NanoDrop Technologies).

### **3.4.3 cDNA synthesis**

First strand cDNA was synthesized in a total volume of 21  $\mu$ l using 2  $\mu$ g of total RNA, 500 ng of oligo-(dT12–18)-primers (Invitrogen) and SuperScript II reverse transcriptase according to the manufacturer's protocol (Invitrogen). In brief, 2  $\mu$ g of total RNA were diluted in nuclease-free water (USB) to a volume of 11  $\mu$ l, oligo-(dT12–18)-primers (1  $\mu$ l of 0.5  $\mu$ g/ml) and dNTP's (1  $\mu$ l, 10 mM each) were added and the solution was incubated at 65 °C for 5 min and then quickly chilled on ice. Next, a reaction mix consisting of 4  $\mu$ l 5 x First Strand Buffer (Invitrogen), 2  $\mu$ l DTT (0.1 M, Invitrogen) and 1  $\mu$ l RNasin (40 U/ $\mu$ l, Promega) was pooled with the RNA/primer mixture and incubated for 2 min at 42 °C. SuperScript II reverse transcriptase (1  $\mu$ l, 200 U/ $\mu$ l, Invitrogen) was added to the reaction mix. The Reverse Transcriptase was allowed to synthesize the cDNA in an incubation step at 42 °C for 2 h

followed by a denaturation step at 70 °C for 15 min. Un-transcribed RNA was digested by adding 1 µl *E. coli* RNase H (Invitrogen, 2 units) and incubation at 37 °C for 20 min.

Reaction Mix		Temperature	Time
RNA (2 µg)	11 µl	65 °C	5 min
Oligo-dT Primers (0.5 µg/ml)	1 µl	→ Ice	1 min
dNTP's (10 mM each)	1 µl		
First Strand Buffer (5 x)	4 µl	42 °C	2 min
DTT (0.1 M)	2 µl		
RNasin (40 U /µl)	1 µl		
SuperScript II reverse transcriptase (200 U/µl)	1 µl	42 °C	2 h
		70 °C	15 min
RNase H (2 U/µl)	1 µl	37 °C	2 min

**Table 8:** cDNA synthesis.

### 3.4.4 Whole Genome Amplification

WGA (whole genome amplified) DNA of purified genomic DNA from primary neuroblastoma specimens and neuroblastoma cell lines was generated using the REPLI-g Kit according to the manufacturer's protocol (Qiagen). DNA concentrations were quantified by using the NanoDrop ND-1000 spectrophotometer (NanoDrop Technologies).

### 3.4.5 Quantitative real-time reverse transcriptase-polymerase chain reaction

For quantitative real-time reverse transcriptase-polymerase chain reaction (qRT-PCR) analysis cells were harvested, washed once with PBS, and subsequently used for RNA isolation and cDNA synthesis. Quantitative RT-PCR was performed using the SYBR Green I reagent on the ABI PRISM 7700 sequence detection system (Applied Biosystems, Foster

City, CA). Quantitative RT-PCR reactions were performed in a total volume of 30  $\mu$ l containing 26.8  $\mu$ l of 1 x SYBR Green PCR master mix (Applied Biosystems), 0.4  $\mu$ l undiluted first strand cDNA, and 1.4  $\mu$ l of 2.5  $\mu$ M forward and reverse primer (Invitrogen) each. To enable calculation of relative expression levels, serial cDNA dilutions (undiluted, 1:5, 1:25, and 1:125) were used for the generation of standard curves of each gene separately. Oligonucleotides hybridizing specifically to corresponding sequences of control genes *HPRT1* and *SDHA* as well as target genes served as primers in PCR reactions (Table 10). Oligonucleotides were selected in successive exons (intron-spanning) for each gene to avoid amplification of contaminating genomic DNA. Quantitative RT-PCR reactions were performed in duplicates using 96-well optical reaction plates with optical caps (Applied Biosystems). Cycling conditions consisted of a single incubation step at 95 °C for 10 minutes, followed by 45 cycles of 15 seconds at 95 °C, 30 seconds at 60 °C and 30 seconds at 72 °C. To evaluate amplification of nonspecific products, aliquots of each reaction mixture were analyzed by agarose gel electrophoresis.

<b>qRT-PCR</b>					
<b>Reaction Mix</b>		<b>Thermal Profile</b>	<b>Temp</b>	<b>Time</b>	<b>Cycle Number</b>
Forward Primer (2.5 $\mu$ M)	1.4 $\mu$ l	Initial Denaturation	95 °C	10 min	1 x
Reverse Primer (2.5 $\mu$ M)	1.4 $\mu$ l	Denaturation Annealing Elongation	95 °C	15 sec	} 45 x
Template cDNA	0.4 $\mu$ l		60 °C	30 sec	
1 x SYBR Green PCR	26.8 $\mu$ l		72 °C	30 sec	
Master Mix					

**Table 9:** qRT-PCR reaction. Abbreviation: Temp, temperature.

qRT-PCR Primer			
Gene Symbol	UCSC Annotation	Primer Sequence	Dir
BAX	chr19:49458117-49464519	5'-CATGTTTTCTGACGGCAACTTC-3' 5'-AGGGCCTTGAGCACCAGTTT-3'	for rev
BCL-2	chr18:60790579-60986613, complement	5'-TCGCCCTGTGGATGACTGA-3' 5'-CAGAGACAGCCAGGAGAAATCA-3'	for rev
REST	chr04:57775079-57802010	5'-AGCTACATGTGAACCCACGGCA-3' 5'-TCAGGCAAGTCAGCCTCTCGT-3'	for rev
PTN	chr07:136912092-137028546, complement	5'-ACAATGCCGAATGCCAGAAG-3' 5'-ACAGGTGACATCTTTTAATC-3'	for rev
NNAT	chr20:36149607-36152090	5'-TCGGCTGAACTGCTCATC-3' 5'-CGAAAAGCGAATCCTAC-3'	for rev
NTRK1	chr01:1567830671-156851642	5'-GAGTGGTCTCCGTTTCG-3' 5'-GTAAGGAGAGGCCCTG-3'	for rev
NGFR	chr17:47572655-47592382	5'-ACAACCTCATCCCTGTCTATTGCT-3' 5'-TGTTCCACCTCTTGAAGGCTATG-3'	for rev
OPHN1	chrX:67262186-67653299, complement	5'-GCGATAGTTAGCTCTCCCTG-3' 5'-CATAACACTTGAGCCTCT-3'	for rev
DNER	chr02:230222345-230579286, complement	5'-AGTCTCAGTGGATTCACCTG-3' 5'-CGTTGTTCTGGCACGGAG-3'	for rev
CD44	chr11:35160417-35253949	5'-CACCATGGACAAGTTTTGG-3' 5'-CACGTGGAATACACCTGCAA-3'	for rev
SNPH	chr20:1246960-1289971	5'-AGCAGCAATTCTGGCTCCTA-3' 5'-GTCCTGTGTGTCCTTCAGC-3'	for rev
NEFM	chr08:24771274-24776606	5'-TATAGAAATCGCTGCGTACAG-3' 5'-GGGTCGGTGTGTATACAGTG-3'	for rev
NEFL	chr08:24808469-24814131, complement	5'-CTCTGAAGGAGAAGCCGAGG-3' 5'-TTCAGACTCTTCCTTGGCAG-3'	for rev
MAP2	chr02:210444403-210598834	5'-GTCATCATGTACCTGGAGG-3' 5'-ATGCCACGCTGGATCTGCCT-3'	for rev
NTS	chr12:86268073-86276770	5'-CATGAAGAGGAGCTTGTTC-3' 5'-TATTCTCATAACAGCTGCCGTT-3'	for rev
SDHA	chr05:218356-256815	5'-TGGGAACAAGAGGGCATCTG-3' 5'-CCACCACTGCATCAAATTCATG-3'	for rev
HPRT1	chrX:133594175-133634698	5'-TGACACTGGCAAACAATGCA-3' 5'-GGTCCTTTTCACCAGCAAGCT-3'	for rev

**Table 10:** qRT-PCR primers. Chromosomal positions are given according to hg 19 assembly at the UCSC Genome Browser. Abbreviations: for, forward; rev, reverse; Dir, Direction.

### 3.4.6 Methylation analysis

*HOXC9* promoter methylation analyses were performed by Sequenom Inc. (Hamburg, Germany) as described elsewhere (214). Genomic DNA was isolated from primary

neuroblastoma specimens and neuroblastoma cell lines (Puregene Blood Core Kit B; Qiagen) and modified by sodium bisulphite using the EZ-96 DNA methylation kit according to the manufacturer's protocol (Zymo Research, Orange, CA, USA). Selected DNA regions located in the *HOXC9* promoter region were amplified by PCR using reverse primers that incorporate the T7 promoter sequence for *in vitro* transcription. PCR primers were designed by using Methprimer ([www.urogene.org/methprimer/](http://www.urogene.org/methprimer/)). Sequenoms MassARRAY platform based on MALDI-TOF mass spectrometry in combination with RNA base-specific cleavage (MassCLEAVE) were used for quantitative methylation analysis. Mass spectra were obtained by using a MassARRAY Compact MALDI-TOF (Sequenom). EpiTyper software 1.0 (Sequenom) was used to generate spectra's methylation ratios.

<b>Methylation Analysis Primer</b>				
<b>Ampl</b>	<b>Amplicon Size (bp)</b>	<b>CpG Sites</b>	<b>Primer Sequence</b>	<b>Dir</b>
1	281	9	5'-ATGGGTATAGGGGTTTTTTAGATGA-3'	for
			5'-TCTACTCACAAAACAATCAAATCAA-3'	rev
2	339	17	5'-TTTTAGTTTATTTGAGAAGTTTTTGTGTT-3'	for
			5'-CCCTACTACTCCTAAAAAAAATACATACA-3'	rev

**Table 11:** Primers for methylation analysis. Abbreviations: Ampl, amplicon; Dir, direction; for, forward; rev, reverse.

### 3.4.7 Sequencing

#### 3.4.7.1 Sequencing of the *HOXC9* locus in neuroblastoma tumors and cell lines

Sequencing was performed by Beckman Coulter Genomics (Danvers, MA, USA). WGA DNA of purified genomic DNA from primary neuroblastoma specimens and neuroblastoma cell lines was generated using the REPLI-g Kit according to the manufacturer's protocol (Qiagen). Amplicons covering the first 500 nucleotides upstream of the *HOXC9*

transcriptional start site, 5' UTR, 3' UTR, exon 1 and exon 2 with exon/intron boundaries were designed using Beckman Coulter Genomics Linux-based amplicon design software. M13 tail sequences were added to the PCR primers. Sanger sequencing of the genomic region of *HOXC9* were performed using BigDye Terminator v3.1 chemistry (Applied Biosystems) and sequences were delineated using an ABI PRISM 3730xl DNA Analyzer (Applied Biosystems).

<b>Amplification Primers</b>			
<b>Ampl</b>	<b>Ampl (bp)</b>	<b>Primer Sequence</b>	<b>Dir</b>
1	580	5'-GTAAAACGACGGCCAGTGGCCAGTGGCAGAAGAACG-3'	for
		5'-CAGGAAACAGCTATGACCAATACGGCGCGGATCAATGC-3'	rev
2	549	5'-GTAAAACGACGGCCAGTCTGCTTATGGGTGGACATGG-3'	for
		5'-CAGGAAACAGCTATGACCACGACGTGCTGAACACTGC-3'	rev
3	535	5'-GTAAAACGACGGCCAGTGGACTCGCTCATCTCTCACG-3'	for
		5'-CAGGAAACAGCTATGACCCCGGTTGTAAAGGAAAATTG-3'	rev
4	590	5'-GTAAAACGACGGCCAGTCGTCACTACGCCCTCAAGC-3'	for
		5'-CAGGAAACAGCTATGACCAGTGTCCCTCACCTCTTC-3'	rev
5	599	5'-GTAAAACGACGGCCAGTGGAGACAGGTTGGGAGAGG-3'	for
		5'-CAGGAAACAGCTATGACCCCTGTGCAATCCTCAGAAGG-3'	rev
6	598	5'-GTAAAACGACGGCCAGTGATTGAGAATGGGGATCAGG-3'	for
		5'-CAGGAAACAGCTATGACCGAATCCCTAAACCCCTCACCC-3'	rev
7	552	5'-GTAAAACGACGGCCAGTCACTGGAGGCCAAACAGG-3'	for
		5'-CAGGAAACAGCTATGACCCCAAATGCAATAACTGAAC-3'	rev
8	537	5'-GTAAAACGACGGCCAGTAGGGGCTTTGATAGCTTTGG-3'	for
		5'-CAGGAAACAGCTATGACCTGTGGGGTTTTTGTTTTTCC-3'	rev
9	600	5'-GTAAAACGACGGCCAGTCCGGGTTCTCAATCTCACC-3'	for
		5'-CAGGAAACAGCTATGACCCAGCCCTCACCCCTCAGC-3'	rev
10	543	5'-GTAAAACGACGGCCAGTGAGAAACTGCGTTCTTTCC-3'	for
		5'-CAGGAAACAGCTATGACCAGAAGGAGCCATTCTCTGG-3'	rev

**Table 12:** Primers for Amplification. Abbreviations: Ampl, amplicon; for, forward; rev, reverse; Dir, direction.

### 3.4.7.2 Sequencing of Plasmid DNA

Sequencing reactions were performed using the BigDye Terminator v3.1 Cycle Sequencing Kit (Applied Biosystems) according to the method of Sanger (215). Sequences were delineated at the Cologne Centre of Genomics (Cologne, Germany) using an ABI PRISM

3730 DNA Analyzer (Applied Biosystems). Sequencing data were evaluated using Chromas Lite 2.01 software (Technelysium Pty Ltd, Queensland, Australia).

Sanger Sequencing					
Reaction Mix		Thermal Profile	Temp	Time	Cycle No
Primer (2.5 $\mu$ M)	0.5 $\mu$ l	Initial Denaturation	95 $^{\circ}$ C	5 min	1 x
Template DNA (60-80 ng)	1.0 $\mu$ l	Denaturation	96 $^{\circ}$ C	10 sec	} 35 x
5 x Sequencing Buffer	2.0 $\mu$ l				
Big Dye Reaction Mix	2.5 $\mu$ l				
ddH <sub>2</sub> O	4.0 $\mu$ l	Elongation	60 $^{\circ}$ C	4 min	

**Table 13:** Sanger sequencing reaction. Abbreviations: Temp, temperature; No, number.

### 3.4.8 Retroviral plasmids and cloning procedure

The human *HOXC9* coding sequence was obtained by PCR from the retroviral vector pBIG2r-*HOXC9*, a kind gift of PD Dr. Malte Buchholz (Division of Gastroenterology, University Hospital, Philipps-Universitaet Marburg, Marburg, Germany). The PCR primer sequences were as follows: 5'-CTC AAG CTT TTA GGA CTG CTC CTT GTC-3' (forward) and 5'-CAG GAT CCA CCA TGT CGG CGA CGG GGC CCA TC-3' (reverse), which contained restriction sites for *HindIII* and *BamHI* respectively. The resulting PCR products were purified using the QIAquick gel extraction kit (Qiagen) according to the manufacturer's instructions. The *HOXC9* coding sequence was cloned into the pRevTRE vector (Clontech) using the restriction enzymes *HindIII/BamHI* (NEB, Frankfurt am Main, Germany). The resulting plasmid was purified (NucleoBond Kit PC 500; Macherey-Nagel, Dueren, Germany), and the nucleotide sequence was confirmed by direct sequencing using the BigDye Terminator v3.1 sequencing kit (Applied Biosystems). The control plasmid pRevTRE-*eGFP-PRE* was generated in parallel using the retroviral vector plasmid MP71-*eGFP-PRE* (216) as template. The enhanced *GFP-PRE* element was cloned by blunt end cloning into the

pRevTRE vector using the restriction enzymes *NotI* and *HindIII*. Blunt end polishing was carried out using Vent DNA Polymerase (NEB).

Vector	Description	Ref.
pRevTet-On	MoMuLV based retroviral vector expressing rtTA (Clontech)	(217)
pRevTRE	MoMuLV based retroviral vector (Clontech)	(217)
pBIG2r- <i>HOXC9</i>	bidirectional doxycycline-regulated retroviral vector expressing <i>HOXC9</i>	(218)
pMP71- <i>eGFP-PRE</i>	retroviral vector containing a enhancer element for GFP expression	(216)
pHIT G	VSV-G expression vector	(219, 220)

**Table 14:** Retroviral plasmids.

### 3.4.9 Immunoblotting

Immunoblots were prepared using the NuPAGE electrophoresis system (Novex Mini Cell; Invitrogen) and semi-dry blotting (Biometra, Goettingen, Germany) (221). For each sample, either 10-50 µg of total protein or cytosolic cell extracts were separated by SDS-PAGE in 4%-12% Bis-Tris gels (Invitrogen) and transferred to 0.2 µm nitrocellulose membranes (Invitrogen) by semi-dry blotting. The membranes were blocked with 5% skim milk powder (Heirler Canovis, Radolfzell, Germany) in 0.05% Tween 20/PBS before incubation with primary antibody and horseradish peroxidase-labeled secondary antibody. The antigen-antibody complex was detected either with Visualizer Spray & Glow (Upstate, Schwalbach, Germany) or with Supersignal West Femto (Thermo Fisher Scientific, Braunschweig, Germany). For isolation of cytosolic cell extracts,  $1 \times 10^7$  cells were washed twice with PBS at 4 °C. Cells were resuspended in 50 µl of buffer A and incubated for 20 min on ice for swelling. After addition of mannitol and sucrose to a final concentration of 220 mM

and to 68 mM (buffer B), respectively, cells were cracked by passing through a 27-gauge needle. Cell breakage was verified microscopically using trypan blue exclusion. Membranes were pelleted at 14000 g and 4 °C for 20 min, and the resulting supernatants were recovered (cytosolic extract). Total protein extracts were isolated either with Cell Lysis Buffer (Biovision, Hannover, Germany) or RIPA Buffer supplemented with PMSF and Complete Protease Inhibitor Cocktail (Roche).

<b>Cell Lysis</b>		
<b>Buffer</b>	<b>Compounds</b>	
RIPA Buffer	Nonidet P 40	1.0%
	Sodium Deoxycholate	0.5%
	SDS	0.1%
	in PBS (pH 7.2)	
Cell Lysis Buffer	PMSF	0.02 mM
	Complete Protease Inhibitor Cocktail	1 mM
	in RIPA Buffer	
Buffer A	PIPES (pH 7.0)	50 mM
(Cytosol Extraction Buffer)	KCl	50 mM
	MgCL <sub>2</sub>	2 mM
	EGTA	5 mM
	Cytochalasin B	1 μM
	Complete Protease Inhibitor Cocktail	1 mM
	DTT	1 mM
Buffer B	Mannitol	220 mM
(Cytosol Extraction Buffer)	Sucrose	68 mM

**Table 15:** Cell lysis buffer.

<b>Immunoblotting</b>		
<b>Solutions</b>	<b>Compounds</b>	
MOPS SDS Running Buffer (Invitrogen)	MOPS	50 mM
	Tris-Base (pH 7.7)	50 mM
	EDTA	1 mM
	SDS	0.1%
Tris-Glycine Transfer Buffer	Tris-Base (pH 8.3)	25 mM
	Glycine	150 mM
	Methanol	10%
Blocking/Hybridization Solution	Skim Milk Powder	5%
	Tween 20 in PBS (pH 7.2)	0.05%

**Table 16:** Solutions for immunoblotting.

<b>Hybridization</b>			
<b>Antibodies</b>	<b>Company</b>	<b>Product No</b>	<b>Dilution</b>
anti-HOXC9	Abcam	ab50839	1 : 100
anti-BCL-2	Dako	M0887	1 : 500
Anti-MYCN	Santa Cruz	sc53993	1 : 1000
anti-cleaved Caspase 3 (Asp 175)	NEB	9664	1 : 1000
anti-cleaved Caspase 7 (Asp 198)	NEB	9491	1 : 1000
anti-cleaved Caspase 9 (Asp 330)	NEB	9501	1 : 1000
anti-cleaved Caspase 9 (Asp 315)	NEB	9505	1 : 1000
polyclonal goat anti-mouse (HRP)	Dako	P0447	1 : 1000
polyclonal goat anti-rabbit (HRP)	NEB	7074S	1 : 1000
polyclonal goat anti-rabbit (HRP)	Dako	P0448	1 : 1000
anti-beta-Actin	Abcam	ab8227	1 : 10000

**Table 17:** Antibodies for immunoblotting. Abbreviation: No, number.

### 3.4.10 Immunofluorescence

#### 3.4.10.1 Hox-C9 immunofluorescence

The localization of transgenic Hox-C9 was determined by immunofluorescence. Cells were seeded on Chamber Slides (Nunc, Wiesbaden, Germany), induced for transgene expression (2 µg/ml) and grown for 48 h. Cells were fixed using 4% paraformaldehyde, and

permeabilized for 5 min using Triton X-100 in PBS. After washing thrice using PBS, cells were blocked with 1% BSA in PBS for 30 minutes. Cells were incubated for 1 h with anti-Hox-C9 antibody (1:5 dilution, Abcam) at RT, washed thrice with PBS and incubated for 30 min with TRITC-labeled polyclonal rabbit anti-mouse antibody (1:20 dilution, Dako) at RT. Images were obtained with a JVC KY-F75U 3-colour CCD camera linked to a Leica DMRA microscope (Leica) using DISKUS Imaging software (Hilgers).

---

### Immunofluorescence

---

Solutions	Compounds	
Fixation	Paraformaldehyde in PBS (pH 7.4)	4%
Permeabilization	Triton X-100 in PBS (pH 7.4)	0.2%
Blocking/Hybridization	BSA in PBS (pH 7.4)	1%

**Table 18:** Solutions for immunofluorescence (Hox-C9 staining).

Antibodies	Company	Product No	Dilution
anti-HOXC9	Abcam	ab50839	1 : 5
rabbit anti-mouse IgG (TRITC)	Dako	R 0270	1 : 20

**Table 19:** Antibodies for immunofluorescence. Abbreviation: No, number.

### 3.4.10.2 F-Actin cytoskeleton staining

The F-Actin cytoskeleton of differentiating IMR-32 cells was stained using Rhodamine Phalloidin (Cytoskeleton Inc., Denver, CO, USA). Cells were seeded on Chamber Slides (Nunc), induced for transgene expression (2 µg/ml) and grown for 18-21 days. Cells were fixed using 4% paraformaldehyde and permeabilized for 5 min using 0.5% Triton X-100 in PBS. After washing thrice with PBS, cells were incubated with 0.1 mM Rhodamine Phalloidin for 30 min at RT. After washing thrice with PBS, cells were counterstained with DAPI. Images were obtained with a JVC KY-F75U 3-colour CCD camera linked to a Leica DMRA microscope (Leica) using DISKUS Imaging software (Hilgers).

---

<b>F-Actin staining</b>		
<b>Solutions</b>	<b>Compounds</b>	
Fixation	Paraformaldehyde in PBS (pH 7.4)	4%
Permeabilization	Triton X-100 in PBS (pH 7.4)	0.5%
Rhodamine Phalloidin	Rhodamine Phalloidin in PBS (pH 7.4)	1 mM
DAPI Staining Solution	in PBS (pH 7.4)	1 mM

---

**Table 20:** Solutions for immunofluorescence (F-Actin staining).

## 4. Results

### 4.1 *HOX* gene expression in neuroblastoma

The expression patterns of 39 class I *HOX* genes were examined in 649 neuroblastoma samples by microarray analysis, and the association with prognostic markers and patient outcome was determined. The expression of the majority of *HOX* genes correlated significantly with clinical covariates in neuroblastoma (Table 21). Elevated expression of *HOXD* genes, particularly *HOXD3*, *HOXD8*, *HOXD9* and *HOXD10*, was predominantly associated with unfavorable prognostic markers and poor patient outcome (Table 21, Figures 5 and 6). Similarly, I observed increased expression levels of more posterior *HOX* genes (*HOXA10*, *HOXA11*, *HOXA13*, *HOXC12*, *HOXC13*) in neuroblastomas with unfavorable characteristics (Table 21). In contrast, elevated expression of the majority of the remaining *HOX* genes was significantly correlated with favorable prognostic markers and beneficial outcome (Table 21). *HOX* gene expression values and the association with prognostic markers and patient outcome are available through Kocak *et al.*, Supplementary Table S1 (222).

Probe ID	Gene	Age	Stage	MYCN	1p	PAM	EFS	OS
A_24_P200854	HOXA2							
A_23_P253982	HOXA4							
A_24_P416370	HOXB4							
A_23_P363316	HOXB5							
A_23_P66682	HOXB6							
A_23_P27013	HOXB9							
A_24_P124558	HOXC8_2							
A_23_P398476	HOXC8							
A_23_P25150	HOXC9							
A_24_P218805	HOXC10							
A_23_P36546	HOXC10_2							
A_23_P501538	HOXA3_2							
A_23_P93772	HOXA5							
A_23_P70968	HOXA7							
A_23_P500998	HOXA9							
A_24_P399220	HOXB3_2							
A_23_P316511	HOXB3							
A_23_P55281	HOXB7							
A_23_P370588	HOXB8							
A_23_P389281	HOXA13_2							
A_24_P914411	HOXC6_2							
A_23_P150974	HOXC4							
A_23_P2344	HOXC6							
A_23_P107283	HOXB2_2							
A_23_P82370	HOXA6							
A_23_P111571	HOXA3							
A_24_P77904	HOXA10_2							
A_23_P47941	HOXC11							
A_23_P120243	HOXD1							
A_23_P165796	HOXD13							
A_23_P253368	HOXA10							
A_23_P64808	HOXC13							
A_23_P323180	HOXD3							
A_23_P210164	HOXD8							
A_23_P429383	HOXD9							
A_23_P381368	HOXD10							
A_23_P31306	HOXA13							
A_23_P162355	HOXC5							
A_23_P345725	HOXD4							
A_23_P154420	HOXD12							
A_24_P365015	HOXB13							
A_23_P143029	HOXD11							
A_23_P335981	HOXC12							
A_23_P42706	HOXA11							
A_23_P145752	HOXA1							
A_23_P118675	HOXB1							
A_24_P33077	HOXB2							

**Table 21:** *HOX* gene expression and association with prognostic markers and patient outcome in neuroblastoma. Age (< 18 months vs. > 18 months), stage (localized vs. 4 vs. 4S), *MYCN* amplification status (non amplified vs. amplified), 1p status (normal vs. aberrant), gene expression-based classification (favorable vs. unfavorable). Green, high expression is significantly associated with favorable prognostic markers/outcome (e.g. age < 18 months,  $p < 0.05$ ); red, high expression is significantly associated with unfavorable prognostic markers/outcome (e.g. age > 18 months,  $p < 0.05$ ); grey, no significant association with the corresponding prognostic marker/outcome. HOX\_2, second HOX probe of the corresponding *HOX* gene on the Array.

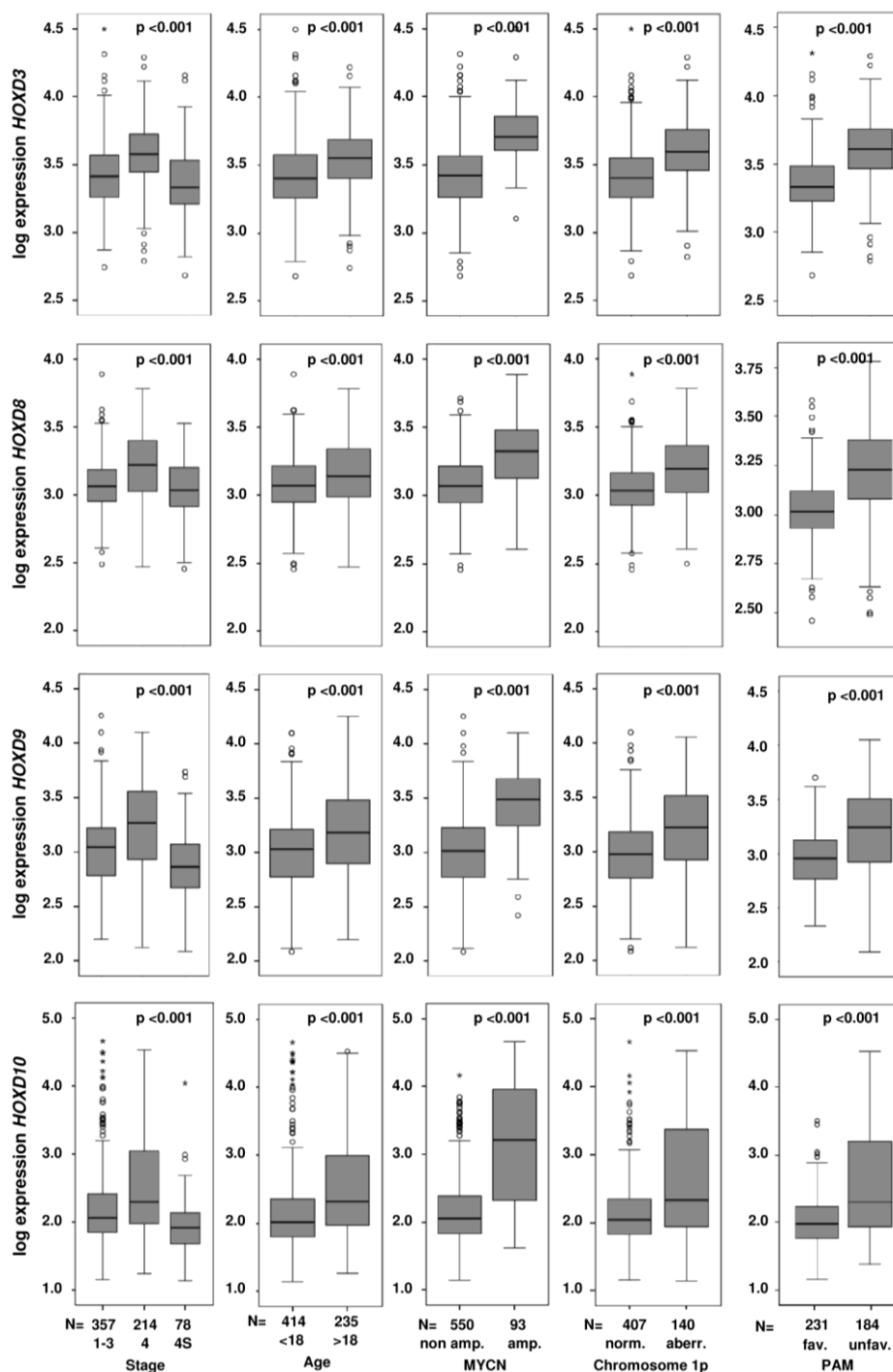


**Figure 5:** Correlation of *HOXD3*, *HOXD8*, *HOXD9* and *HOXD10* expression levels with prognostic markers in neuroblastoma. Association of tumor stage, age at diagnosis, *MYCN* amplification status, chromosome 1p status and gene expression-based classification (PAM classifier) with *HOX* transcript levels in 649 neuroblastoma samples as determined by oligonucleotide-microarray experiments. Boxes, median expression values (horizontal line) and 25th and 75th percentiles; whiskers, distances from the end of the box to the largest and smallest observed values that are less than 1.5 box lengths from either end of the box; open circles, outlying values; asterisks, extreme outlying values. Abbreviations: amp., amplification; norm., normal, aberr., aberration; fav., favorable; unfav., unfavorable.

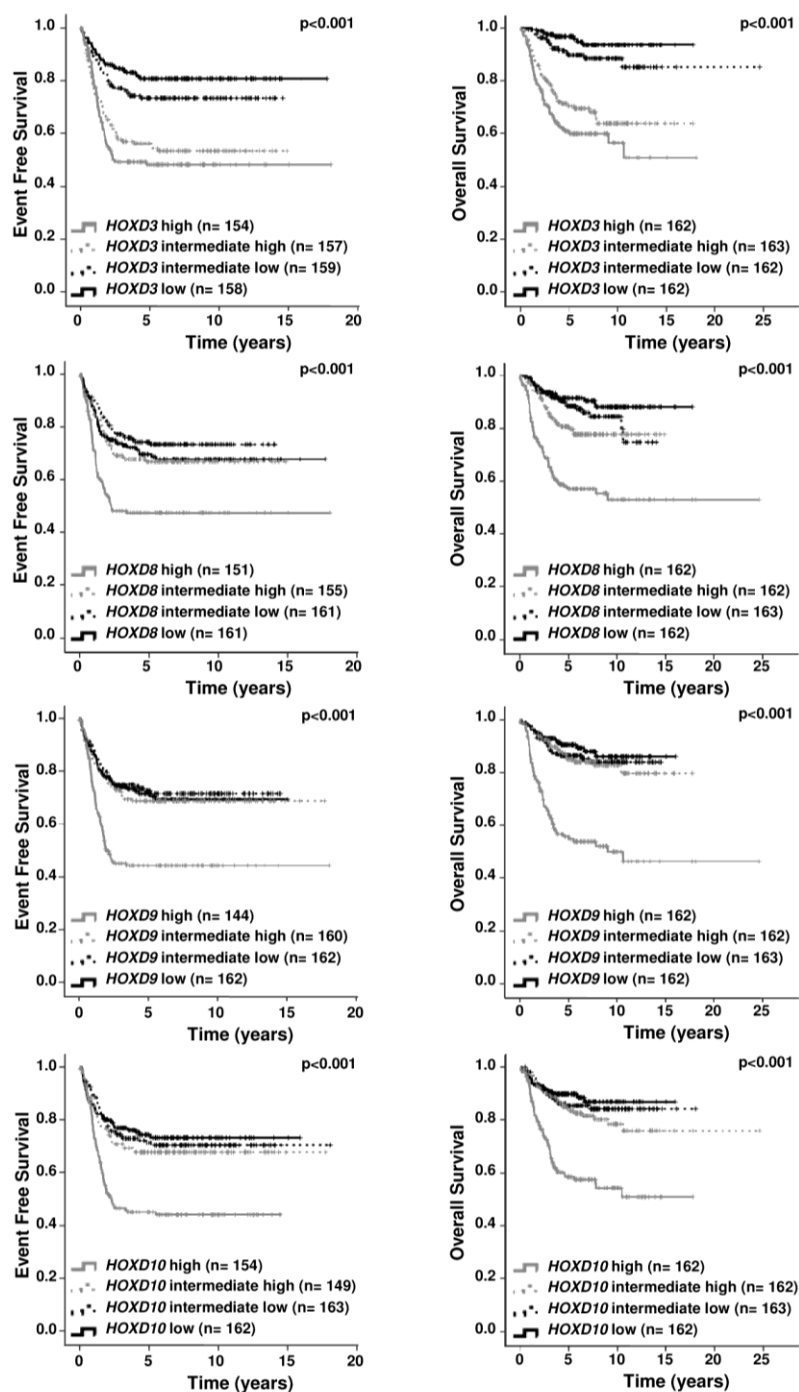


**Figure 6:** Survival of neuroblastoma patients according to expression levels of *HOXD3*, *HOXD8*, *HOXD9* and *HOXD10*. Kaplan-Meier curves show the probability of EFS and OS according to *HOXD3*, *HOXD8*, *HOXD9* and *HOXD10* expression as determined by microarray analysis. “*HOX* high”, “*HOX* intermediate-high”, “*HOX* intermediate-low” or “*HOX* low” indicate patients with *HOX* mRNA levels defined as high (> 75th percentile), intermediate-high (> 50th and < 75th percentile), intermediate-low (< 50 and > 25th percentile) or low (< 25th percentile), respectively.

---

### 4.1.1 Prediction of neuroblastoma outcome based on a *HOX* gene expression-based classifier

To assess the impact of class I *HOX* gene expression on neuroblastoma outcome, we developed a *HOX* gene expression-based classifier (Table 22) using a training cohort of 75 neuroblastoma patients with maximal divergent clinical outcome (as described in Materials and Methods). In the training set, the classification accuracy was 85% as assessed by cross-validation (Table 23). In an independent validation subset of 215 patients who matched the outcome criteria of the training set, the 33 *HOX* gene signature predicted patient outcome with an accuracy of 76% (Table 24). In the entire validation set (n= 574), the classifier accurately discriminated patients with favorable and unfavorable outcome (favorable, n= 265; 5-year EFS  $80.7 \pm 2.6\%$ , 5-year OS  $96.0 \pm 1.2\%$ ; unfavorable, n= 309; 5-year EFS  $49.5 \pm 3.0\%$ , 5-year OS  $67.1 \pm 2.8\%$ ; both  $p < 0.001$ ; Figure 7a and b). In multivariate Cox regression models based on EFS and OS, the *HOX* classifier predicted patient outcome independently from age, stage and *MYCN* amplification status (Table 25).

Probe ID	Gene Symbol	Selection frequency of HOX probes (5CVx10repeats)
A_23_P25150	HOXC9	50
A_24_P218805	HOXC10	50
A_23_P398476	HOXC8	50
A_23_P36546	HOXC10_2	50
A_23_P345725	HOXD4	50
A_23_P150974	HOXC4	50
A_24_P124558	HOXC8_2	50
A_23_P27013	HOXB9	50
A_23_P55281	HOXB7	50
A_23_P389281	HOXA13_2	50
A_23_P429383	HOXD9	49
A_23_P323180	HOXD3	49
A_23_P47941	HOXC11	49
A_24_P77904	HOXA10_2	48
A_23_P107283	HOXB2_2	48
A_23_P500998	HOXA9	48
A_23_P70968	HOXA7	48
A_23_P335981	HOXC12	47
A_23_P381368	HOXD10	47
A_23_P363316	HOXB5	46
A_23_P66682	HOXB6	45
A_23_P210164	HOXD8	45
A_23_P253368	HOXA10	44
A_23_P501538	HOXA3_2	44
A_23_P370588	HOXB8	44
A_24_P416370	HOXB4	44
A_23_P64808	HOXC13	43
A_23_P2344	HOXC6	42
A_24_P200854	HOXA2	42
A_23_P253982	HOXA4	42
A_23_P154420	HOXD12	41
A_24_P365015	HOXB13	40
A_24_P33077	HOXB2	40
A_24_P399220	HOXB3_2	38
A_24_P914411	HOXC6_2	38
A_23_P82370	HOXA6	37
A_23_P93772	HOXA5	36
A_23_P162355	HOXC5	36
A_23_P316511	HOXB3	34
A_23_P31306	HOXA13	32

**Table 22:** HOX classifier probes. Selection frequency of HOX probes in 50 models generated in the iterative cross-validation process. Probes were selected for the final classifier when they were included in at least 65% of the models. HOX\_2, second HOX probe of the corresponding *HOX* gene on the array. Abbreviation: CV, cross validation.

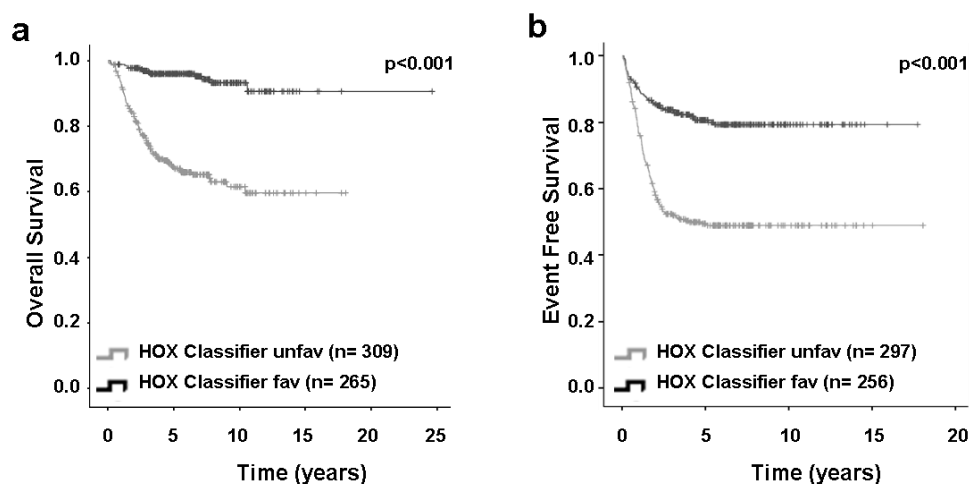


**Figure 7:** Survival curves of neuroblastoma patients according to classification results of the HOX classifier. Kaplan-Meier estimates for (a) OS and (b) EFS of the entire validation set (n= 574) according to classification results of the HOX classifier. Abbreviations: unfav., unfavorable; fav., favorable.

#### Classification performance of the HOX classifier in the training set

Classifier	Patients (N)	Probes (N)	(%)		
			Accuracy	Sensitivity	Specificity
NB_d75_hox52_fsPAM_predSVM	75	52	85	58	96

**Table 23:** Classification performance of the HOX classifier in the training set.

#### Classification performance of the HOX classifier in the selected test set

Classifier	Patients (N)	Probes (N)	(%)		
			Accuracy	Sensitivity	Specificity
NB_d75_hox52_fsPAM_predSVM	215	40	76	63	90

**Table 24:** Classification performance of the HOX classifier in the test set matching the criteria of the training set.

<b>Multivariate Cox regression models for the entire test set based on EFS and OS considering single prognostic markers and the HOX classifier</b>					
<b>Marker</b>	<b>Patients (N)</b>	<b>Available Cases (N)</b>	<b>Hazard Ratio</b>	<b>95% CI</b>	<b>p</b>
<b>Model considering single prognostic markers and the <i>HOX</i> classifier based on EFS</b>					
Age (< 18 months vs. > 18 months)	574	547	2.06	1.48 – 2.87	< 0.001
Stage (1-3, 4S vs. 4)			1.49	1.49 – 2.07	0.018
<i>MYCN</i> status (normal vs. amplified)			1.44	1.44 – 2.03	0.041
HOX classifier (favorable vs. unfavorable)			2.13	1.48 – 3.06	< 0.001
<b>Model considering single prognostic markers and the <i>HOX</i> classifier based on OS</b>					
Age (< 18 months vs. > 18 months)	574	568	4.44	2.61 – 7.53	< 0.001
Stage (1-3, 4S vs. 4)			2.24	1.39 – 3.58	< 0.001
<i>MYCN</i> status (normal vs. amplified)			2.62	1.77 – 3.88	< 0.001
HOX classifier (favorable vs. unfavorable)			3.10	1.67 – 5.76	< 0.001

**Table 25:** Multivariate Cox regression models for the complete test set based on EFS and OS considering single prognostic markers and the HOX classifier. Abbreviation: CI, Confidence Interval.

## **4.2 Elevated *HOXC9* expression is associated with favorable prognostic markers, beneficial patient outcome and spontaneous regression in neuroblastoma**

*HOXC9* was most strongly associated with the clinical neuroblastoma phenotype. Elevated *HOXC9* expression levels strongly correlated with lower stages, age < 18 months at diagnosis, lack of *MYCN* amplification, lack of 1p loss, and favorable gene expression-based classification according to the PAM classifier (Figure 8a). Multivariate Cox regression models based on EFS and OS considering established risk markers (*MYCN* status, tumor stage and patient age at diagnosis) identified *HOXC9* expression as a significant independent prognostic marker for both EFS and OS (Table 26). I also investigated *HOXC9* expression levels in infant neuroblastoma that had regressed without any chemotherapy, and compared these to infant stage 4 neuroblastoma. Notably, *HOXC9* transcript levels were significantly

higher in neuroblastoma showing spontaneous regression (Figure 8b). Furthermore, patients with high *HOXC9* expression levels had a significantly better outcome with a 5-year OS of  $95 \pm 2\%$  as compared to patients with low *HOXC9* expression (5-year OS of  $56 \pm 5\%$ ; Figure 8c). Likewise, *HOXC9* expression levels strongly correlated with EFS (high *HOXC9* expression, 5-year EFS  $82 \pm 4\%$  vs. low *HOXC9* expression, 5-year EFS  $37 \pm 5\%$ ; Figure 8d). Taken together, these results demonstrate that *HOXC9* transcript levels discriminate neuroblastoma patients with favorable and unfavorable outcome and indicate that elevated *HOXC9* expression is associated with spontaneous regression in neuroblastoma.

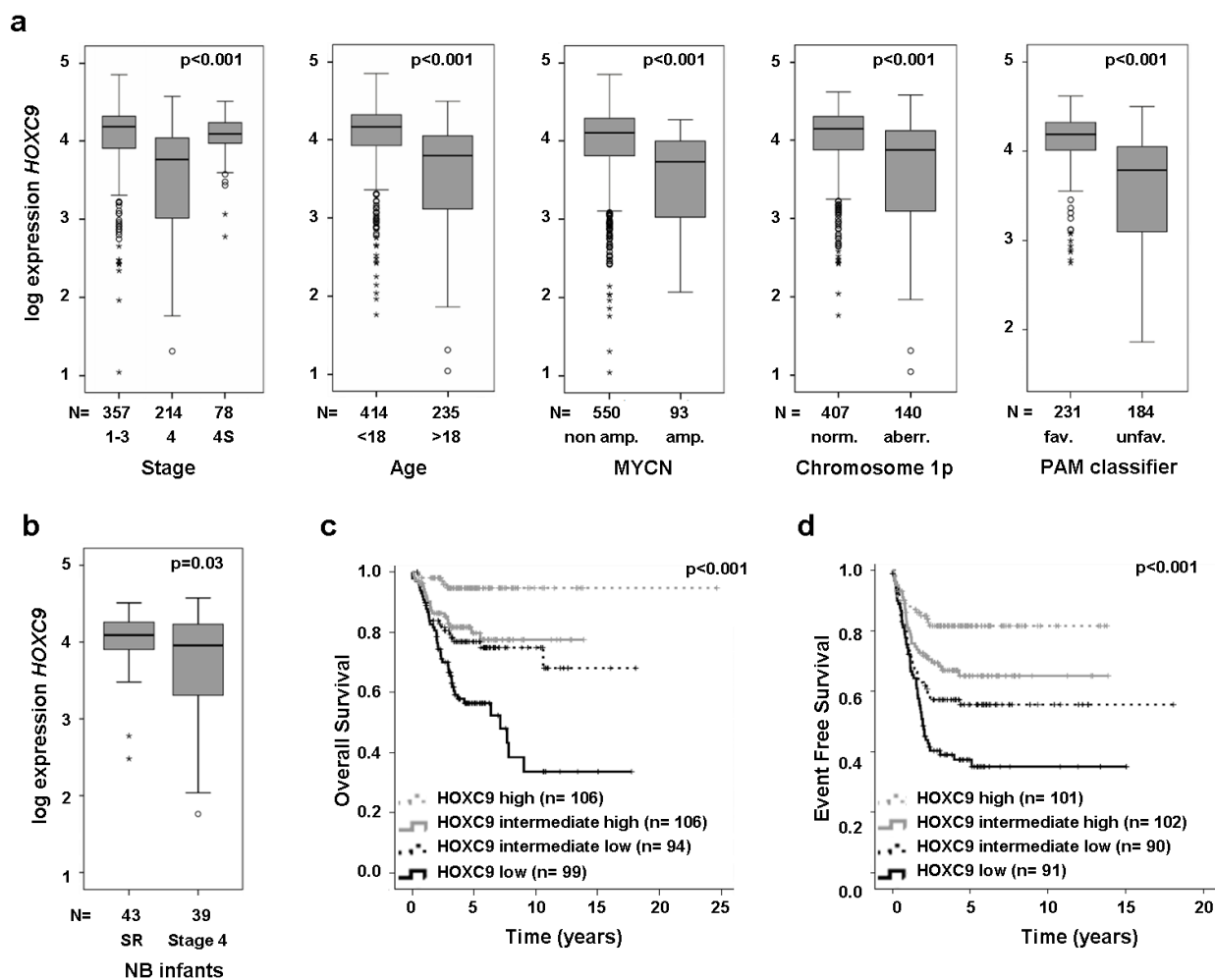


**Figure 8:** Association of *HOXC9* expression with prognostic markers and survival in neuroblastoma. (a) Association of *HOXC9* expression with prognostic markers in 649 neuroblastomas as determined by microarray analysis. PAM classifier, gene expression-based classifier as defined in the main text. Boxes, median expression values (horizontal line) and 25th and 75th percentiles; whiskers, distances from the end of the box to the largest and smallest observed values that are less than 1.5 box lengths from either end of the box; open circles, outlying values; asterisks, extreme outlying values. (b) *HOXC9* expression levels in spontaneously regressing and stage 4 infant neuroblastomas. (c) OS probability of neuroblastoma patients according to *HOXC9* expression. (d) EFS probability of neuroblastoma patients according to *HOXC9* expression. Abbreviations: amp., amplification; norm., normal; aberr., aberration; fav., favorable; unfav., unfavorable; SR, spontaneous regressive; NB, neuroblastoma.

---

**Multivariate Cox regression models based on EFS and OS considering single prognostic markers and *HOXC9* expression**

---

Marker	Patients (N)	Available Cases (N)	Hazard Ratio	95% CI	p
Model considering single prognostic markers and <i>HOXC9</i> expression based on EFS					
Age (> 18 months vs. < 18 months)	649	622	0.48	0.34 – 0.66	< 0.001
Stage (4 vs. 1-3, 4S)			0.52	0.38 – 0.72	< 0.001
<i>MYCN</i> status (amplified vs. normal)			0.57	0.42 – 0.79	0.001
<i>HOXC9</i> expression (continuous)			0.75	0.60 – 0.93	0.012
Model considering single prognostic markers and <i>HOXC9</i> expression based on OS					
Age (> 18 months vs. < 18 months)	649	643	0.24	0.15 – 0.39	< 0.001
Stage (4 vs. 1-3, 4S)			0.33	0.26 – 0.52	< 0.001
<i>MYCN</i> status (amplified vs. normal)			0.32	0.22 – 0.46	< 0.001
<i>HOXC9</i> expression (continuous)			0.73	0.55 – 0.97	0.030

---

**Table 26:** Multivariate Cox regression models based on EFS and OS considering single prognostic markers and *HOXC9* expression. Multivariate Cox regression models based on EFS and OS considering age at diagnosis (> 18 months vs. < 18 months), stage (4 vs. 1-3, 4S), *MYCN* status (amplified vs. normal) and *HOXC9* expression (continuous). Abbreviation: CI, Confidence Interval.

### 4.2.1 Elevated *HOXC9* expression is associated with abdominal neuroblastoma

Since the expression of class I *HOX* genes is not only temporally but also spatially regulated during embryonic development, *HOXC9* expression in neuroblastoma was investigated according to the primary tumor site. I observed significantly higher *HOXC9* expression levels in tumors with abdominal location in comparison to neuroblastomas located at the neck/chest or at the adrenal glands (Figure 9a), which is in line with the embryonal expression pattern of *HOX* genes: *HOX* genes located more 5' in the *HOX* cluster, such as *HOXC9*, are expressed more posterior in the body during development (Figure 4). Analogous expression patterns were observed for *HOXA9*, *HOXA10* and *HOXC10* (Figure 10). The remaining 5' located *HOX* genes showed no significant correlation with the primary tumor localization (Figure 10). Interestingly, the spatial expression pattern of *HOXC9* does not correlate with the general

association of primary tumor sites with patient outcome. In line with previous reports (223-225), I observed a better outcome of patients with neck/chest neuroblastoma in comparison to tumors located at the adrenal glands or in the abdomen (neck/chest vs. adrenal glands vs. abdomen, 5-year EFS,  $84 \pm 5\%$  vs.  $69 \pm 3\%$  vs.  $63 \pm 4\%$ , respectively; 5-year OS,  $97 \pm 2\%$  vs.  $83 \pm 2\%$  vs.  $85 \pm 3\%$ , respectively; Figure 9b and 9c).

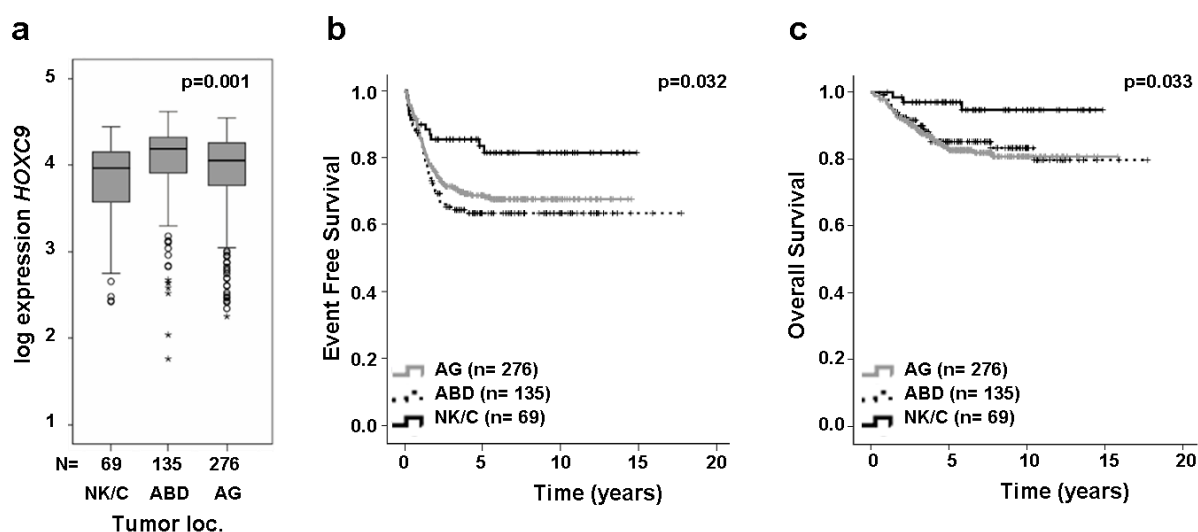


**Figure 9:** Association of *HOXC9* expression with tumor localization and survival of neuroblastoma patients according to the site of primary tumor. **(a)** Association of *HOXC9* expression with tumor localization in 480 neuroblastomas as determined by microarray analysis. Boxes, median expression values (horizontal line) and 25th and 75th percentiles; whiskers, distances from the end of the box to the largest and smallest observed values that are less than 1.5 box lengths from either end of the box; open circles, outlying values; asterisks, extreme outlying values. Survival of neuroblastoma patients. **(b)** EFS and **(c)** OS probability of neuroblastoma patients according to the site of primary tumor. Abbreviations: NK/C, neck/chest; ABD, abdomen; AG, adrenal glands, loc., localization.

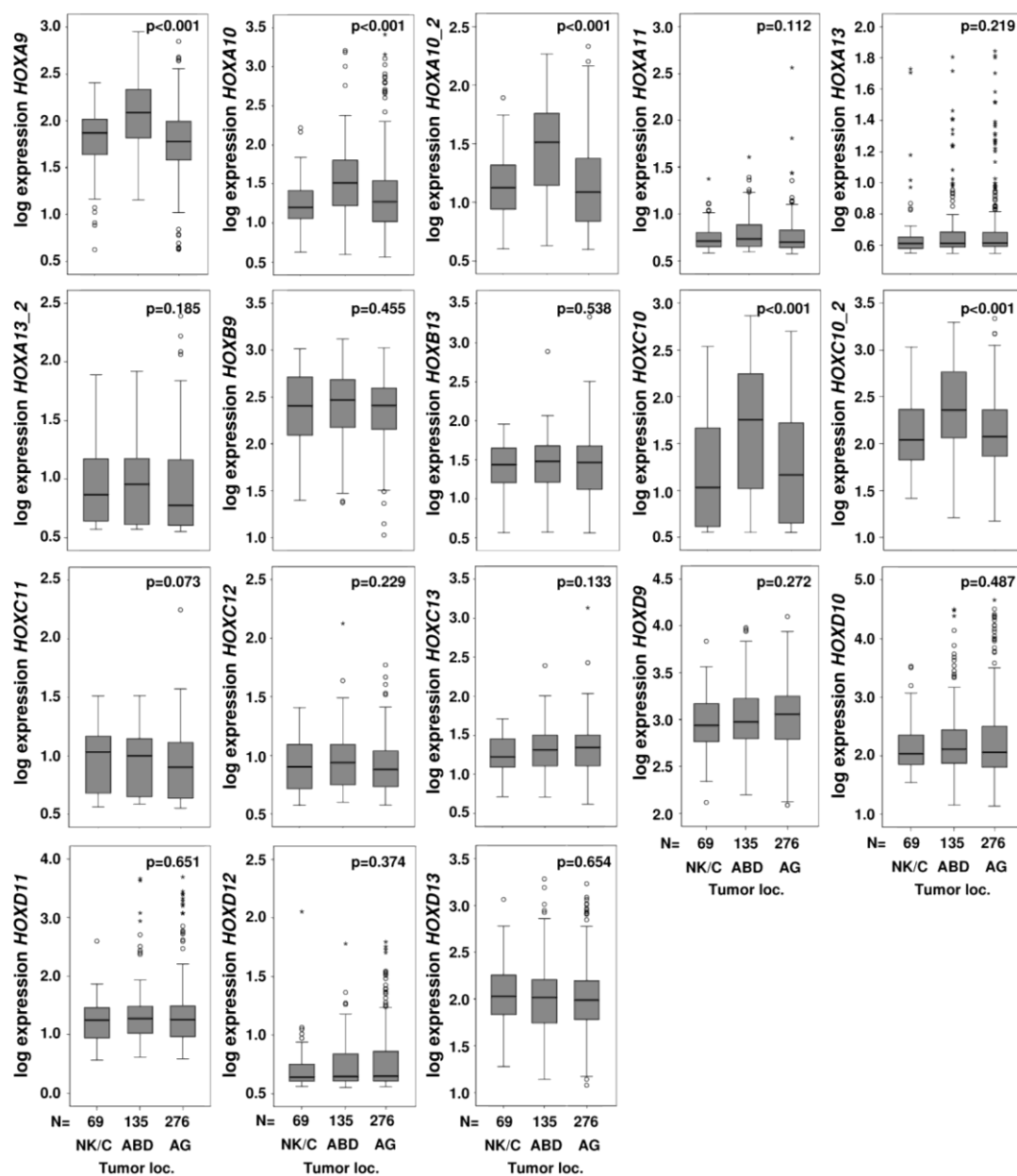


**Figure 10:** Expression of 5' clustered *HOX* genes according to primary tumor localization. Boxes, median expression values (horizontal line) and 25th and 75th percentiles; whiskers, distances from the end of the box to the largest and smallest observed values that are less than 1.5 box lengths from either end of the box; open circles, outlying values; asterisks, extreme outlying values. Abbreviations: NK/C, neck/chest; ABD, abdomen; AG, adrenal glands, loc., localization.

## 4.3 Molecular basis for differential expression of *HOXC9* in neuroblastoma

### 4.3.1 Numerical gain of chromosome 12 correlates with elevated expression of *HOXC9*

I next aimed to evaluate whether genetic or epigenetic aberrations of the *HOXC9* locus (12q13.3) are associated with *HOXC9* expression levels. First, I analyzed aCGH profiles of 209 neuroblastoma samples and compared the results with corresponding microarray gene expression data of the same tumors. Genomic aberrations of chromosome 12 were detected in 92/209 of the samples (44%, Table 27, Figure 11a). I most frequently observed numerical gains of the entire chromosome (n= 64, 30.6%). Numerical chromosome 12 loss occurred in 4 cases. Segmental alterations of chromosome 12 were detected in 24 tumors (11.5%), most of which were segmental gains not affecting the *HOXC9* locus (n= 18, 8.6%). Analysis of *HOXC9* gene expression data revealed significantly higher transcript levels in tumors with numerical chromosome 12 gains in comparison to tumors in which the *HOXC9* locus was not affected by genomic alterations (Figure 11b).

Aberration	Patients (N)
No Aberrations	117
Whole Chromosome gain	64
Whole Chromosome loss	4
Segmental gain ( <i>HOXC9</i> affected)	2
Segmental gain ( <i>HOXC9</i> not affected)	18
Segmental loss ( <i>HOXC9</i> affected)	0
Segmental loss ( <i>HOXC9</i> not affected)	4
Total	209

**Table 27:** Aberrations on chromosome 12 as determined by aCGH.

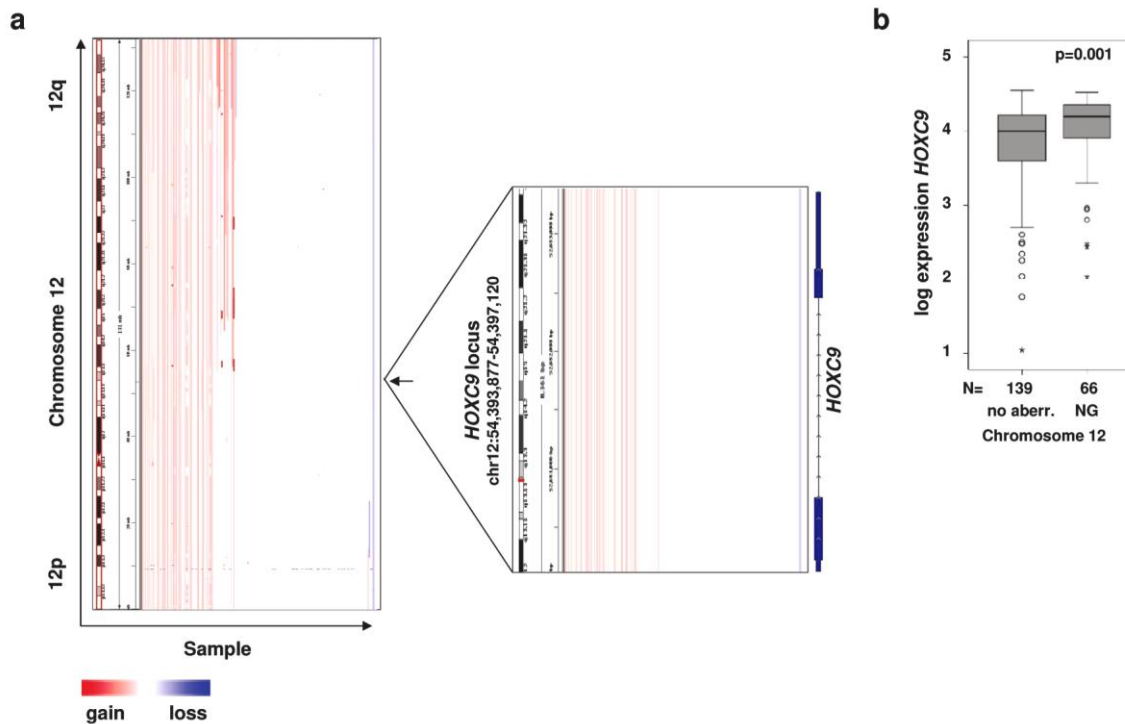


**Figure 11:** Aberrations at chromosome 12 and correlation with *HOXC9* expression. (a) Chromosomal aberrations of the *HOXC9* locus in primary neuroblastomas (n= 200). (b) Association of whole chromosome 12 gain with *HOXC9* expression in primary neuroblastomas. Abbreviations: aberr., aberration; NG, numerical gain.

### 4.3.2 Sequencing of *HOXC9*

To examine whether inactivating mutations might contribute to diminished *HOXC9* expression in neuroblastoma, we sequenced the genomic *HOXC9* locus of 46 primary tumors which showed low *HOXC9* expression. A total of 16 unique sequence variants were detected (Table 28). Eight of these represented known SNP's, while the remaining sequence variants were novel. The latter variants affected either non-coding sequences or were synonymous, and occurred infrequently in our cohort. Together, these data suggest that mutations in the *HOXC9* locus are not a major cause of reduced *HOXC9* expression levels in unfavorable neuroblastoma.

Chromosomal Position	A 1	A 2	REG	DB SNP	AA (A 1)	AA (A 2)	AA CO	AA CD	Freq
chr12:52,679,605	T	A	Intr				0		1
chr12:52,679,904	T	G	Intr				0		1
chr12:52,680,032	G	C	Intr				0		3
chr12:52,680,037	A	G	Intr	56368105			0		29
chr12:52,680,041	G	A	Intr	12817092			0		35
chr12:52,680,050	G	C	Intr	56154542			0		27
chr12:52,680,263	T	C	Cod		Ser	Ser	8	AG_	1
chr12:52,680,551	C	T	Cod	34079606	Val	Val	104	GT_	1
chr12:52,680,764	C	T	Cod	2241820	Ala	Ala	175	GC_	33
chr12:52,680,844	C	A	Intr				0		2
chr12:52,681,051	A	G	Intr	67918869			0		10
chr12:52,682,790	A	G	UTR3				0		1
chr12:52,683,065	A	G	UTR3				0		2
chr12:52,683,165	C	G	UTR3	72033532			0		3
chr12:52,683,238	A	G	UTR3	1867297			0		3
chr12:52,683,242	C	G	UTR3				0		1

**Table 28:** Sequence variations in the genomic region of *HOXC9*. Chromosomal positions are given according to hg 18 assembly at the UCSC Genome Browser. Abbreviations: A, Allele; REG, Region; Intr, intronic; Cod, coding; AA Amino Acid; CO, coordinate; CD, Codon; Freq; Frequency.

### 4.3.3 Methylation pattern of the promoter region of *HOXC9*

To determine whether epigenetic regulation might contribute to differences in *HOXC9* expression in neuroblastoma, we analyzed the methylation status of 26 CpG sites located in the *HOXC9* promoter region. DNA samples from 46 neuroblastoma tumors with differing *HOXC9* expression levels (high and low *HOXC9* expression as defined in Materials and Methods, n= 23 per subgroup) and 2 neuroblastoma cell lines (SK-N-AS and IMR-32) with loss of *HOXC9* expression were analyzed (Table 29). Unsupervised one-way hierarchical clustering of CpG site methylation revealed a largely homogeneous methylation pattern in tumors of both subgroups and cell lines (Figure 12), suggesting that down-regulation of *HOXC9* does not result from differences in CpG methylation patterns.

Design statistics of genomic regions analyzed for methylation	
Number of DNA samples	48
Number of genomic regions	1
Number of amplicons	2
Number of CpG units	26
Median amplicon length	310 bp (min= 281; max= 339)
Median CpG/amplicon	13 CpG/amplicon (min= 9; max= 17)

**Table 29:** *HOXC9* promoter methylation analyses. Design statistics of genomic regions analyzed for methylation. Abbreviations: min, minimum; max, maximum.

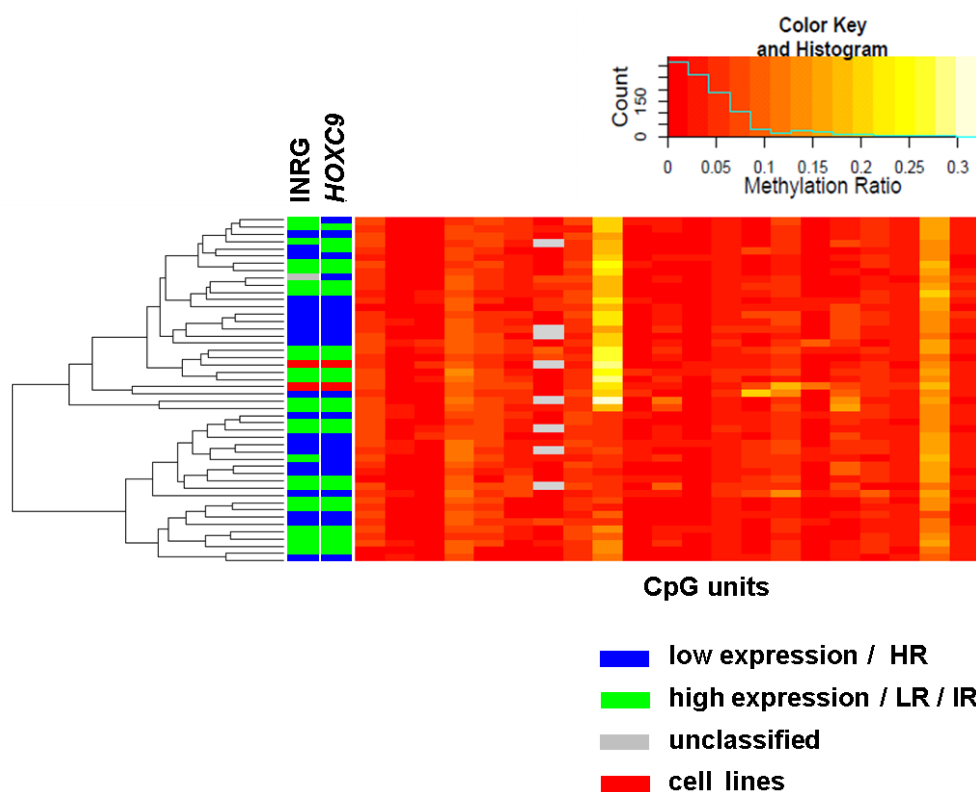


**Figure 12:** Hierarchical clustering of methylation ratios. A total of 26 CpG units of *HOXC9* were analyzed in 46 tumor samples and 2 cell lines (red, upper: SK-N-AS; lower: IMR-32). *HOXC9* expression (blue, low; green, high) and risk group according to INRG (blue, HR; green, LR/IR and grey, unclassified) are indicated aside. DNA methylation values are indicated by colors ranging from dark red (non-methylated) to bright yellow (30% methylated). Poor quality data are indicated in grey. A histogram is given in the inset that indicates the frequency of each color in the hierarchical clustering. Abbreviations: HR, high-risk; LR, low-risk; IR, intermediate-risk; INRG, International Neuroblastoma Risk Group.

## **4.4 Functional investigation of *HOXC9* in neuroblastoma**

### **4.4.1 Doxycycline-inducible expression of *HOXC9* in neuroblastoma cell lines**

The expression of *HOXC9* was restored in three neuroblastoma cell lines to analyze its functional effects on growth characteristics of neuroblastoma. To mirror the broad spectrum of neuroblastoma disease, I selected two *MYCN*-amplified (IMR-32 and CHP-212) cell lines and one non-amplified (SK-N-AS) cell line. Either *HOXC9* or *GFP* control cDNA was placed under a tetracycline-regulated promoter. Transgenic polyclonal cell lines were further verified for Hox-C9 expression by Western blot analysis (Figure 13a and b) and immunohistochemistry (Figure 14). Recombinant Hox-C9 expression, which was already detected under uninduced conditions due to promoter leakage of the pRevTRE vector system, increased in a time dependent manner upon treatment with doxycycline (Figure 13b) and reached protein levels in the range of physiological levels observed in neuroblastoma patients with high expression of Hox-C9 (Figure 13c). The expression of recombinant Hox-C9 was observed in the nucleus (Figure 14).

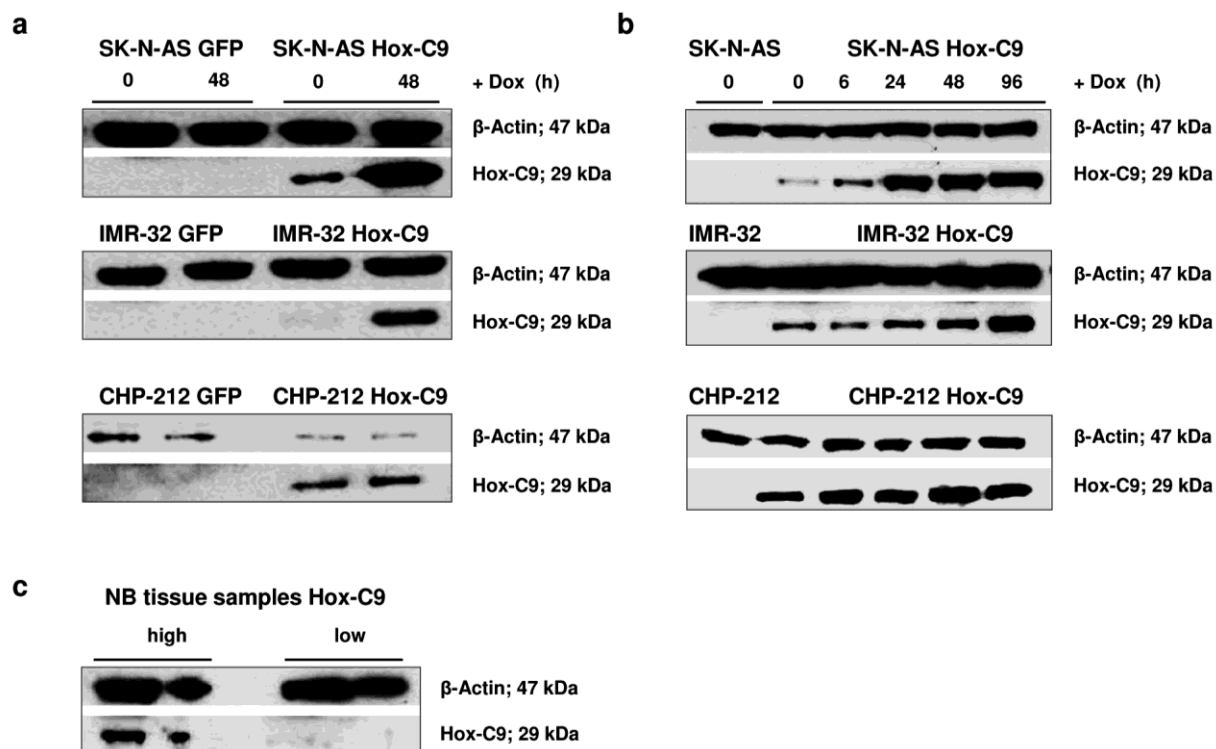


**Figure 13:** Inducible expression of Hox-C9 in SK-N-AS, IMR-32 and CHP-212 cells and physiological Hox-C9 levels in primary neuroblastomas as determined by Western blot analysis. **(a)** Inducible expression of Hox-C9 vs. GFP-expressing control cells. **(b)** Time course of Hox-C9 expression. **(c)** Representative neuroblastoma tumor samples with high and low Hox-C9 expression (high and low *HOXC9* expression as defined in Materials and Methods).

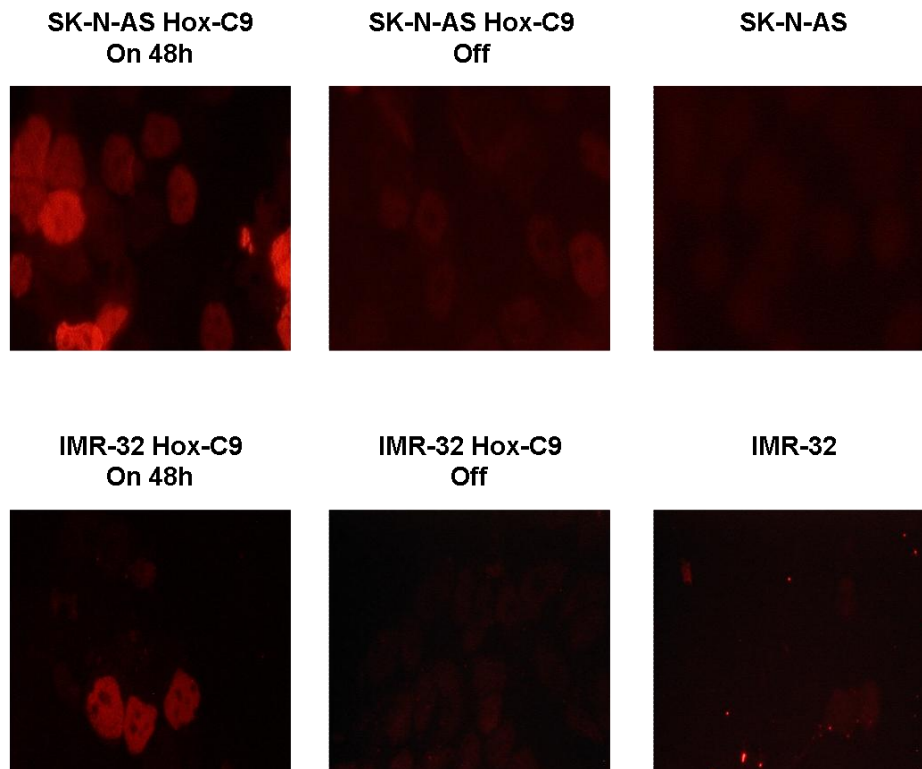


**Figure 14:** Inducible expression of Hox-C9 in SK-N-AS and IMR-32 cells as determined by immunohistochemistry. Hox-C9 On vs. Hox-C9 Off vs. parental neuroblastoma cell lines.

## 4.4.2 *HOXC9* expression inhibits neuroblastoma cell growth

### 4.4.2.1 *HOXC9* expression inhibits growth of neuroblastoma cells *in vitro*

To investigate whether *HOXC9* expression affects growth properties of neuroblastoma cell lines, polyclonal *HOXC9*-expressing SK-N-AS, IMR-32 and CHP-212 cells were compared with polyclonal *GFP*-expressing controls. Cell proliferation was assayed for up to 8 days using trypan blue dye exclusion tests. In all cell lines, the number of viable cells at day 8 was significantly lower compared to *GFP*-induced controls (Figure 15a).

To determine whether reduced proliferation upon *HOXC9* re-expression might be due to impaired cell cycle progression, the DNA content of *HOXC9*-expressing cells was assessed by flow cytometry. I observed a significant increase of the G<sub>0</sub>/G<sub>1</sub> peak at day 7 after Hox-C9 induction in all three cell lines (Figure 15b).

To investigate the influence of *HOXC9* on anchorage-independent clonal growth, I performed soft agar assays with SK-N-AS and IMR-32 cells which show anchorage independent growth potential. A marked reduction in colony formation was observed in both *HOXC9*-expressing SK-N-AS and IMR-32 cell lines in comparison to *GFP*-expressing control cells (Figure 15c).

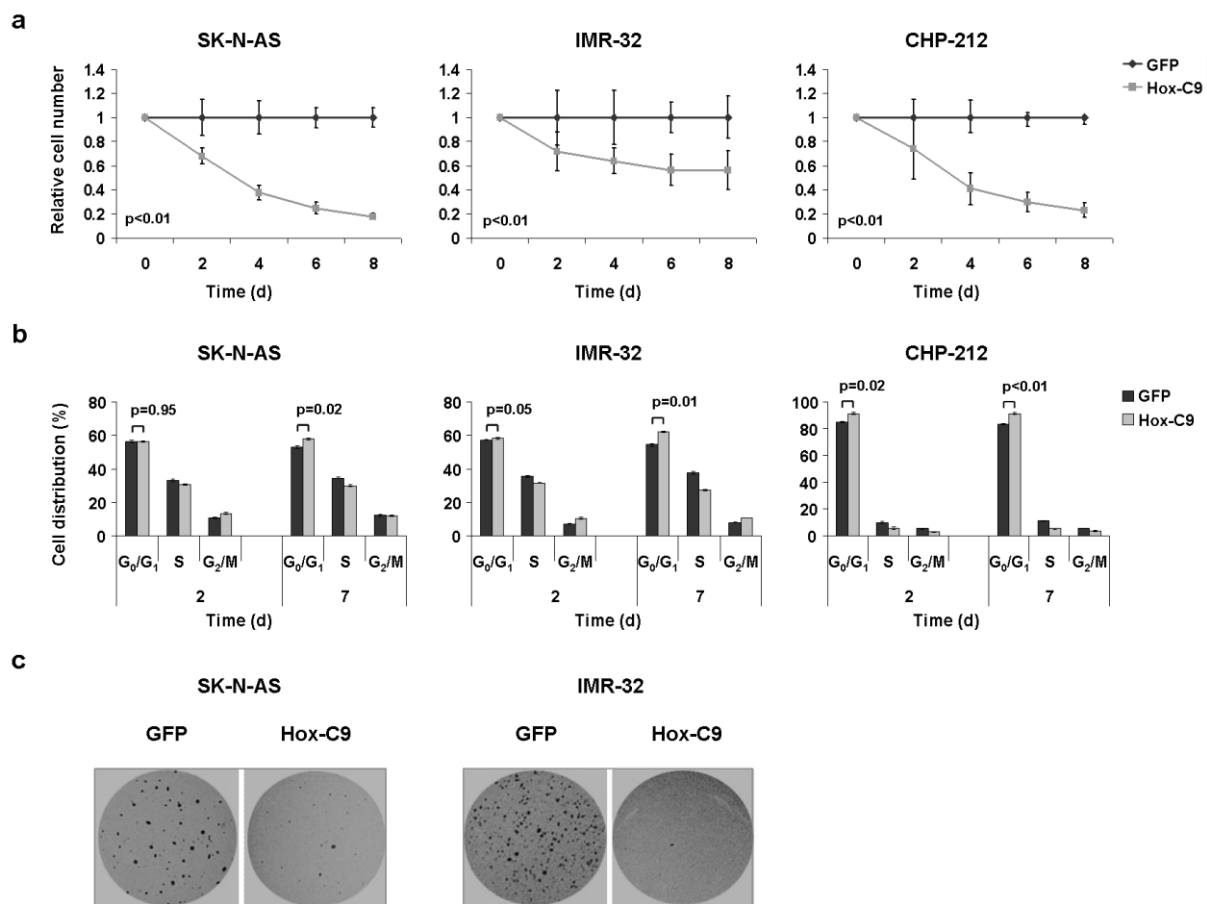


**Figure 15:** *HOXC9* re-expression inhibits growth of neuroblastoma cells in vitro. Hox-C9 induced changes in (a) cell proliferation (trypan blue dye exclusion), (b) cell cycle distribution (FACS) and (c) soft agar colony formation.

#### 4.4.2.2 *HOXC9* expression abrogates neuroblastoma tumor growth *in vivo*

Two xenograft mouse model systems were used to assess the effect of Hox-C9 on neuroblastoma tumor growth *in vivo*. First, tumor growth was investigated in neuroblastoma cells induced for transgene expression 48h before xenografting. *GFP*-expressing SK-N-AS and IMR-32 control cells formed rapidly growing tumors with mean tumor volumes of  $1905 \pm 295 \text{ mm}^3$  at day 17 and  $1323 \pm 404 \text{ mm}^3$  at day 22, respectively. In contrast, tumor growth was almost completely abrogated in mice inoculated with *HOXC9* expressing SK-N-S and IMR-32 (tumor volumes of  $79 \pm 31 \text{ mm}^3$  at day 17 and  $173 \pm 129 \text{ mm}^3$  at day 22, respectively; Figure 16a).

To investigate the impact of Hox-C9 in already established tumors, SK-N-AS *HOXC9*-off and SK-N-AS *GFP*-off cells were subcutaneously injected in the lateral thoracic wall of athymic Nude- Foxn1<sup>nu</sup> mice. Transgene expression was induced after the tumor had reached a mean tumor volume of  $144 \pm 41 \text{ mm}^3$  ( $120 \pm 25 \text{ mm}^3$  in the control group and  $174 \pm 36 \text{ mm}^3$  in the *HOXC9* group) by switching from standard diet to doxycycline containing diet. Induction of transgene expression was started 8 days after tumor inoculation in the control group and after 18 to 34 days in the *HOXC9* group, indicating a slower initial tumor growth probably due to low-level Hox-C9 expression under uninduced conditions (Figure 13b). *GFP* expressing control cells formed tumors that exceeded  $1 \text{ cm}^3$  and had to be sacrificed 10 days after transgene induction, while the *HOXC9* expressing group formed tumors accounted for  $5.3 \pm 2\%$  the tumor volumes of the control group (Figure 16b).

Histological examination of neuroblastoma xenograft tumors revealed that Hox-C9 expression led to stroma rich tumors containing less mitotic cells than in *GFP* expressing control tumors, which contained extensive amounts of mitotic cells with atypical mitotic figures (Figure 17).

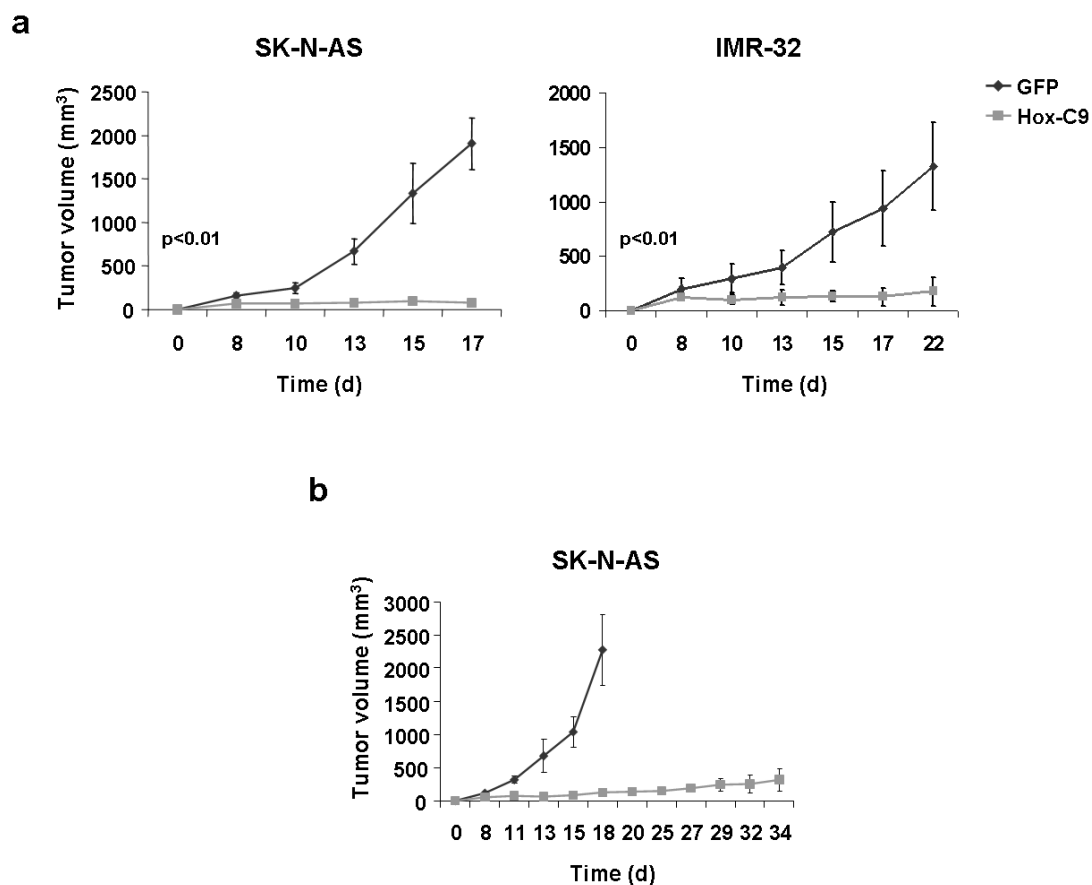


**Figure 16:** *HOXC9* re-expression inhibits growth of neuroblastoma cells *in vivo*. (a) Hox-C9 expression impedes tumor growth in SK-N-AS and IMR-32 neuroblastoma xenografts (n= 8 mice per group). (b) Hox-C9 induction in already established xenograft tumors. Error bars indicate standard deviation (SD), p-values (unpaired, two-tailed Students t-test).

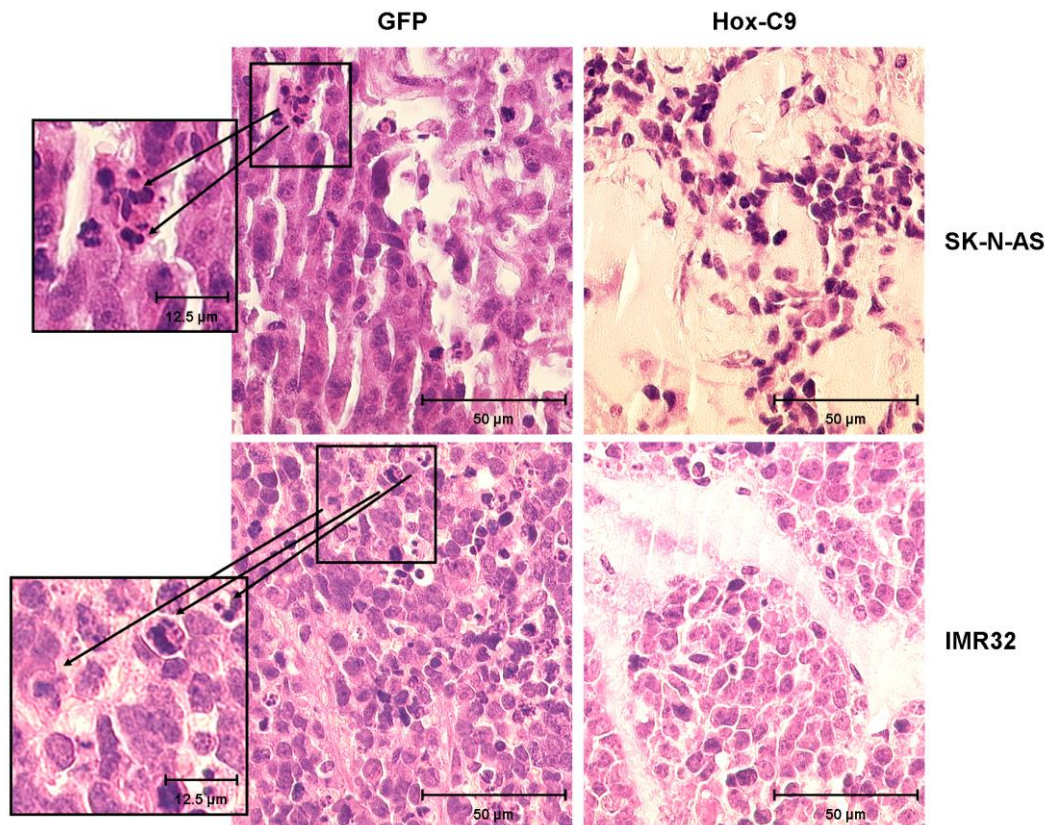


**Figure 17:** Histological features of neuroblastoma xenografts. Histological evaluation was done using paraffin-embedded sections stained with Meyer's hematoxylin and eosin. Arrows indicate tumor cells with atypical mitotic figures.

### 4.4.3 Hox-C9 induces neuronal differentiation in neuroblastoma

#### 4.4.3.1 Hox-C9-induced neuronal differentiation of IMR-32 cells is accompanied by down-regulation of *REST*

Morphological signs of neuronal differentiation were assessed by microscopic examination in all three cell lines after *HOXC9* re-expression. In IMR-32 cells, *HOXC9* re-expression led to a neuronal-like phenotype with a large network of cells interconnected by long neurite elongations (Figure 18), while similar changes were not observed in the other cell lines. To determine whether this morphological alteration induced by Hox-C9 was accompanied by up-regulation of genes involved in neuronal differentiation, I analyzed expression levels of the

neuron-related markers *PTN* (226-228), *NNAT* (229), *NEFL* (52), *TRKA* (100, 230), *DNER* (231) and *NTS* (232) by qRT-PCR and microarray analysis. In line with the morphological changes, all markers were up-regulated upon *HOXC9* re-expression (Figure 19a and b). At the same time, the RE1-silencing transcription factor *REST*, a master negative regulator of neurogenesis, was down-regulated in Hox-C9-induced IMR-32 cells (Figure 19c and 19d).

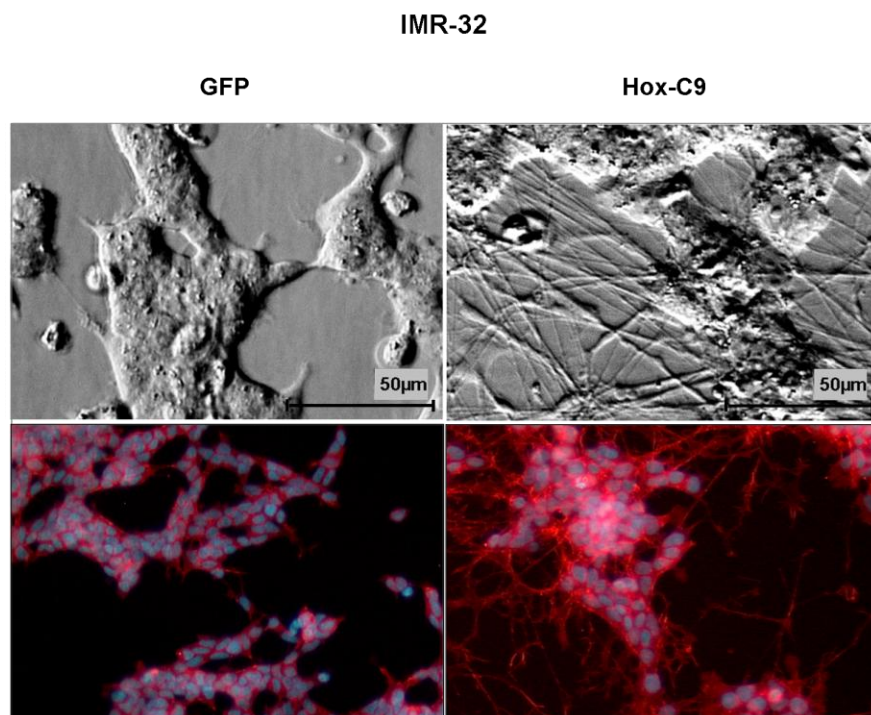


**Figure 18:** Hox-C9 induces neuronal differentiation in IMR-32 cells. Morphological changes of IMR-32 cells at 21 days after Hox-C9 and GFP induction. White light images and F-Actin cytoskeleton organization (labeled with Rhodamine Phalloidin (red) and counterstained with DAPI (blue)).

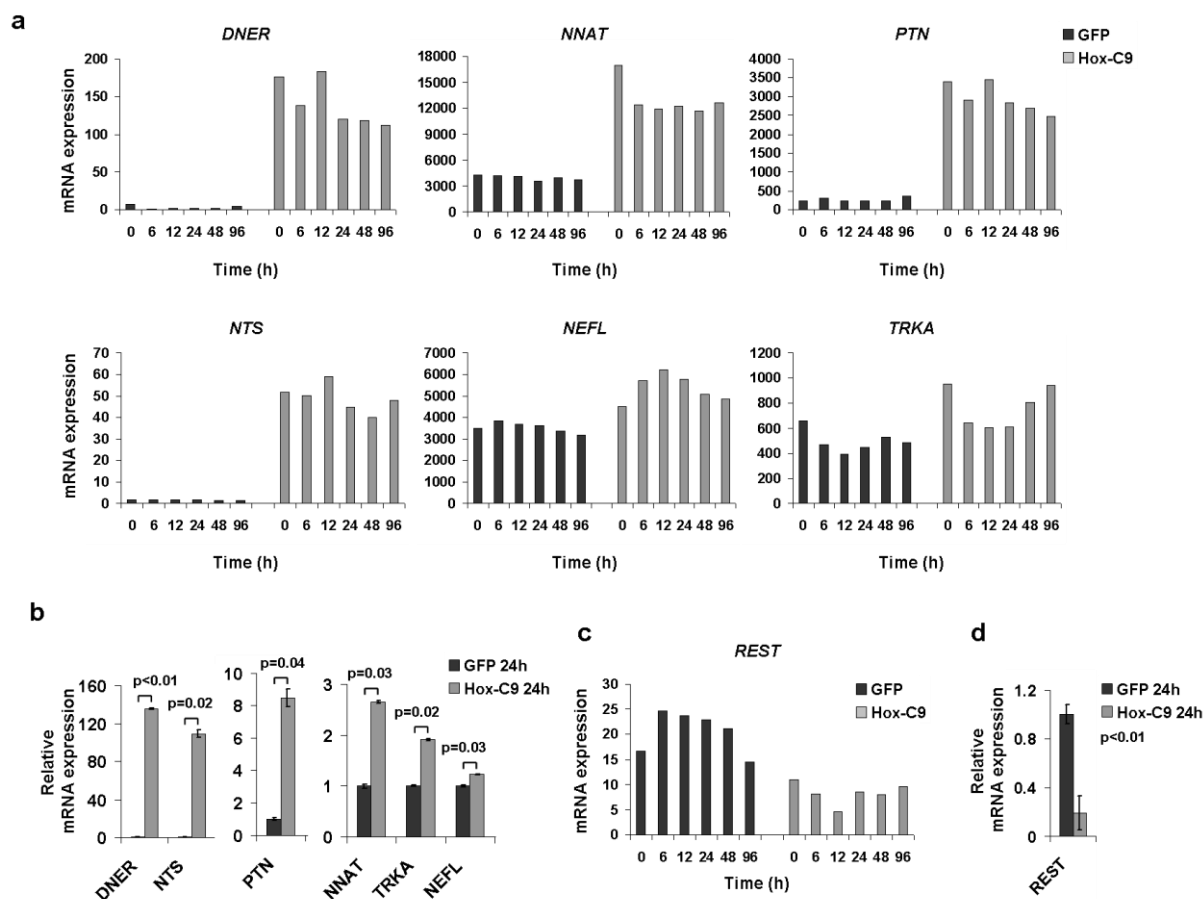


**Figure 19:** *HOXC9* expression up-regulates neuron-related markers in IMR-32 cells (a) as determined by oligonucleotide-microarrays and (b) qRT-PCR. Hox-C9 expression down-regulates REST (c) as determined by oligonucleotide-microarrays and (d) qRT-PCR. Error bars indicate SD, p-values (unpaired, two-tailed Students t-test).

#### 4.4.4 *HOXC9* re-expression induces apoptosis in neuroblastoma cell lines

I next examined whether apoptosis contributes to inhibition of neuroblastoma cell growth after *HOXC9* re-expression. First, externalization of phosphatidylserine was analyzed by flow cytometry using Annexin-V staining. I observed a significant increase of the Annexin-V binding fraction in SK-N-AS and CHP-212 cells 168h after *HOXC9* re-expression in comparison to control cells (Figure 20a). Second, DNA fragmentation was assessed using the TUNEL assay in SK-N-AS, IMR-32 and CHP-212 cells. *HOXC9* expressing neuroblastoma cells showed a significantly higher fraction of cells with fragmented DNA as compared to

*GFP*-expressing controls (Figure 20b). These results were supported by FACS analysis following *Hox-C9* induction in SK-N-AS, IMR-32 and CHP-212 cells, in which Nicoletti labeling and assessment of the fraction of sub-G<sub>1</sub> events indicated an accumulation of cells with fragmented DNA. In all investigated cell lines, the sub-G<sub>1</sub> fraction was significantly increased by *HOXC9* re-expression as compared to *GFP*-induced controls (Figure 20c). Together, these findings indicate that *Hox-C9* affects growth properties in human neuroblastoma cells not only by cell cycle regulation but also by induction of apoptosis.

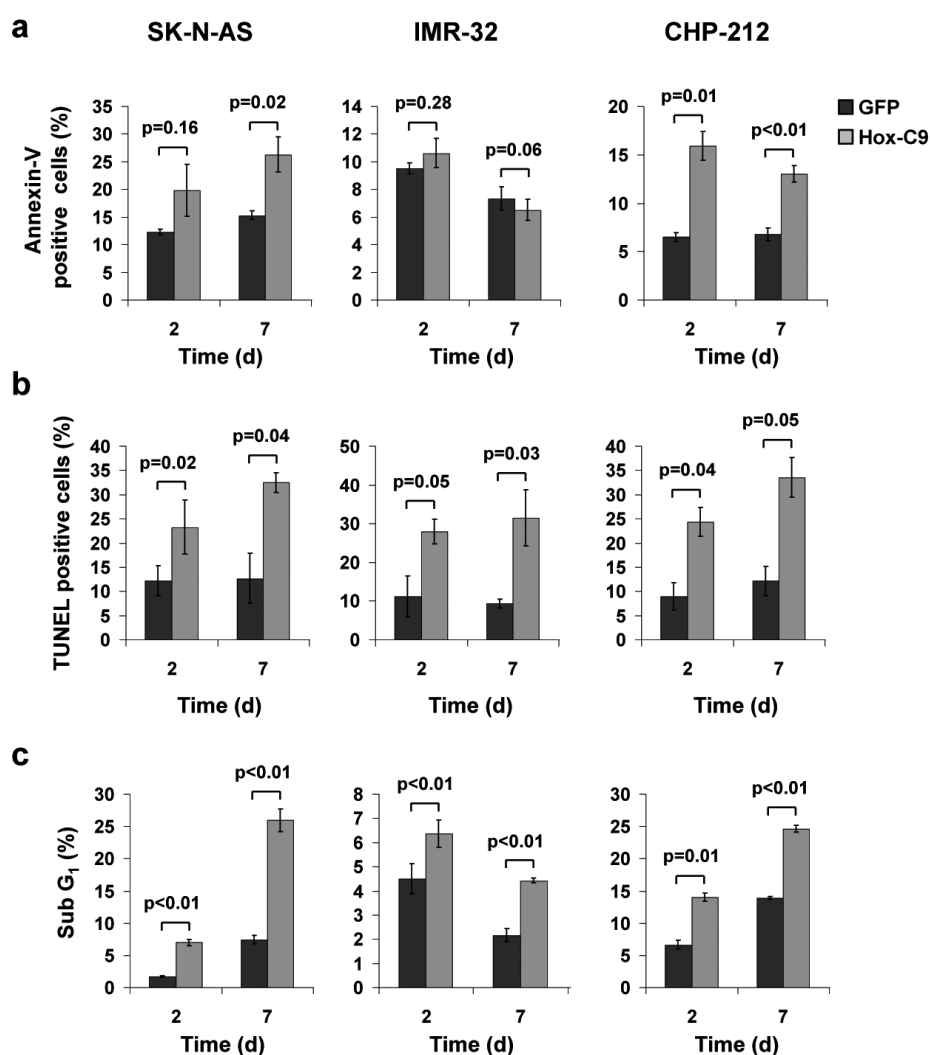


**Figure 20:** *Hox-C9* induces apoptosis in neuroblastoma cell lines. (a) Proportion of Annexin-V positive cells as determined by FACS. (b) Proportion of cells showing apoptotic nuclei as determined by fluorescence microscopy (TUNEL). (c) Proportion of cells with subnormal DNA content as determined by FACS.

#### 4.4.4.1 Hox-C9 activates the intrinsic pathway of apoptosis

To further analyze Hox-C9-induced cell death, the expression of pro- and anti-apoptotic regulators was examined by immunoblot, qRT-PCR and microarray analysis in *HOXC9*-expressing and control neuroblastoma cells. Apoptotic cell death was associated with a strong increase of cytochrome c in the cytosolic fraction of Hox-C9-induced cells (Figure 21a) suggesting a loss of mitochondrial membrane potential and involvement of mitochondria in Hox-C9-induced cell death. In IMR-32 cells, I observed down-regulation of *BCL-2* both on the transcript and protein level, while expression levels remained unchanged in SK-N-AS and CHP-212 cells (Figure 21a, b and c). In the latter cell lines, however, I observed a marked up-regulation of *BAX* mRNA expression upon induction of Hox-C9 (Figure 21b and c). These data suggest that apoptosis induced by *HOXC9* re-expression may be conferred by a shifted *BCL-2/BAX* ratio as a consequence of either increased expression of pro-apoptotic *BAX* or decreased expression of anti-apoptotic Bcl-2. Subsequently, I investigated whether procaspase 9, the initial caspase in the mitochondrial apoptotic cascade, is activated upon cytochrome c release. I observed an increase of cleaved 35 kDa fragments of activated caspase 9 in all cell lines upon *HOXC9* re-expression (Figure 21a). In addition, a 37 kDa cleaved fragment of caspase 9 was observed in SK-N-AS and CHP-212 cells (Figure 21a), which is indicative of a feedback amplification loop induced by activated caspase 3 (233). Finally, I observed an increased activation of the downstream effector caspases 3 and 7 in all three cell lines (Figure 21a) upon *HOXC9* re-expression. Together, these data indicate that *HOXC9* expression can activate the intrinsic apoptosis pathway and thereby triggers neuroblastoma cell death.

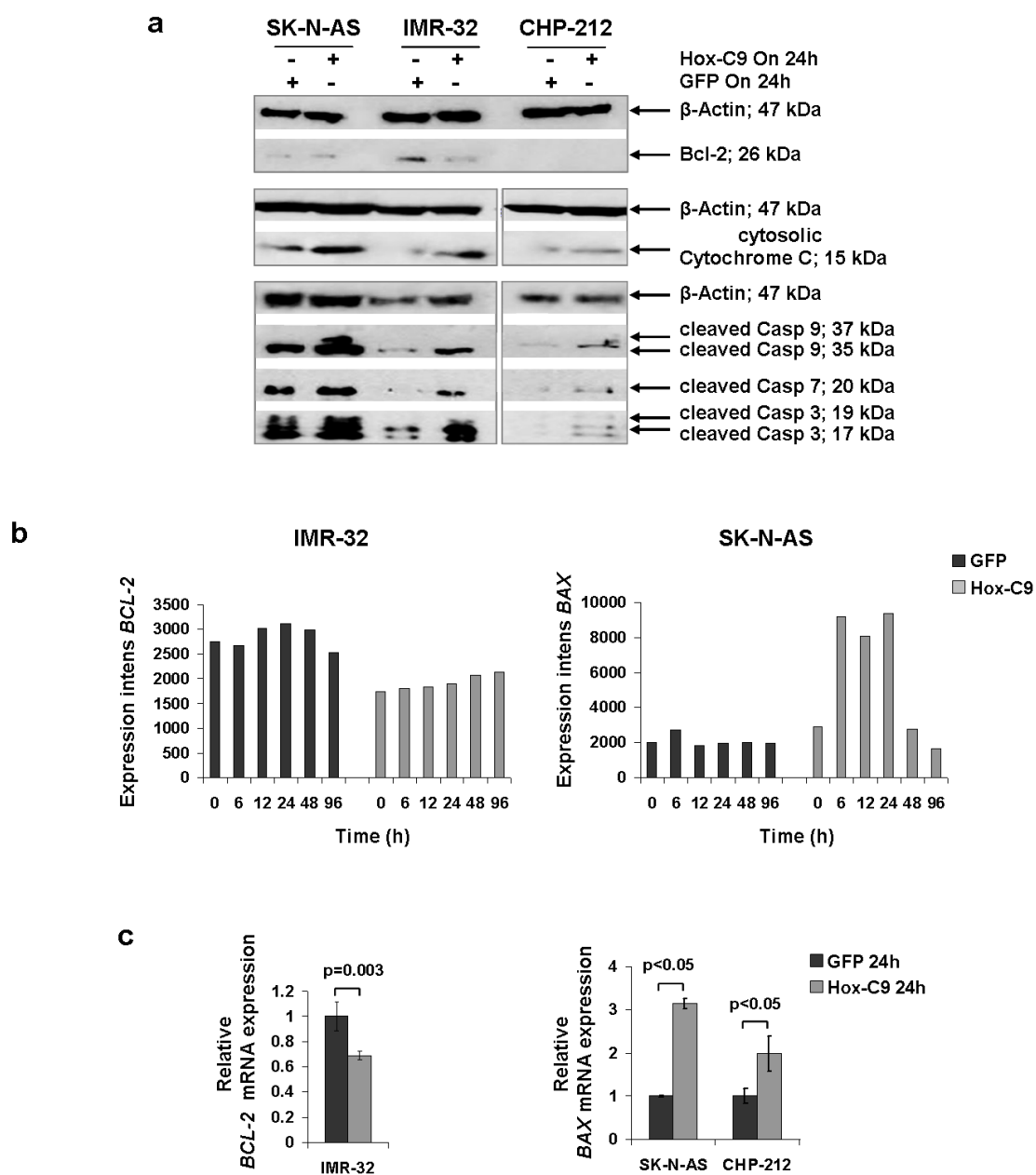


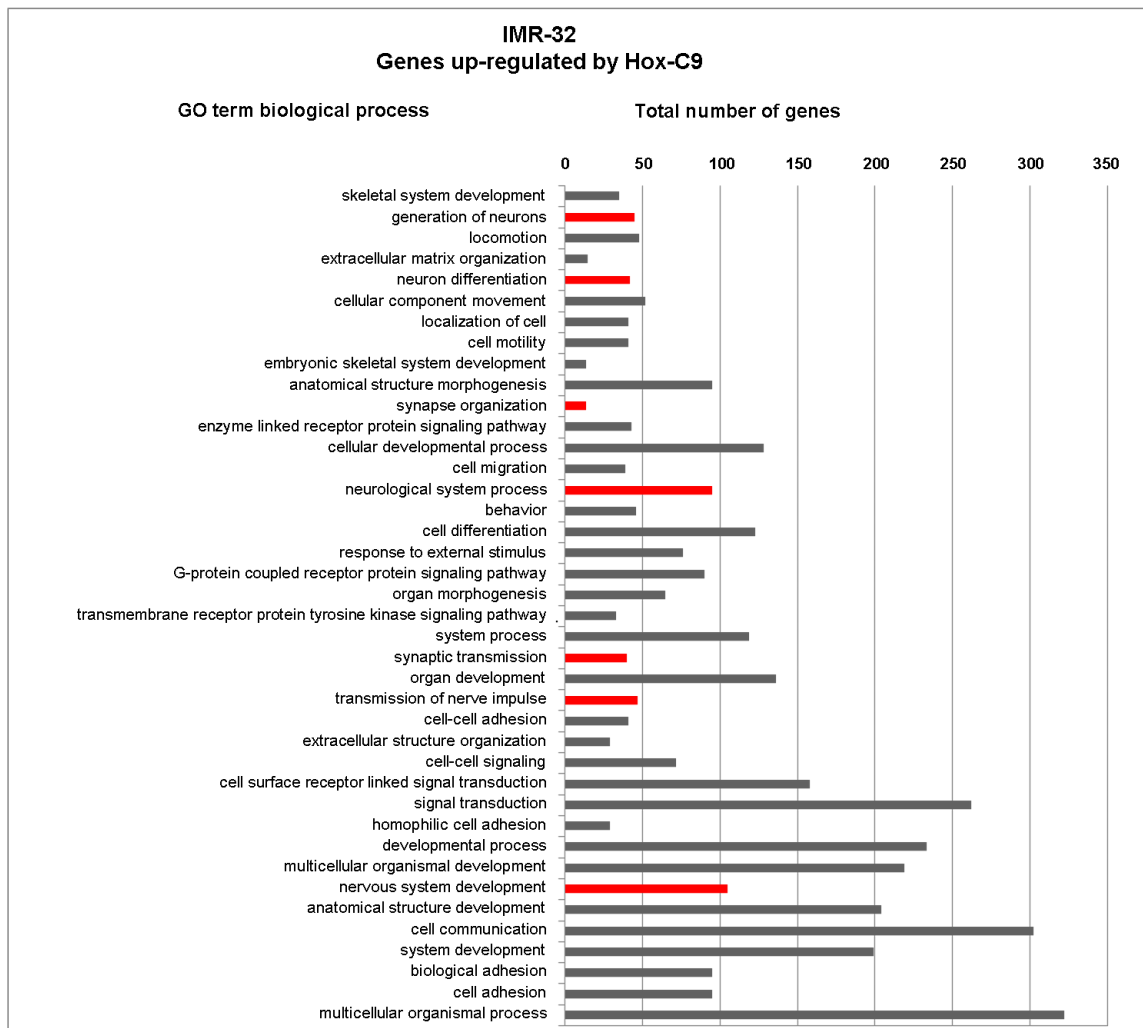
**Figure 21:** Hox-C9 induces apoptosis in neuroblastoma cell lines by activating the intrinsic apoptotic pathway. (a) Protein expression of Bcl-2, cytosolic cytochrome c, and cleaved caspase 9, caspase 7 and caspase 3 upon Hox-C9 and GFP induction. (b) *BCL-2* and *BAX* expression in IMR-32 and SK-N-AS cells following Hox-C9 induction as determined by microarrays. (c) *BCL-2* expression in IMR-32 and *BAX* expression in SK-N-AS and CHP-212 cells following Hox-C9 induction as determined by qRT-PCR. Error bars indicate SD, p-values (unpaired, two-tailed Students t-test). Abbreviation: Casp, Caspase.

---

#### 4.4.5 *HOXC9* expression affects transcriptional pathways regulating differentiation and cell death

To gain further insights into the biological processes occurring upon *HOXC9* re-expression, I analyzed gene expression profiles of IMR-32 and SK-N-AS cells after Hox-C9 induction using microarrays. I used GO annotations to find classes of genes which are significantly overrepresented in gene sets that were either up-regulated or down-regulated after *HOXC9* re-expression. Many GO categories significantly enriched for genes up-regulated in *HOXC9*-expressing IMR-32 cells were related to neuronal functions and differentiation, thereby reflecting the Hox-C9-associated differentiation phenotype in IMR-32 cells (Figure 22a). Of note, I also observed that *MYCN* is down-regulated upon *HOXC9* re-expression in *MYCN*-amplified IMR-32 cells (Figure 23a). Accordingly, N-Myc protein levels decreased in both *HOXC9* expressing IMR-32 and CHP-212 cells (Figure 23b), suggesting that down-regulation of *MYCN* might contribute to the favorable phenotype observed in *HOXC9*-expressing neuroblastoma. In SK-N-AS cells, many GO categories significantly enriched for genes up-regulated by Hox-C9 were associated with cell death (Figure 22c). These results are well in line with the observed phenotypes of these two neuroblastoma cell lines after *HOXC9* re-expression: While growth inhibition mediated by apoptosis is the predominant characteristic of *HOXC9*-expressing SK-N-AS cells, neuronal differentiation is mainly observed in IMR-32 cells. Complete data tables for significantly differentially expressed genes between *HOXC9*- and *GFP*-induced SK-N-AS and IMR-32 cells and the complete list of GO annotations are available through Kocak *et al.* (234), Supplementary Table S6.

a

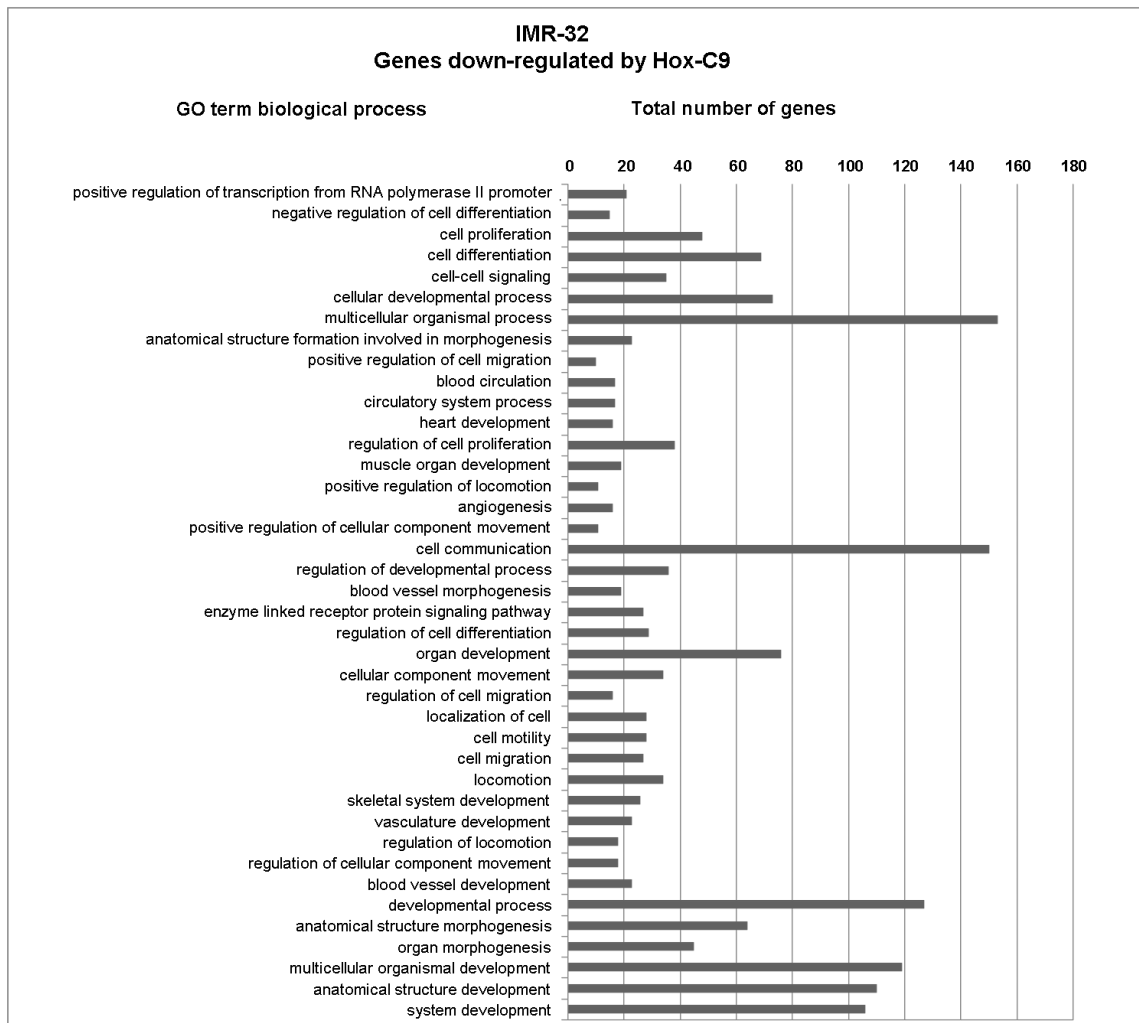


■ GO terms associated with neuronal functions and differentiation

■ GO terms associated with cell death

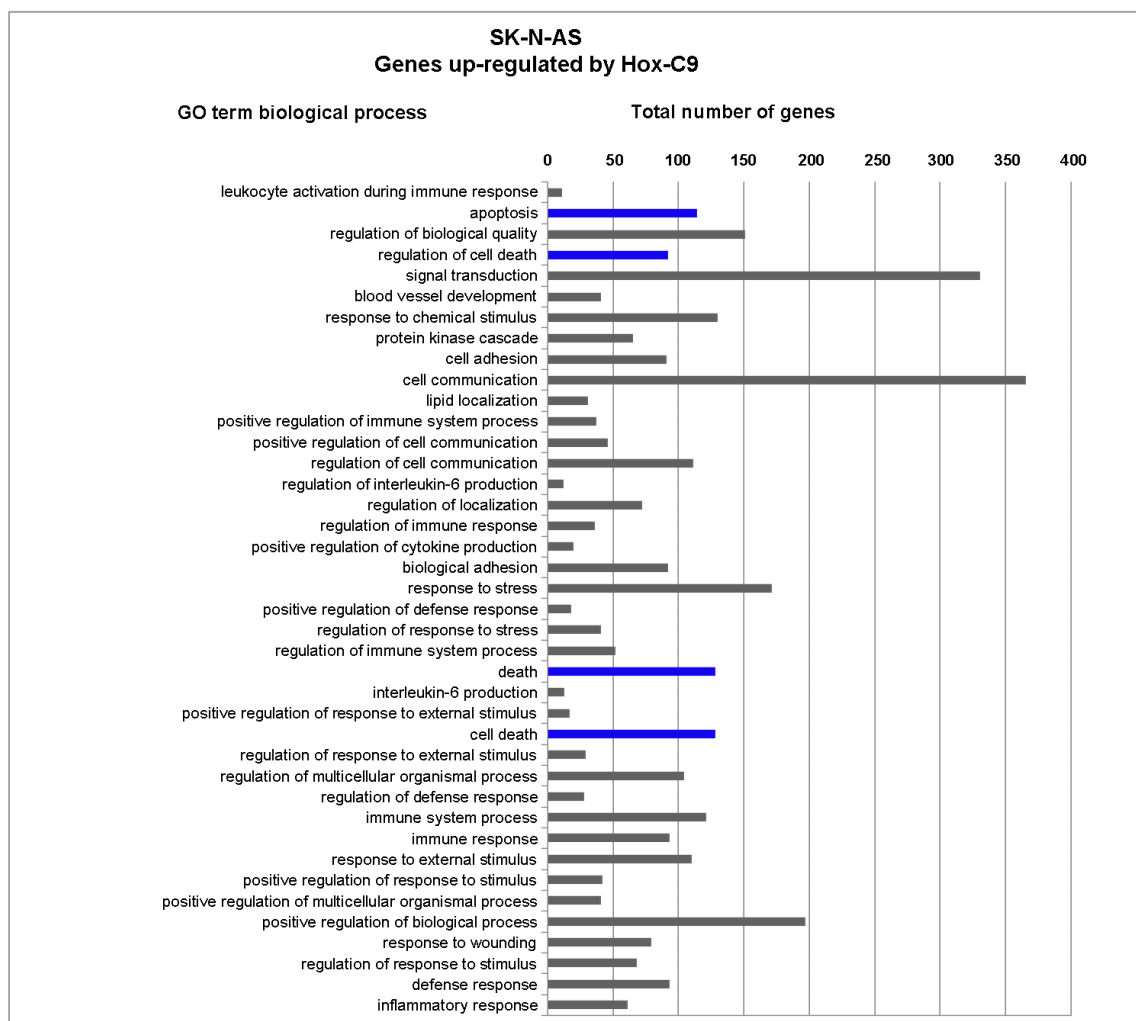
■ Others

b



- GO terms associated with neuronal functions and differentiation
- GO terms associated with cell death
- Others

C



■ GO terms associated with neuronal functions and differentiation

■ GO terms associated with cell death

■ Others

d

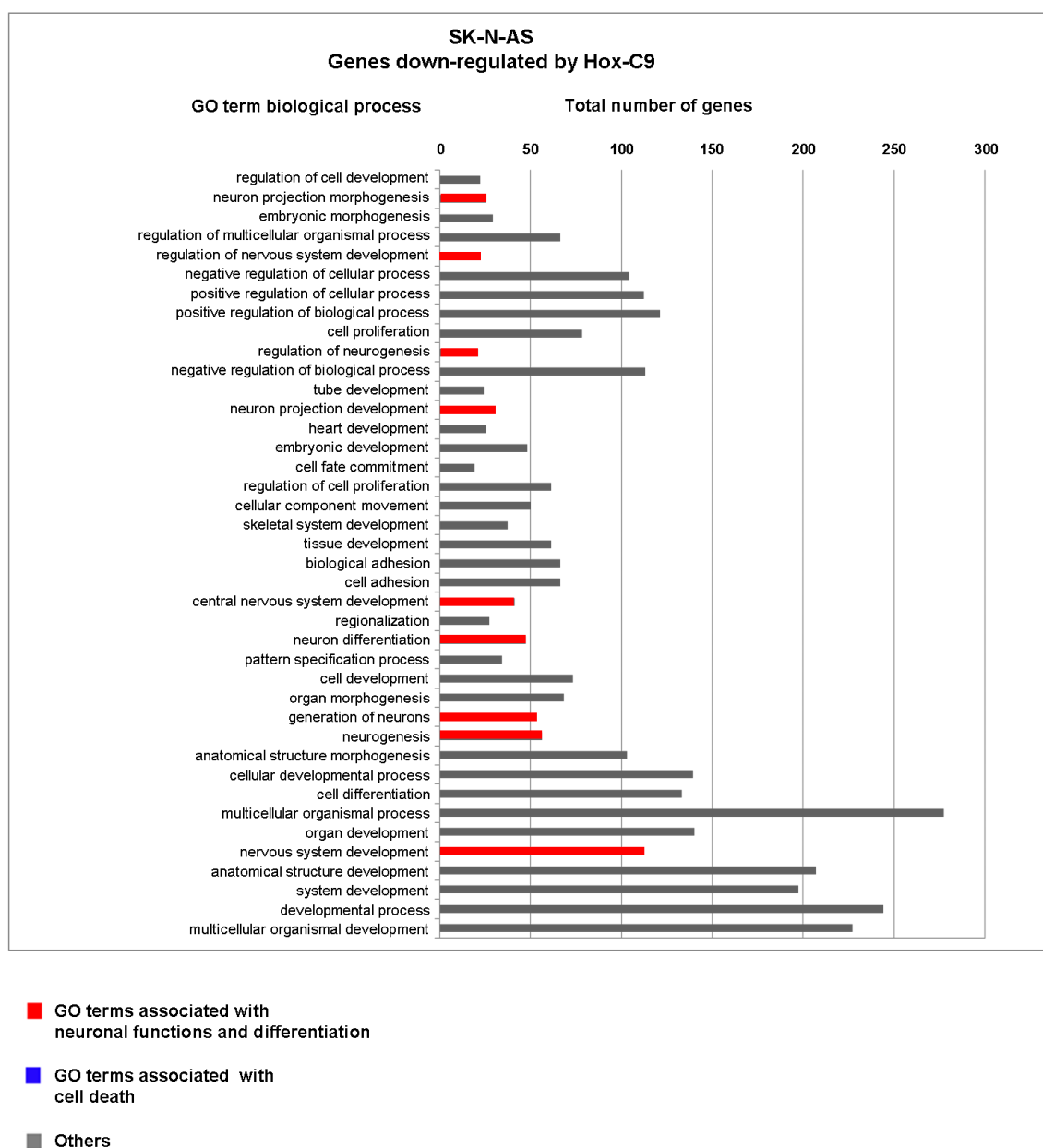


**Figure 22:** Gene Ontology (GO) annotations for significantly differentially expressed genes. (a) GO terms for up-regulated or (b) down-regulated genes by Hox-C9 in IMR-32 cells. (c) GO terms for up-regulated or (d) down-regulated genes by Hox-C9 in SK-N-AS cells. Only GO terms for “biological process” with corrected p-values < 0.01 are shown. GO terms associated with neuronal functions and differentiation are highlighted in red, GO terms associated with cell death are highlighted in blue. Abbreviation: GO, Gene Ontology.

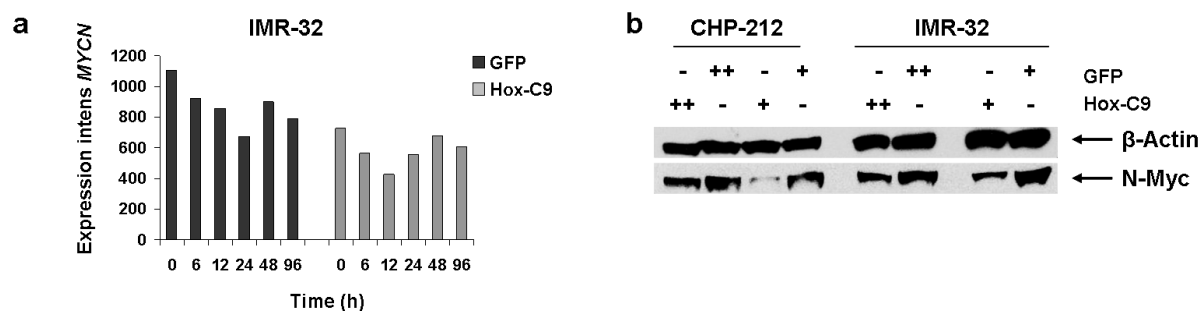


**Figure 23:** *HOXC9* leads to reduced expression of *MYCN*. (a) *MYCN* expression in *MYCN*-amplified IMR-32 cells after *HOXC9* re-expression as determined by microarrays. (b) N-Myc expression in IMR-32 and CHP-212 cells upon Hox-C9 and GFP induction as determined by Western blot analysis. +, transgene is weakly expressed under uninduced conditions; ++ transgene is induced by doxycycline treatment for 48 h. Abbreviation: Intens, Intensity.

## 5 Discussion

### 5.1 Expression patterns of *HOX* genes in neuroblastoma

In this study, I report that expression of the majority of class I *HOX* genes is associated with clinical phenotypes of neuroblastoma. *HOX* genes play essential roles in morphogenesis and cell differentiation during embryonic development (103). Since neuroblastoma is an embryonal tumor capable of differentiating into less aggressive ganglioneuroblastoma or benign ganglioneuroma, it has been suggested that Hox transcription factors may be involved in these processes (102, 184). Accordingly, it has been reported that morphological differentiation of neuroblastoma cells upon treatment with RA is accompanied by increased expression of a number of *HOX* genes (102, 184, 235). In line with these results, I here show that expression of most *HOX* genes is significantly associated with prognostic markers and clinical outcome in primary neuroblastoma, suggesting that *HOX* genes are essentially involved in neuroblastoma pathogenesis.

The potential relevance of these genes is further emphasized by the finding that a *HOX* gene expression-based classifier was able to accurately predict neuroblastoma patient outcome independently of the prognostic markers age at diagnosis, stage of disease and amplification status of the proto-oncogene *MYCN*. I observed that *HOX* genes of the A, B and C cluster were mainly up-regulated in favorable neuroblastoma, while genes of the D cluster, particularly *HOXD3*, *HOXD8*, *HOXD9* and *HOXD10*, were up-regulated in unfavorable tumors. These findings are in contrast to a recent study of Mao *et al.* (195), who investigated the prognostic value of a panel of *HOX* genes (*HOXA9*, *HOXB9*, *HOXD1*, *HOXD8*, *HOXD9*) in primary neuroblastoma, and did not observe any correlation of the expression and clinical outcome for most of these. The difference between the two studies might be explained by the fact that Mao and co-workers examined a limited number of samples comprising metastasized

neuroblastoma without *MYCN* amplification only (24), while a large tumor cohort representing the entire spectrum of the disease has been analyzed in my study.

In another study, the group of Han-Fei Ding showed that induction of Hox-D8, Hox-D9 and Hox-D10 results in growth arrest and neuronal differentiation in neuroblastoma using the cell line BE(2)-C as a model system (185). In addition, Hox-D8 was suggested to mediate its functional effects by directly activating Hox-C9, which implicates that *HOXD8* and *HOXC9* expression levels are positively correlated. The expression analysis of primary tumors in my study does not support this suggestion, as I observed a modest negative correlation of *HOXD8* and *HOXC9* expression levels (data not shown). These discrepant results could be explained by the fact that a single neuroblastoma cell line has been used for functional studies of *HOXD* genes in the study of Zha *et al.*, which probably is not representative of the entire biological and clinical spectrum of neuroblastoma. In addition, one may speculate that the biological function of these *HOX* genes may depend on specific expression thresholds. This suggestion is supported by specific patterns of survival curves of patients stratified according to quartiles of *HOXD8*, *HOXD9* and *HOXD10* expression levels in my study (Figure 6). For all three genes, patients with low, intermediate-low and intermediate-high expression levels had similar outcomes, whereas the outcome of those with high expression levels was substantially inferior. These findings may indicate that expression of *HOXD8*, *HOXD9* and *HOXD10* is of prognostic relevance only if specific expression thresholds are exceeded.

Spatial and temporal co-linearity is a hallmark of clustered *HOX* genes (236, 237). *HOX* genes located more 5' in the *HOX* cluster, such as *HOXC9*, are expressed later and more posterior during early development. In accordance with this embryonic expression pattern of *HOX* genes, I here show a significant correlation of increased *HOXC9* expression levels in neuroblastomas from abdominal sites in comparison to tumors of the neck and chest. This finding contrasts with previous speculations (195), which suggested that *HOXC9* expression

might be higher in tumors of the neck and thorax because of their association with a better outcome (223, 224) and a more differentiated histology (225). Indeed tumors located at the neck/chest appear to have a slightly better outcome compared to tumors located at the adrenal glands or abdomen (Figure 9b and c). While the correlation of *HOXC9* with the primary tumor site fits well to the embryonal expression pattern of *HOX* genes, most of the other 5' located *HOX* genes do not show such an expression pattern, suggesting that multiple factors may influence *HOX* gene expression in neuroblastoma.

## **5.2 Expression patterns of *HOXC9* in neuroblastoma**

Among all *HOX* genes, *HOXC9* expression was most prominently associated with favorable prognostic markers and beneficial clinical outcome in neuroblastoma. The prognostic impact of *HOXC9* is underlined by the fact that this gene was selected in all predictive models generated during the training phase of the *HOX* classifier generation process (Table 22), and that it was one of 144 predictive genes of a prognostic classifier reported previously (25). Using gene expression data from our group and others, low expression of *HOXC9* has also been described to be associated with the unfavorable clinical phenotype of neuroblastoma in a recent study (195).

Since genetic and epigenetic changes can lead to altered gene expression and, thereby, trigger cancer development, I questioned which genetic or epigenetic factors might influence *HOXC9* expression in primary neuroblastoma. A gain of chromosome 12, which comprises the *HOXC9* locus, was associated with elevated *HOXC9* transcript levels, suggesting that a gene-dosage effect might account for *HOXC9* expression differences in neuroblastoma. These findings are in line with previous reports showing that numerical chromosomal aberrations including chromosome 12 gain (238, 239) are associated with lower stages (205) and better outcome in neuroblastoma (240). Diminished *HOX* gene expression was reported to be

associated with promoter hypermethylation in numerous malignancies (155, 163-166) and seems to be a major mechanism of *HOX* gene de-regulation in cancer. By contrast, I neither detected hypermethylation of the promoter region of *HOXC9* nor inactivating mutations at the *HOXC9* locus as a potential cause of decreased *HOXC9* expression in unfavorable tumors. Mao and co-workers (195) showed that the *HOXC9* promoter is associated with the chromatin silencing marker H3K27me3 in RA-resistant SK-N-AS cells. Whether this finding represents a common regulatory mechanism for *HOXC9* gene silencing in the unfavorable subgroup of neuroblastoma remains to be elucidated. Alternatively, other mechanisms, such as regulatory RNA's (241) or upstream transcriptional regulators (36) may control *HOXC9* expression in neuroblastoma. In human embryonic stem (ES) cells Myc and Miz-1 control *HOX* gene expression (242), which may represent a further possibility for transcriptional regulation of *HOXC9* in neuroblastoma.

## **5.3 The functional relevance of *HOXC9* expression in neuroblastoma**

### **5.3.1 *HOXC9* leads to neuronal differentiation in IMR-32 cells**

Neuroblastoma is an embryonal tumor with the potential to differentiate into less aggressive ganglioneuroblastoma or benign ganglioneuroma, and *HOX* genes have been suggested to be involved in these processes (102, 184). In line with this hypothesis, it has been reported that the expression of a number of *HOX* genes increases by induction of neuroblastoma cell differentiation using RA, which is implemented in the post-consolidation therapy of stage 4 neuroblastoma (243). In this study, I substantiate that Hox-C9 may induce neuronal differentiation in a fraction of neuroblastomas. The induction of neuron associated marker genes and neurogenesis-like processes by re-expression of *HOXC9* in IMR-32 cells points

towards a role of *HOXC9* in neuroblastoma cell differentiation. In human cells, *MYC* has been shown to repress *HOX* gene expression to maintain ES cell pluripotency (242). Given the inverse correlation of *MYCN* amplification and *HOXC9* expression in our cohort (Figure 8a), one may speculate that such a mechanism may also exist in neuroblastoma. Conversely, I observed that morphological differentiation of *MYCN*-amplified IMR-32 cells upon *HOXC9* re-expression is accompanied by decreased *MYCN* expression. Since down-regulation of *MYCN* is a general feature of neural differentiation (244), it might be possible that Hox-C9 mediates differentiation by repression of *MYCN*. In addition, I observed down-regulation of *REST* after *HOXC9* re-expression. *REST* is a well-known master negative regulator of neurogenesis (245), and has been reported to be degraded upon RA induced neuroblastoma cell differentiation (246). While *REST* has been described as a potent tumor suppressor gene in several non-neural tumors including small cell lung cancer and breast cancer (247, 248), oncogenic functions have been described in neuroblastoma (249) and medulloblastoma (250). *REST* expression has been observed in ES cells and neural progenitor cells (251-253), where it represses several terminal neuronal differentiation genes (253-255). However, *REST* down-regulation in neural progenitors during neurogenesis de-represses its target genes. While *REST* down-regulation is mediated by proteasomal degradation during the differentiation of ES cells into neural progenitors, its down-regulation during differentiation of neural progenitors into mature neurons occurs by transcriptional repression (255, 256). Taking these findings into account, it seems likely that Hox-C9 promotes a more differentiated neuroblastoma phenotype by transcriptional repression of *REST*.

### **5.3.2 *HOXC9* suppresses growth of neuroblastoma cells *in vitro* and *in vivo***

A consistently low expression of *HOXC9* in unfavorable neuroblastomas was observed in our patient cohort and led to the suggestion that down-regulation of *HOXC9* might mediate a selective advantage for tumor cells. By contrast, re-expression of *HOXC9* in neuroblastoma cell lines showing diminished *HOXC9* levels may inhibit features of malignancy. In line with this hypothesis, I observed that re-expression of *HOXC9* suppressed neuroblastoma cell proliferation and induced accumulation of cells in the G<sub>0</sub>/G<sub>1</sub>-phase of the cell cycle. In support of our hypothesis, Mao and co-workers demonstrated that *HOXC9* represses the transcription of cyclins and cyclin dependent kinases and thereby trigger an G<sub>0</sub>/G<sub>1</sub>-phase cell cycle arrest in neuroblastoma cell lines (195). The fact that *HOXC9* inhibited anchorage independent growth and *in vivo* growth of IMR-32 and SK-N-AS cells further strengthens the role of *HOXC9* as a tumor suppressor candidate gene. A potential tumor suppressive function of *HOXC9* in already established xenograft tumors could not be clarified due to limitations of the leaky promoter system used in this study. Histological examination of neuroblastoma xenograft tumors revealed that Hox-C9 expression resulted in stroma rich xenograft tumors containing lower contents of mitotic cells, supporting the hypothesis that Hox-C9 affects cell cycle progression in a dominant negative manner (195).

### **5. 3.3 *HOXC9* induces apoptosis in neuroblastoma cells**

The strong effect of Hox-C9 re-expression on neuroblastoma growth arrest observed here and by others (195) suggested that additional mechanisms beyond cell cycle arrest may contribute to this phenotype. Accordingly, I here provide substantial evidence that Hox-C9 promotes apoptosis in neuroblastoma in general, as indicated by a strong increase of the sub-G<sub>1</sub> fraction and an increase of TUNEL-positive cells after *HOXC9* induction in all three cell lines

analyzed. I demonstrate that *HOXC9* expression activates the intrinsic pathway of apoptosis, probably by increasing the *BAX:BCL-2* ratio, which in turn may lead to the release of cytochrome c from the mitochondria into the cytosol and to activation of the intrinsic cascade of caspases. The putative role of *HOXC9* in promoting apoptotic processes in neuroblastoma is further supported by the results of the GO analysis described here, which correspond to the apoptotic phenotype of Hox-C9 expressing neuroblastoma cell lines. The data presented here suggest that a combination of G<sub>0</sub>/G<sub>1</sub>-phase arrest associated with induction of cell differentiation and the initiation of apoptotic processes lead to the favorable phenotype of neuroblastoma with high *HOXC9* expression. Such a broad spectrum of regulatory effects is not uncommon for transcriptional regulators (257-259) and has been described for *HOX* genes in particular (reviewed in (179)).

## **5.4 *HOXC9* expression and the association with spontaneous tumor regression in neuroblastoma**

Neuroblastoma is an embryonal tumor derived from fetal precursors of the sympathetic nervous system, and has the highest frequency of spontaneous regression observed in human malignancies. Mass screening studies for neuroblastoma conducted in the 1990's resulted in a substantially increased incidence of neuroblastoma cases. These results led to the suggestion that spontaneous regression of neuroblastoma occurs far more often than previously thought, and that the cases detected by mass screening studies represent neuroblastomas that would have never become clinically evident. It has thus been suggested that spontaneous regression may represent a delayed activation of developmentally regulated apoptotic pathways (99, 100). However, the molecular mechanisms of this peculiar phenomenon have remained enigmatic. Since expression of Hox transcription factor genes is tightly regulated during embryogenesis and fundamental for a normal embryonic development, I hypothesized a role

of these genes in neuroblastoma pathogenesis in general and in spontaneous regression in particular. I found that elevated *HOXC9* expression is not only associated with favorable prognostic markers and beneficial outcome in primary neuroblastoma, but also correlates with spontaneous tumor regression. Molecularly, spontaneous regressing neuroblastomas are characterized by a near-triploid DNA content and absence of structural chromosomal alterations (57, 260). Considering the correlation of high *HOXC9* expression with favorable molecular characteristics of the tumor, favorable patient outcome and spontaneous regression, and its pro-apoptotic function in neuroblastoma cells, I hypothesize that Hox-C9 may represent a critical factor for the process of spontaneous regression in neuroblastoma.

## 6 Conclusion

In summary, I here demonstrate that distinct *HOX* gene expression patterns are associated with clinical phenotypes of neuroblastoma. I show that *HOXC9* expression does not only correlate with favorable prognostic markers and beneficial clinical outcome, but also with spontaneous regression in infant neuroblastoma. Re-expression of *HOXC9* in neuroblastoma cell lines consistently leads to strong growth arrest and activates the intrinsic pathway of apoptosis. Taken together, I conclude from these data that *HOX* genes may contribute to neuroblastoma pathogenesis, and that Hox-C9 might be involved in the molecular process of spontaneous regression.

---

## 7 References

1. Maris JM, Hogarty MD, Bagatell R, Cohn SL. Neuroblastoma. *Lancet* 2007;369(9579):2106-20.
2. van Noesel MM, Versteeg R. Pediatric neuroblastomas: genetic and epigenetic 'danse macabre'. *Gene* 2004;325:1-15.
3. Westermann F, Schwab M. Genetic parameters of neuroblastomas. *Cancer Lett* 2002;184(2):127-47.
4. Maris JM, Matthay KK. Molecular biology of neuroblastoma. *J Clin Oncol* 1999;17(7):2264-79.
5. Cooper MJ, Hutchins GM, Cohen PS, Helman LJ, Mennie RJ, Israel MA. Human neuroblastoma tumor cell lines correspond to the arrested differentiation of chromaffin adrenal medullary neuroblasts. *Cell Growth Differ* 1990;1(4):149-59.
6. Hoehner JC, Gestblom C, Hedborg F, Sandstedt B, Olsen L, Pahlman S. A developmental model of neuroblastoma: differentiating stroma-poor tumors' progress along an extra-adrenal chromaffin lineage. *Lab Invest* 1996;75(5):659-75.
7. Nakagawara A, Arima-Nakagawara M, Scavarda NJ, Azar CG, Cantor AB, Brodeur GM. Association between high levels of expression of the TRK gene and favorable outcome in human neuroblastoma. *N Engl J Med* 1993;328(12):847-54.
8. Brodeur GM, Pritchard J, Berthold F, *et al.* Revisions of the international criteria for neuroblastoma diagnosis, staging, and response to treatment. *J Clin Oncol* 1993;11(8):1466-77.
9. D'Angio GJ, Evans AE, Koop CE. Special pattern of widespread neuroblastoma with a favourable prognosis. *Lancet* 1971;1(7708):1046-9.
10. Oberthuer A, Theissen J, Westermann F, Hero B, Fischer M. Molecular characterization and classification of neuroblastoma. *Future Oncol* 2009;5(5):625-39.
11. Evans AE, D'Angio GJ, Randolph J. A proposed staging for children with neuroblastoma. *Children's cancer study group A. Cancer* 1971;27(2):374-8.
12. London WB, Castleberry RP, Matthay KK, *et al.* Evidence for an age cutoff greater than 365 days for neuroblastoma risk group stratification in the Children's Oncology Group. *J Clin Oncol* 2005;23(27):6459-65.
13. Brodeur GM, Seeger RC, Schwab M, Varmus HE, Bishop JM. Amplification of N-myc in untreated human neuroblastomas correlates with advanced disease stage. *Science* 1984;224(4653):1121-4.
14. Brodeur GM, Seeger RC, Barrett A, *et al.* International criteria for diagnosis, staging, and response to treatment in patients with neuroblastoma. *J Clin Oncol* 1988;6(12):1874-81.
15. Cohn SL, Pearson AD, London WB, *et al.* The International Neuroblastoma Risk Group (INRG) classification system: an INRG Task Force report. *J Clin Oncol* 2009;27(2):289-97.
16. Shimada H, Ambros IM, Dehner LP, *et al.* The International Neuroblastoma Pathology Classification (the Shimada system). *Cancer* 1999;86(2):364-72.
17. Attiyeh EF, London WB, Mosse YP, *et al.* Chromosome 1p and 11q deletions and outcome in neuroblastoma. *N Engl J Med* 2005;353(21):2243-53.
18. Cohn SL, Tweddle DA. MYCN amplification remains prognostically strong 20 years after its "clinical debut". *Eur J Cancer* 2004;40(18):2639-42.
19. Look AT, Hayes FA, Nitschke R, McWilliams NB, Green AA. Cellular DNA content as a predictor of response to chemotherapy in infants with unresectable neuroblastoma. *N Engl J Med* 1984;311(4):231-5.

20. Oberthuer A, Hero B, Berthold F, *et al.* Prognostic impact of gene expression-based classification for neuroblastoma. *J Clin Oncol* 2010;28(21):3506-15.
21. Brodeur GM. Neuroblastoma: biological insights into a clinical enigma. *Nat Rev Cancer* 2003;3(3):203-16.
22. Maris JM. The biologic basis for neuroblastoma heterogeneity and risk stratification. *Curr Opin Pediatr* 2005;17(1):7-13.
23. Vermeulen J, De Preter K, Naranjo A, *et al.* Predicting outcomes for children with neuroblastoma using a multigene-expression signature: a retrospective SIOPEX/COG/GPOH study. *Lancet Oncol* 2009;10(7):663-71.
24. Asgharzadeh S, Pique-Regi R, Sposto R, *et al.* Prognostic significance of gene expression profiles of metastatic neuroblastomas lacking MYCN gene amplification. *J Natl Cancer Inst* 2006;98(17):1193-203.
25. Oberthuer A, Berthold F, Warnat P, *et al.* Customized oligonucleotide microarray gene expression-based classification of neuroblastoma patients outperforms current clinical risk stratification. *J Clin Oncol* 2006;24(31):5070-8.
26. Oberthuer A, Warnat P, Kahlert Y, *et al.* Classification of neuroblastoma patients by published gene-expression markers reveals a low sensitivity for unfavorable courses of MYCN non-amplified disease. *Cancer Lett* 2007;250(2):250-67.
27. Brodeur GM, Seeger RC. Gene amplification in human neuroblastomas: basic mechanisms and clinical implications. *Cancer Genet Cytogenet* 1986;19(1-2):101-11.
28. Brodeur GM, Hayes FA, Green AA, *et al.* Consistent N-myc copy number in simultaneous or consecutive neuroblastoma samples from sixty individual patients. *Cancer Res* 1987;47(16):4248-53.
29. Schwab M. Amplification of N-myc as a prognostic marker for patients with neuroblastoma. *Semin Cancer Biol* 1993;4(1):13-8.
30. Schwab M, Alitalo K, Klempnauer KH, *et al.* Amplified DNA with limited homology to myc cellular oncogene is shared by human neuroblastoma cell lines and a neuroblastoma tumour. *Nature* 1983;305(5931):245-8.
31. Kohl NE, Gee CE, Alt FW. Activated expression of the N-myc gene in human neuroblastomas and related tumors. *Science* 1984;226(4680):1335-7.
32. Nisen PD, Waber PG, Rich MA, *et al.* N-myc oncogene RNA expression in neuroblastoma. *J Natl Cancer Inst* 1988;80(20):1633-7.
33. Slavic I, Ellenbogen R, Jung WH, *et al.* myc gene amplification and expression in primary human neuroblastoma. *Cancer Res* 1990;50(5):1459-63.
34. Seeger RC, Wada R, Brodeur GM, *et al.* Expression of N-myc by neuroblastomas with one or multiple copies of the oncogene. *Prog Clin Biol Res* 1988;271:41-9.
35. Schwab M, Ellison J, Busch M, Rosenau W, Varmus HE, Bishop JM. Enhanced expression of the human gene N-myc consequent to amplification of DNA may contribute to malignant progression of neuroblastoma. *Proc Natl Acad Sci U S A* 1984;81(15):4940-4.
36. Alaminos M, Mora J, Cheung NK, *et al.* Genome-wide analysis of gene expression associated with MYCN in human neuroblastoma. *Cancer Res* 2003;63(15):4538-46.
37. Berwanger B, Hartmann O, Bergmann E, *et al.* Loss of a FYN-regulated differentiation and growth arrest pathway in advanced stage neuroblastoma. *Cancer Cell* 2002;2(5):377-86.
38. Prescott JE, Osthus RC, Lee LA, *et al.* A novel c-Myc-responsive gene, JPO1, participates in neoplastic transformation. *J Biol Chem* 2001;276(51):48276-84.
39. Chiarle R, Martinengo C, Mastini C, *et al.* The anaplastic lymphoma kinase is an effective oncoantigen for lymphoma vaccination. *Nat Med* 2008;14(6):676-80.
40. Chen Y, Takita J, Choi YL, *et al.* Oncogenic mutations of ALK kinase in neuroblastoma. *Nature* 2008;455(7215):971-4.

41. Janoueix-Lerosey I, Lequin D, Brugieres L, *et al.* Somatic and germline activating mutations of the ALK kinase receptor in neuroblastoma. *Nature* 2008;455(7215):967-70.
42. Mosse YP, Laudenslager M, Longo L, *et al.* Identification of ALK as a major familial neuroblastoma predisposition gene. *Nature* 2008;455(7215):930-5.
43. De Brouwer S, De Preter K, Kumps C, *et al.* Meta-analysis of neuroblastomas reveals a skewed ALK mutation spectrum in tumors with MYCN amplification. *Clin Cancer Res*;16(17):4353-62.
44. Berry T, Luther W, Bhatnagar N, *et al.* The ALK(F1174L) mutation potentiates the oncogenic activity of MYCN in neuroblastoma. *Cancer Cell*;22(1):117-30.
45. Azarova AM, Gautam G, George RE. Emerging importance of ALK in neuroblastoma. *Semin Cancer Biol*;21(4):267-75.
46. Schulte JH, Lindner S, Bohrer A, *et al.* MYCN and ALKF1174L are sufficient to drive neuroblastoma development from neural crest progenitor cells. *Oncogene*.
47. White PS, Maris JM, Beltinger C, *et al.* A region of consistent deletion in neuroblastoma maps within human chromosome 1p36.2-36.3. *Proc Natl Acad Sci U S A* 1995;92(12):5520-4.
48. Gehring M, Berthold F, Edler L, Schwab M, Amler LC. The 1p deletion is not a reliable marker for the prognosis of patients with neuroblastoma. *Cancer Res* 1995;55(22):5366-9.
49. Martinsson T, Sjoberg RM, Hedborg F, Kogner P. Deletion of chromosome 1p loci and microsatellite instability in neuroblastomas analyzed with short-tandem repeat polymorphisms. *Cancer Res* 1995;55(23):5681-6.
50. White PS, Thompson PM, Seifried BA, *et al.* Detailed molecular analysis of 1p36 in neuroblastoma. *Med Pediatr Oncol* 2001;36(1):37-41.
51. White PS, Thompson PM, Gotoh T, *et al.* Definition and characterization of a region of 1p36.3 consistently deleted in neuroblastoma. *Oncogene* 2005;24(16):2684-94.
52. Henrich KO, Fischer M, Mertens D, *et al.* Reduced expression of CAMTA1 correlates with adverse outcome in neuroblastoma patients. *Clin Cancer Res* 2006;12(1):131-8.
53. Okawa ER, Gotoh T, Manne J, *et al.* Expression and sequence analysis of candidates for the 1p36.31 tumor suppressor gene deleted in neuroblastomas. *Oncogene* 2008;27(6):803-10.
54. Wang Q, Diskin S, Rappaport E, *et al.* Integrative genomics identifies distinct molecular classes of neuroblastoma and shows that multiple genes are targeted by regional alterations in DNA copy number. *Cancer Res* 2006;66(12):6050-62.
55. Welch C, Chen Y, Stallings RL. MicroRNA-34a functions as a potential tumor suppressor by inducing apoptosis in neuroblastoma cells. *Oncogene* 2007;26(34):5017-22.
56. Plantaz D, Vandesompele J, Van Roy N, *et al.* Comparative genomic hybridization (CGH) analysis of stage 4 neuroblastoma reveals high frequency of 11q deletion in tumors lacking MYCN amplification. *Int J Cancer* 2001;91(5):680-6.
57. Vandesompele J, Speleman F, Van Roy N, *et al.* Multicentre analysis of patterns of DNA gains and losses in 204 neuroblastoma tumors: how many genetic subgroups are there? *Med Pediatr Oncol* 2001;36(1):5-10.
58. Vandesompele J, Van Roy N, Van Gele M, *et al.* Genetic heterogeneity of neuroblastoma studied by comparative genomic hybridization. *Genes Chromosomes Cancer* 1998;23(2):141-52.
59. Spitz R, Betts DR, Simon T, *et al.* Favorable outcome of triploid neuroblastomas: a contribution to the special oncogenesis of neuroblastoma. *Cancer Genet Cytogenet* 2006;167(1):51-6.
60. Bown N, Cotterill S, Lastowska M, *et al.* Gain of chromosome arm 17q and adverse outcome in patients with neuroblastoma. *N Engl J Med* 1999;340(25):1954-61.

61. Lastowska M, Cullinane C, Variend S, *et al.* Comprehensive genetic and histopathologic study reveals three types of neuroblastoma tumors. *J Clin Oncol* 2001;19(12):3080-90.
62. Spitz R, Hero B, Ernestus K, Berthold F. Gain of distal chromosome arm 17q is not associated with poor prognosis in neuroblastoma. *Clin Cancer Res* 2003;9(13):4835-40.
63. Look AT, Hayes FA, Shuster JJ, *et al.* Clinical relevance of tumor cell ploidy and N-myc gene amplification in childhood neuroblastoma: a Pediatric Oncology Group study. *J Clin Oncol* 1991;9(4):581-91.
64. Oberthuer A, Kaderali L, Kahlert Y, *et al.* Subclassification and individual survival time prediction from gene expression data of neuroblastoma patients by using CASPAR. *Clin Cancer Res* 2008;14(20):6590-601.
65. Kogner P, Barbany G, Dominici C, Castello MA, Raschella G, Persson H. Coexpression of messenger RNA for TRK protooncogene and low affinity nerve growth factor receptor in neuroblastoma with favorable prognosis. *Cancer Res* 1993;53(9):2044-50.
66. Eggert A, Grotzer MA, Zuzak TJ, *et al.* Resistance to tumor necrosis factor-related apoptosis-inducing ligand (TRAIL)-induced apoptosis in neuroblastoma cells correlates with a loss of caspase-8 expression. *Cancer Res* 2001;61(4):1314-9.
67. Teitz T, Wei T, Valentine MB, *et al.* Caspase 8 is deleted or silenced preferentially in childhood neuroblastomas with amplification of MYCN. *Nat Med* 2000;6(5):529-35.
68. Shojaei-Brosseau T, Chompret A, Abel A, *et al.* Genetic epidemiology of neuroblastoma: a study of 426 cases at the Institut Gustave-Roussy in France. *Pediatr Blood Cancer* 2004;42(1):99-105.
69. Maris JM, Kyemba SM, Rebbeck TR, *et al.* Molecular genetic analysis of familial neuroblastoma. *Eur J Cancer* 1997;33(12):1923-8.
70. Amiel J, Laudier B, Attie-Bitach T, *et al.* Polyalanine expansion and frameshift mutations of the paired-like homeobox gene PHOX2B in congenital central hypoventilation syndrome. *Nat Genet* 2003;33(4):459-61.
71. Mosse YP, Laudenslager M, Khazi D, *et al.* Germline PHOX2B mutation in hereditary neuroblastoma. *Am J Hum Genet* 2004;75(4):727-30.
72. van Limpt V, Schramm A, van Lakeman A, *et al.* The Phox2B homeobox gene is mutated in sporadic neuroblastomas. *Oncogene* 2004;23(57):9280-8.
73. O'Rahilly R, Muller F. The development of the neural crest in the human. *J Anat* 2007;211(3):335-51.
74. White PM, Morrison SJ, Orimoto K, Kubu CJ, Verdi JM, Anderson DJ. Neural crest stem cells undergo cell-intrinsic developmental changes in sensitivity to instructive differentiation signals. *Neuron* 2001;29(1):57-71.
75. Nakagawara A, Ohira M. Comprehensive genomics linking between neural development and cancer: neuroblastoma as a model. *Cancer Lett* 2004;204(2):213-24.
76. Shah NM, Anderson DJ. Integration of multiple instructive cues by neural crest stem cells reveals cell-intrinsic biases in relative growth factor responsiveness. *Proc Natl Acad Sci U S A* 1997;94(21):11369-74.
77. Shah NM, Groves AK, Anderson DJ. Alternative neural crest cell fates are instructively promoted by TGFbeta superfamily members. *Cell* 1996;85(3):331-43.
78. Huber K, Bruhl B, Guillemot F, Olson EN, Ernsberger U, Unsicker K. Development of chromaffin cells depends on MASH1 function. *Development* 2002;129(20):4729-38.
79. Anderson DJ. Molecular control of cell fate in the neural crest: the sympathoadrenal lineage. *Annu Rev Neurosci* 1993;16:129-58.
80. Stanke M, Junghans D, Geissen M, Goridis C, Ernsberger U, Rohrer H. The Phox2 homeodomain proteins are sufficient to promote the development of sympathetic neurons. *Development* 1999;126(18):4087-94.

81. Patzke H, Reissmann E, Stanke M, Bixby JL, Ernsberger U. BMP growth factors and Phox2 transcription factors can induce synaptotagmin I and neurexin I during sympathetic neuron development. *Mech Dev* 2001;108(1-2):149-59.
82. Pattyn A, Morin X, Cremer H, Goridis C, Brunet JF. The homeobox gene Phox2b is essential for the development of autonomic neural crest derivatives. *Nature* 1999;399(6734):366-70.
83. Mohlin SA, Wigerup C, Pahlman S. Neuroblastoma aggressiveness in relation to sympathetic neuronal differentiation stage. *Semin Cancer Biol*;21(4):276-82.
84. Voth H, Oberthuer A, Simon T, Kahlert Y, Berthold F, Fischer M. Co-regulated expression of HAND2 and DEIN by a bidirectional promoter with asymmetrical activity in neuroblastoma. *BMC Mol Biol* 2009;10:28.
85. Anderson DJ, Groves A, Lo L, *et al.* Cell lineage determination and the control of neuronal identity in the neural crest. *Cold Spring Harb Symp Quant Biol* 1997;62:493-504.
86. Soderholm H, Ortoft E, Johansson I, *et al.* Human achaete-scute homologue 1 (HASH-1) is downregulated in differentiating neuroblastoma cells. *Biochem Biophys Res Commun* 1999;256(3):557-63.
87. Ichimiya S, Nimura Y, Seki N, Ozaki T, Nagase T, Nakagawara A. Downregulation of hASH1 is associated with the retinoic acid-induced differentiation of human neuroblastoma cell lines. *Med Pediatr Oncol* 2001;36(1):132-4.
88. Hirsch MR, Tiveron MC, Guillemot F, Brunet JF, Goridis C. Control of noradrenergic differentiation and Phox2a expression by MASH1 in the central and peripheral nervous system. *Development* 1998;125(4):599-608.
89. Pattyn A, Morin X, Cremer H, Goridis C, Brunet JF. Expression and interactions of the two closely related homeobox genes Phox2a and Phox2b during neurogenesis. *Development* 1997;124(20):4065-75.
90. Rohrer T, Trachsel D, Engelcke G, Hammer J. Congenital central hypoventilation syndrome associated with Hirschsprung's disease and neuroblastoma: case of multiple neurocristopathies. *Pediatr Pulmonol* 2002;33(1):71-6.
91. Yamashiro DJ, Nakagawara A, Ikegaki N, Liu XG, Brodeur GM. Expression of TrkC in favorable human neuroblastomas. *Oncogene* 1996;12(1):37-41.
92. Beckwith JB, Perrin EV. In Situ Neuroblastomas: A Contribution to the Natural History of Neural Crest Tumors. *Am J Pathol* 1963;43:1089-104.
93. Woods WG, Tuchman M, Robison LL, *et al.* A population-based study of the usefulness of screening for neuroblastoma. *Lancet* 1996;348(9043):1682-7.
94. Kerbl R, Urban CE, Ambros IM, *et al.* Neuroblastoma mass screening in late infancy: insights into the biology of neuroblastic tumors. *J Clin Oncol* 2003;21(22):4228-34.
95. Schilling FH, Spix C, Berthold F, *et al.* Neuroblastoma screening at one year of age. *N Engl J Med* 2002;346(14):1047-53.
96. Bessho F, Hashizume K, Nakajo T, Kamoshita S. Mass screening in Japan increased the detection of infants with neuroblastoma without a decrease in cases in older children. *J Pediatr* 1991;119(2):237-41.
97. Nakagawara A. Molecular basis of spontaneous regression of neuroblastoma: role of neurotrophic signals and genetic abnormalities. *Hum Cell* 1998;11(3):115-24.
98. van Noesel MM. Neuroblastoma stage 4S: a multifocal stem-cell disease of the developing neural crest. *Lancet Oncol*;13(3):229-30.
99. Pritchard J, Hickman JA. Why does stage 4s neuroblastoma regress spontaneously? *Lancet* 1994;344(8926):869-70.
100. Nakagawara A. Neural crest development and neuroblastoma: the genetic and biological link. *Prog Brain Res* 2004;146:233-42.
101. Seeger RC, Brodeur GM, Sather H, *et al.* Association of multiple copies of the N-myc oncogene with rapid progression of neuroblastomas. *N Engl J Med* 1985;313(18):1111-6.

102. Manohar CF, Furtado MR, Salwen HR, Cohn SL. Hox gene expression in differentiating human neuroblastoma cells. *Biochem Mol Biol Int* 1993;30(4):733-41.
103. Gehring WJ, Hiromi Y. Homeotic genes and the homeobox. *Annu Rev Genet* 1986;20:147-73.
104. Abate-Shen C. Deregulated homeobox gene expression in cancer: cause or consequence? *Nat Rev Cancer* 2002;2(10):777-85.
105. Chuai M, Weijer CJ. Regulation of cell migration during chick gastrulation. *Curr Opin Genet Dev* 2009;19(4):343-9.
106. Falaschi A, Abdurashidova G, Biamonti G. DNA replication, development and cancer: a homeotic connection? *Crit Rev Biochem Mol Biol* 2010;45(1):14-22.
107. Serpente P, Tumpel S, Ghyselinck NB, *et al.* Direct crossregulation between retinoic acid receptor {beta} and Hox genes during hindbrain segmentation. *Development* 2005;132(3):503-13.
108. Stobe P, Stein MA, Habring-Muller A, *et al.* Multifactorial regulation of a hox target gene. *PLoS Genet* 2009;5(3):e1000412.
109. van den Akker WM, Durston AJ, Spaink HP. Identification of *hoxb1b* downstream genes: *hoxb1b* as a regulatory factor controlling transcriptional networks and cell movement during zebrafish gastrulation. *Int J Dev Biol* 2010;54(1):55-62.
110. Abdel-Fattah R, Xiao A, Bomgardner D, Pease CS, Lopes MB, Hussaini IM. Differential expression of HOX genes in neoplastic and non-neoplastic human astrocytes. *J Pathol* 2006;209(1):15-24.
111. Nolte C, Krumlauf R. Expression of Hox Genes in the Nervous System of Vertebrates.: Landes Bioscience; 2000.
112. Cantile M, Schiavo G, Terracciano L, Cillo C. Homeobox genes in normal and abnormal vasculogenesis. *Nutr Metab Cardiovasc Dis* 2008;18(10):651-8.
113. Rastegar M, Kobrossy L, Kovacs EN, Rambaldi I, Featherstone M. Sequential histone modifications at *Hoxd4* regulatory regions distinguish anterior from posterior embryonic compartments. *Mol Cell Biol* 2004;24(18):8090-103.
114. Barber BA, Rastegar M. Epigenetic control of Hox genes during neurogenesis, development, and disease. *Ann Anat* 2010;192(5):261-74.
115. Bel-Vialar S, Itasaki N, Krumlauf R. Initiating Hox gene expression: in the early chick neural tube differential sensitivity to FGF and RA signaling subdivides the HoxB genes in two distinct groups. *Development* 2002;129(22):5103-15.
116. Nordstrom U, Maier E, Jessell TM, Edlund T. An early role for WNT signaling in specifying neural patterns of *Cdx* and *Hox* gene expression and motor neuron subtype identity. *PLoS Biol* 2006;4(8):e252.
117. Simeone A, Acampora D, Arcioni L, Andrews PW, Boncinelli E, Mavilio F. Sequential activation of HOX2 homeobox genes by retinoic acid in human embryonal carcinoma cells. *Nature* 1990;346(6286):763-6.
118. Diez del Corral R, Breitkreuz DN, Storey KG. Onset of neuronal differentiation is regulated by paraxial mesoderm and requires attenuation of FGF signalling. *Development* 2002;129(7):1681-91.
119. Diez del Corral R, Olivera-Martinez I, Goriely A, Gale E, Maden M, Storey K. Opposing FGF and retinoid pathways control ventral neural pattern, neuronal differentiation, and segmentation during body axis extension. *Neuron* 2003;40(1):65-79.
120. Han L, Witmer PD, Casey E, Valle D, Sukumar S. DNA methylation regulates MicroRNA expression. *Cancer Biol Ther* 2007;6(8):1284-8.
121. Sessa L, Breiling A, Lavorgna G, Silvestri L, Casari G, Orlando V. Noncoding RNA synthesis and loss of Polycomb group repression accompanies the colinear activation of the human HOXA cluster. *RNA* 2007;13(2):223-39.

122. Sasaki YT, Sano M, Kin T, Asai K, Hirose T. Coordinated expression of ncRNAs and HOX mRNAs in the human HOXA locus. *Biochem Biophys Res Commun* 2007;357(3):724-30.
123. Rinn JL, Kertesz M, Wang JK, *et al.* Functional demarcation of active and silent chromatin domains in human HOX loci by noncoding RNAs. *Cell* 2007;129(7):1311-23.
124. Manzanares M, Bel-Vialar S, Ariza-McNaughton L, *et al.* Independent regulation of initiation and maintenance phases of Hoxa3 expression in the vertebrate hindbrain involve auto- and cross-regulatory mechanisms. *Development* 2001;128(18):3595-607.
125. Gould A, Morrison A, Sproat G, White RA, Krumlauf R. Positive cross-regulation and enhancer sharing: two mechanisms for specifying overlapping Hox expression patterns. *Genes Dev* 1997;11(7):900-13.
126. Arcioni L, Simeone A, Guazzi S, Zappavigna V, Boncinelli E, Mavilio F. The upstream region of the human homeobox gene HOX3D is a target for regulation by retinoic acid and HOX homeoproteins. *EMBO J* 1992;11(1):265-77.
127. Moens CB, Selleri L. Hox cofactors in vertebrate development. *Dev Biol* 2006;291(2):193-206.
128. Chang CP, Shen WF, Rozenfeld S, Lawrence HJ, Largman C, Cleary ML. Pbx proteins display hexapeptide-dependent cooperative DNA binding with a subset of Hox proteins. *Genes Dev* 1995;9(6):663-74.
129. Lu Q, Knoepfler PS, Scheele J, Wright DD, Kamps MP. Both Pbx1 and E2A-Pbx1 bind the DNA motif ATCAATCAA cooperatively with the products of multiple murine Hox genes, some of which are themselves oncogenes. *Mol Cell Biol* 1995;15(7):3786-95.
130. Neuteboom ST, Peltenburg LT, van Dijk MA, Murre C. The hexapeptide LFPWMR in Hoxb-8 is required for cooperative DNA binding with Pbx1 and Pbx2 proteins. *Proc Natl Acad Sci U S A* 1995;92(20):9166-70.
131. Phelan ML, Featherstone MS. Distinct HOX N-terminal arm residues are responsible for specificity of DNA recognition by HOX monomers and HOX.PBX heterodimers. *J Biol Chem* 1997;272(13):8635-43.
132. Shen WF, Montgomery JC, Rozenfeld S, *et al.* AbdB-like Hox proteins stabilize DNA binding by the Meis1 homeodomain proteins. *Mol Cell Biol* 1997;17(11):6448-58.
133. Moskow JJ, Bullrich F, Huebner K, Daar IO, Buchberg AM. Meis1, a PBX1-related homeobox gene involved in myeloid leukemia in BXH-2 mice. *Mol Cell Biol* 1995;15(10):5434-43.
134. Huang H, Rastegar M, Bodner C, Goh SL, Rambaldi I, Featherstone M. MEIS C termini harbor transcriptional activation domains that respond to cell signaling. *J Biol Chem* 2005;280(11):10119-27.
135. Spieker N, van Sluis P, Beitsma M, *et al.* The MEIS1 oncogene is highly expressed in neuroblastoma and amplified in cell line IMR32. *Genomics* 2001;71(2):214-21.
136. Muragaki Y, Mundlos S, Upton J, Olsen BR. Altered growth and branching patterns in synpolydactyly caused by mutations in HOXD13. *Science* 1996;272(5261):548-51.
137. Mortlock DP, Innis JW. Mutation of HOXA13 in hand-foot-genital syndrome. *Nat Genet* 1997;15(2):179-80.
138. Utsch B, McCabe CD, Galbraith K, *et al.* Molecular characterization of HOXA13 polyalanine expansion proteins in hand-foot-genital syndrome. *Am J Med Genet A* 2007;143A(24):3161-8.
139. Dobbs MB, Gurnett CA, Pierce B, *et al.* HOXD10 M319K mutation in a family with isolated congenital vertical talus. *J Orthop Res* 2006;24(3):448-53.
140. Ester AR, Weymouth KS, Burt A, *et al.* Altered transmission of HOX and apoptotic SNPs identify a potential common pathway for clubfoot. *Am J Med Genet A* 2009;149A(12):2745-52.

141. Thompson AA, Nguyen LT. Amegakaryocytic thrombocytopenia and radio-ulnar synostosis are associated with HOXA11 mutation. *Nat Genet* 2000;26(4):397-8.
142. Tischfield MA, Bosley TM, Salih MA, *et al.* Homozygous HOXA1 mutations disrupt human brainstem, inner ear, cardiovascular and cognitive development. *Nat Genet* 2005;37(10):1035-7.
143. Bodey B, Bodey B, Jr., Siegel SE, Kaiser HE. Immunocytochemical detection of the homeobox B3, B4, and C6 gene products in breast carcinomas. *Anticancer Res* 2000;20(5A):3281-6.
144. Hung YC, Ueda M, Terai Y, *et al.* Homeobox gene expression and mutation in cervical carcinoma cells. *Cancer Sci* 2003;94(5):437-41.
145. Jung C, Kim RS, Lee SJ, Wang C, Jeng MH. HOXB13 homeodomain protein suppresses the growth of prostate cancer cells by the negative regulation of T-cell factor 4. *Cancer Res* 2004;64(9):3046-51.
146. Economides KD, Capecchi MR. Hoxb13 is required for normal differentiation and secretory function of the ventral prostate. *Development* 2003;130(10):2061-9.
147. Wang Z, Dahiya S, Provencher H, *et al.* The prognostic biomarkers HOXB13, IL17BR, and CHDH are regulated by estrogen in breast cancer. *Clin Cancer Res* 2007;13(21):6327-34.
148. Zhang X, Hamada J, Nishimoto A, *et al.* HOXC6 and HOXC11 increase transcription of S100beta gene in BrdU-induced in vitro differentiation of GOTO neuroblastoma cells into Schwannian cells. *J Cell Mol Med* 2007;11(2):299-306.
149. Armstrong SA, Golub TR, Korsmeyer SJ. MLL-rearranged leukemias: insights from gene expression profiling. *Semin Hematol* 2003;40(4):268-73.
150. Argiropoulos B, Humphries RK. Hox genes in hematopoiesis and leukemogenesis. *Oncogene* 2007;26(47):6766-76.
151. Tedeschi FA, Zalazar FE. HOXA9 gene expression in the chronic myeloid leukemia progression. *Leuk Res* 2006;30(11):1453-6.
152. Golub TR, Slonim DK, Tamayo P, *et al.* Molecular classification of cancer: class discovery and class prediction by gene expression monitoring. *Science* 1999;286(5439):531-7.
153. Takahashi O, Hamada J, Abe M, *et al.* Dysregulated expression of HOX and ParaHOX genes in human esophageal squamous cell carcinoma. *Oncol Rep* 2007;17(4):753-60.
154. Abe M, Hamada J, Takahashi O, *et al.* Disordered expression of HOX genes in human non-small cell lung cancer. *Oncol Rep* 2006;15(4):797-802.
155. Rauch T, Wang Z, Zhang X, *et al.* Homeobox gene methylation in lung cancer studied by genome-wide analysis with a microarray-based methylated CpG island recovery assay. *Proc Natl Acad Sci U S A* 2007;104(13):5527-32.
156. Manohar CF, Salwen HR, Furtado MR, Cohn SL. Up-regulation of HOXC6, HOXD1, and HOXD8 homeobox gene expression in human neuroblastoma cells following chemical induction of differentiation. *Tumour Biol* 1996;17(1):34-47.
157. Miao J, Wang Z, Provencher H, *et al.* HOXB13 promotes ovarian cancer progression. *Proc Natl Acad Sci U S A* 2007;104(43):17093-8.
158. Hong JH, Lee JK, Park JJ, Lee NW, Lee KW, Na JY. Expression pattern of the class I homeobox genes in ovarian carcinoma. *J Gynecol Oncol*;21(1):29-37.
159. Alami Y, Castronovo V, Belotti D, Flagiello D, Clause N. HOXC5 and HOXC8 expression are selectively turned on in human cervical cancer cells compared to normal keratinocytes. *Biochem Biophys Res Commun* 1999;257(3):738-45.
160. Zhai Y, Kuick R, Nan B, *et al.* Gene expression analysis of preinvasive and invasive cervical squamous cell carcinomas identifies HOXC10 as a key mediator of invasion. *Cancer Res* 2007;67(21):10163-72.

161. Jung C, Kim RS, Zhang HJ, Lee SJ, Jeng MH. HOXB13 induces growth suppression of prostate cancer cells as a repressor of hormone-activated androgen receptor signaling. *Cancer Res* 2004;64(24):9185-92.
162. Waltregny D, Alami Y, Clausse N, de Leval J, Castronovo V. Overexpression of the homeobox gene HOXC8 in human prostate cancer correlates with loss of tumor differentiation. *Prostate* 2002;50(3):162-9.
163. Chen H, Zhang H, Lee J, *et al.* HOXA5 acts directly downstream of retinoic acid receptor beta and contributes to retinoic acid-induced apoptosis and growth inhibition. *Cancer Res* 2007;67(17):8007-13.
164. Raman V, Martensen SA, Reisman D, *et al.* Compromised HOXA5 function can limit p53 expression in human breast tumours. *Nature* 2000;405(6789):974-8.
165. Chen H, Chung S, Sukumar S. HOXA5-induced apoptosis in breast cancer cells is mediated by caspases 2 and 8. *Mol Cell Biol* 2004;24(2):924-35.
166. Chu MC, Selam FB, Taylor HS. HOXA10 regulates p53 expression and matrigel invasion in human breast cancer cells. *Cancer Biol Ther* 2004;3(6):568-72.
167. Rubin E, Wu X, Zhu T, *et al.* A role for the HOXB7 homeodomain protein in DNA repair. *Cancer Res* 2007;67(4):1527-35.
168. Chen H, Lee JS, Liang X, *et al.* Hoxb7 inhibits transgenic HER-2/neu-induced mouse mammary tumor onset but promotes progression and lung metastasis. *Cancer Res* 2008;68(10):3637-44.
169. Wu X, Chen H, Parker B, *et al.* HOXB7, a homeodomain protein, is overexpressed in breast cancer and confers epithelial-mesenchymal transition. *Cancer Res* 2006;66(19):9527-34.
170. Ma XJ, Wang Z, Ryan PD, *et al.* A two-gene expression ratio predicts clinical outcome in breast cancer patients treated with tamoxifen. *Cancer Cell* 2004;5(6):607-16.
171. Jerevall PL, Brommesson S, Strand C, *et al.* Exploring the two-gene ratio in breast cancer--independent roles for HOXB13 and IL17BR in prediction of clinical outcome. *Breast Cancer Res Treat* 2008;107(2):225-34.
172. Armstrong SA, Staunton JE, Silverman LB, *et al.* MLL translocations specify a distinct gene expression profile that distinguishes a unique leukemia. *Nat Genet* 2002;30(1):41-7.
173. Faber J, Krivtsov AV, Stubbs MC, *et al.* HOXA9 is required for survival in human MLL-rearranged acute leukemias. *Blood* 2009;113(11):2375-85.
174. Ghannam G, Takeda A, Camarata T, Moore MA, Viale A, Yaseen NR. The oncogene Nup98-HOXA9 induces gene transcription in myeloid cells. *J Biol Chem* 2004;279(2):866-75.
175. Kawagoe H, Humphries RK, Blair A, Sutherland HJ, Hogge DE. Expression of HOX genes, HOX cofactors, and MLL in phenotypically and functionally defined subpopulations of leukemic and normal human hematopoietic cells. *Leukemia* 1999;13(5):687-98.
176. Jung C, Kim RS, Zhang H, *et al.* HOXB13 is downregulated in colorectal cancer to confer TCF4-mediated transactivation. *Br J Cancer* 2005;92(12):2233-9.
177. Cillo C, Barba P, Freschi G, Bucciarelli G, Magli MC, Boncinelli E. HOX gene expression in normal and neoplastic human kidney. *Int J Cancer* 1992;51(6):892-7.
178. Buccoliero AM, Castiglione F, Rossi Degl'Innocenti D, *et al.* Hox-D genes expression in pediatric low-grade gliomas: real-time-PCR study. *Cell Mol Neurobiol* 2009;29(1):1-6.
179. Shah N, Sukumar S. The Hox genes and their roles in oncogenesis. *Nat Rev Cancer* 2010;10(5):361-71.
180. Abbracchio MP, Cattabeni F, Clementi F, Sher E. Adenosine receptors linked to adenylate cyclase activity in human neuroblastoma cells: modulation during cell differentiation. *Neuroscience* 1989;30(3):819-25.

- 
181. Horii Y, Sugimoto T, Sawada T, Imanishi J, Tsuboi K, Hatanaka M. Differential expression of N-myc and c-src proto-oncogenes during neuronal and schwannian differentiation of human neuroblastoma cells. *Int J Cancer* 1989;43(2):305-9.
  182. Cushing H, Wolbach SB. The Transformation of a Malignant Paravertebral Sympathicoblastoma into a Benign Ganglioneuroma. *Am J Pathol* 1927;3(3):203-16 7.
  183. Shimada H, Ambros IM, Dehner LP, Hata J, Joshi VV, Roald B. Terminology and morphologic criteria of neuroblastic tumors: recommendations by the International Neuroblastoma Pathology Committee. *Cancer* 1999;86(2):349-63.
  184. Peverali FA, D'Esposito M, Acampora D, *et al.* Expression of HOX homeogenes in human neuroblastoma cell culture lines. *Differentiation* 1990;45(1):61-9.
  185. Zha Y, Ding E, Yang L, *et al.* Functional dissection of HOXD cluster genes in regulation of neuroblastoma cell proliferation and differentiation. *PLoS One*;7(8):e40728.
  186. Jung H, Lacombe J, Mazzoni EO, *et al.* Global control of motor neuron topography mediated by the repressive actions of a single hox gene. *Neuron*;67(5):781-96.
  187. Miano JM, Firulli AB, Olson EN, Hara P, Giachelli CM, Schwartz SM. Restricted expression of homeobox genes distinguishes fetal from adult human smooth muscle cells. *Proc Natl Acad Sci U S A* 1996;93(2):900-5.
  188. Chung N, Jee BK, Chae SW, Jeon YW, Lee KH, Rha HK. HOX gene analysis of endothelial cell differentiation in human bone marrow-derived mesenchymal stem cells. *Mol Biol Rep* 2009;36(2):227-35.
  189. Pruett ND, Visconti RP, Jacobs DF, *et al.* Evidence for Hox-specified positional identities in adult vasculature. *BMC Dev Biol* 2008;8:93.
  190. Thisse B, Heyer V, Lux A, *et al.* Spatial and temporal expression of the zebrafish genome by large-scale in situ hybridization screening. *Methods Cell Biol* 2004;77:505-19.
  191. Korff T, Augustin HG. Integration of endothelial cells in multicellular spheroids prevents apoptosis and induces differentiation. *J Cell Biol* 1998;143(5):1341-52.
  192. Stoll SJ, Bartsch S, Augustin HG, Kroll J. The transcription factor HOXC9 regulates endothelial cell quiescence and vascular morphogenesis in zebrafish via inhibition of interleukin 8. *Circ Res*;108(11):1367-77.
  193. Kikuyama M, Takeshima H, Kinoshita T, *et al.* Development of a novel approach, the epigenome-based outlier approach, to identify tumor-suppressor genes silenced by aberrant DNA methylation. *Cancer Lett*;322(2):204-12.
  194. Lin Q, Geng J, Ma K, *et al.* RASSF1A, APC, ESR1, ABCB1 and HOXC9, but not p16INK4A, DAPK1, PTEN and MT1G genes were frequently methylated in the stage I non-small cell lung cancer in China. *J Cancer Res Clin Oncol* 2009;135(12):1675-84.
  195. Mao L, Ding J, Zha Y, *et al.* HOXC9 links cell-cycle exit and neuronal differentiation and is a prognostic marker in neuroblastoma. *Cancer Res*;71(12):4314-24.
  196. Lopez R, Garrido E, Vazquez G, *et al.* A subgroup of HOX Abd-B gene is differentially expressed in cervical cancer. *Int J Gynecol Cancer* 2006;16(3):1289-96.
  197. Okamoto OK, Oba-Shinjo SM, Lopes L, Nagahashi Marie SK. Expression of HOXC9 and E2F2 are up-regulated in CD133(+) cells isolated from human astrocytomas and associate with transformation of human astrocytes. *Biochim Biophys Acta* 2007;1769(7-8):437-42.
  198. Suemori H, Takahashi N, Noguchi S. Hoxc-9 mutant mice show anterior transformation of the vertebrae and malformation of the sternum and ribs. *Mech Dev* 1995;51(2-3):265-73.
  199. Hero B, Simon T, Spitz R, *et al.* Localized infant neuroblastomas often show spontaneous regression: results of the prospective trials NB95-S and NB97. *J Clin Oncol* 2008;26(9):1504-10.
  200. Bolstad BM, Irizarry RA, Astrand M, Speed TP. A comparison of normalization methods for high density oligonucleotide array data based on variance and bias. *Bioinformatics* 2003;19(2):185-93.

- 
201. Tibshirani R, Hastie T, Narasimhan B, Chu G. Diagnosis of multiple cancer types by shrunken centroids of gene expression. *Proc Natl Acad Sci U S A* 2002;99(10):6567-72.
  202. Li X, Rao S, Wang Y, Gong B. Gene mining: a novel and powerful ensemble decision approach to hunting for disease genes using microarray expression profiling. *Nucleic Acids Res* 2004;32(9):2685-94.
  203. Vapnik VN. An overview of statistical learning theory. *IEEE Trans Neural Netw* 1999;10(5):988-99.
  204. Zhang B, Schmoyer D, Kirov S, Snoddy J. GOTree Machine (GOTM): a web-based platform for interpreting sets of interesting genes using Gene Ontology hierarchies. *BMC Bioinformatics* 2004;5:16.
  205. Spitz R, Oberthuer A, Zapatka M, *et al.* Oligonucleotide array-based comparative genomic hybridization (aCGH) of 90 neuroblastomas reveals aberration patterns closely associated with relapse pattern and outcome. *Genes Chromosomes Cancer* 2006;45(12):1130-42.
  206. Fischer M, Bauer T, Oberthuer A, *et al.* Integrated genomic profiling identifies two distinct molecular subtypes with divergent outcome in neuroblastoma with loss of chromosome 11q. *Oncogene* 2009.
  207. Venkatraman ES, Olshen AB. A faster circular binary segmentation algorithm for the analysis of array CGH data. *Bioinformatics* 2007;23(6):657-63.
  208. Robinson JT, Thorvaldsdottir H, Winckler W, *et al.* Integrative genomics viewer. *Nat Biotechnol*;29(1):24-6.
  209. Sugimoto T, Tatsumi E, Kemshead JT, Helson L, Green AA, Minowada J. Determination of cell surface membrane antigens common to both human neuroblastoma and leukemia-lymphoma cell lines by a panel of 38 monoclonal antibodies. *J Natl Cancer Inst* 1984;73(1):51-7.
  210. Tumilowicz JJ, Nichols WW, Cholon JJ, Greene AE. Definition of a continuous human cell line derived from neuroblastoma. *Cancer Res* 1970;30(8):2110-8.
  211. Schlesinger HR, Gerson JM, Moorhead PS, Maguire H, Hummeler K. Establishment and characterization of human neuroblastoma cell lines. *Cancer Res* 1976;36(9 pt.1):3094-100.
  212. Otto FJ. High-resolution analysis of nuclear DNA employing the fluorochrome DAPI. *Methods Cell Biol* 1994;41:211-7.
  213. Nicoletti I, Migliorati G, Pagliacci MC, Grignani F, Riccardi C. A rapid and simple method for measuring thymocyte apoptosis by propidium iodide staining and flow cytometry. *J Immunol Methods* 1991;139(2):271-9.
  214. Ehrich M, Nelson MR, Stanssens P, *et al.* Quantitative high-throughput analysis of DNA methylation patterns by base-specific cleavage and mass spectrometry. *Proc Natl Acad Sci U S A* 2005;102(44):15785-90.
  215. Sanger F, Nicklen S, Coulson AR. DNA sequencing with chain-terminating inhibitors. *Proc Natl Acad Sci U S A* 1977;74(12):5463-7.
  216. Schambach A, Wodrich H, Hildinger M, Bohne J, Krausslich HG, Baum C. Context dependence of different modules for posttranscriptional enhancement of gene expression from retroviral vectors. *Mol Ther* 2000;2(5):435-45.
  217. Gossen M, Bujard H. Tight control of gene expression in mammalian cells by tetracycline-responsive promoters. *Proc Natl Acad Sci U S A* 1992;89(12):5547-51.
  218. Strathdee CA, McLeod MR, Hall JR. Efficient control of tetracycline-responsive gene expression from an autoregulated bi-directional expression vector. *Gene* 1999;229(1-2):21-9.
  219. Fouchier RA, Meyer BE, Simon JH, Fischer U, Malim MH. HIV-1 infection of non-dividing cells: evidence that the amino-terminal basic region of the viral matrix protein is important for Gag processing but not for post-entry nuclear import. *EMBO J* 1997;16(15):4531-9.

220. Howard BD, Boenicke L, Schniewind B, Henne-Bruns D, Kalthoff H. Transduction of human pancreatic tumor cells with vesicular stomatitis virus G-pseudotyped retroviral vectors containing a herpes simplex virus thymidine kinase mutant gene enhances bystander effects and sensitivity to ganciclovir. *Cancer Gene Ther* 2000;7(6):927-38.
221. Ackermann S, Goeser F, Schulte JH, *et al.* Polo-like kinase 1 is a therapeutic target in high-risk neuroblastoma. *Clin Cancer Res* 2011;17(4):731-41.
222. Kocak H, Ackermann S, Hero B, *et al.* Hox-C9 activates the intrinsic pathway of apoptosis and is associated with spontaneous regression in neuroblastoma. *Cell Death Dis*;4:e586.
223. Shimada H, Chatten J, Newton WA, Jr., *et al.* Histopathologic prognostic factors in neuroblastic tumors: definition of subtypes of ganglioneuroblastoma and an age-linked classification of neuroblastomas. *J Natl Cancer Inst* 1984;73(2):405-16.
224. Hughes M, Marsden HB, Palmer MK. Histologic patterns of neuroblastoma related to prognosis and clinical staging. *Cancer* 1974;34(5):1706-11.
225. Joshi VV, Cantor AB, Altshuler G, *et al.* Recommendations for modification of terminology of neuroblastic tumors and prognostic significance of Shimada classification. A clinicopathologic study of 213 cases from the Pediatric Oncology Group. *Cancer* 1992;69(8):2183-96.
226. Nakagawara A, Milbrandt J, Muramatsu T, *et al.* Differential expression of pleiotrophin and midkine in advanced neuroblastomas. *Cancer Res* 1995;55(8):1792-7.
227. Li R, Morris SW. Development of anaplastic lymphoma kinase (ALK) small-molecule inhibitors for cancer therapy. *Med Res Rev* 2008;28(3):372-412.
228. Li YS, Milner PG, Chauhan AK, *et al.* Cloning and expression of a developmentally regulated protein that induces mitogenic and neurite outgrowth activity. *Science* 1990;250(4988):1690-4.
229. Higashi M, Tajiri T, Kinoshita Y, *et al.* High expressions of neuronatin isoforms in favorable neuroblastoma. *J Pediatr Hematol Oncol* 2007;29(8):551-6.
230. Ho R, Minturn JE, Simpson AM, *et al.* The effect of P75 on Trk receptors in neuroblastomas. *Cancer Lett*;305(1):76-85.
231. Sun P, Xia S, Lal B, *et al.* DNER, an epigenetically modulated gene, regulates glioblastoma-derived neurosphere cell differentiation and tumor propagation. *Stem Cells* 2009;27(7):1473-86.
232. Schulte JH, Kirfel J, Lim S, *et al.* Transcription factor AP2alpha (TFAP2a) regulates differentiation and proliferation of neuroblastoma cells. *Cancer Lett* 2008;271(1):56-63.
233. Liu X, Kim CN, Yang J, Jemmerson R, Wang X. Induction of apoptotic program in cell-free extracts: requirement for dATP and cytochrome c. *Cell* 1996;86(1):147-57.
234. Kocak H, Ackermann S, Hero B, *et al.* Hox-C9 activates the intrinsic pathway of apoptosis and is associated with spontaneous regression in neuroblastoma. *Cell Death Dis* 2013;4:e586.
235. Merrill RA, Ahrens JM, Kaiser ME, Federhart KS, Poon VY, Clagett-Dame M. All-trans retinoic acid-responsive genes identified in the human SH-SY5Y neuroblastoma cell line and their regulated expression in the nervous system of early embryos. *Biol Chem* 2004;385(7):605-14.
236. Graham A, Papalopulu N, Krumlauf R. The murine and *Drosophila* homeobox gene complexes have common features of organization and expression. *Cell* 1989;57(3):367-78.
237. Lewis EB. A gene complex controlling segmentation in *Drosophila*. *Nature* 1978;276(5688):565-70.
238. Chen QR, Bilke S, Wei JS, *et al.* cDNA array-CGH profiling identifies genomic alterations specific to stage and MYCN-amplification in neuroblastoma. *BMC Genomics* 2004;5:70.

- 
239. Coco S, Theissen J, Scaruffi P, *et al.* Age-dependent accumulation of genomic aberrations and deregulation of cell cycle and telomerase genes in metastatic neuroblastoma. *Int J Cancer*.
240. Janoueix-Lerosey I, Schleiermacher G, Michels E, *et al.* Overall genomic pattern is a predictor of outcome in neuroblastoma. *J Clin Oncol* 2009;27(7):1026-33.
241. Yekta S, Tabin CJ, Bartel DP. MicroRNAs in the Hox network: an apparent link to posterior prevalence. *Nat Rev Genet* 2008;9(10):789-96.
242. Varlakhanova N, Cotterman R, Bradnam K, Korf I, Knoepfler PS. Myc and Miz-1 have coordinate genomic functions including targeting Hox genes in human embryonic stem cells. *Epigenetics Chromatin*;4:20.
243. Matthay KK, Villablanca JG, Seeger RC, *et al.* Treatment of high-risk neuroblastoma with intensive chemotherapy, radiotherapy, autologous bone marrow transplantation, and 13-cis-retinoic acid. Children's Cancer Group. *N Engl J Med* 1999;341(16):1165-73.
244. Galderisi U, Jori FP, Giordano A. Cell cycle regulation and neural differentiation. *Oncogene* 2003;22(33):5208-19.
245. Gao Z, Ure K, Ding P, *et al.* The master negative regulator REST/NRSF controls adult neurogenesis by restraining the neurogenic program in quiescent stem cells. *J Neurosci*;31(26):9772-86.
246. Singh A, Rokes C, Gireud M, *et al.* Retinoic acid induces REST degradation and neuronal differentiation by modulating the expression of SCF(beta-TRCP) in neuroblastoma cells. *Cancer*;117(22):5189-202.
247. Coulson JM, Edgson JL, Woll PJ, Quinn JP. A splice variant of the neuron-restrictive silencer factor repressor is expressed in small cell lung cancer: a potential role in derepression of neuroendocrine genes and a useful clinical marker. *Cancer Res* 2000;60(7):1840-4.
248. Reddy BY, Greco SJ, Patel PS, Trzaska KA, Rameshwar P. RE-1-silencing transcription factor shows tumor-suppressor functions and negatively regulates the oncogenic TAC1 in breast cancer cells. *Proc Natl Acad Sci U S A* 2009;106(11):4408-13.
249. Palm K, Metsis M, Timmusk T. Neuron-specific splicing of zinc finger transcription factor REST/NRSF/XBR is frequent in neuroblastomas and conserved in human, mouse and rat. *Brain Res Mol Brain Res* 1999;72(1):30-9.
250. Lawinger P, Venugopal R, Guo ZS, *et al.* The neuronal repressor REST/NRSF is an essential regulator in medulloblastoma cells. *Nat Med* 2000;6(7):826-31.
251. Gopalakrishnan V. REST and the RESTless: in stem cells and beyond. *Future Neurol* 2009;4(3):317-29.
252. Kagalwala MN, Singh SK, Majumder S. Stemness is only a state of the cell. *Cold Spring Harb Symp Quant Biol* 2008;73:227-34.
253. Ballas N, Mandel G. The many faces of REST oversee epigenetic programming of neuronal genes. *Curr Opin Neurobiol* 2005;15(5):500-6.
254. Schoenherr CJ, Anderson DJ. The neuron-restrictive silencer factor (NRSF): a coordinate repressor of multiple neuron-specific genes. *Science* 1995;267(5202):1360-3.
255. Ballas N, Grunseich C, Lu DD, Speh JC, Mandel G. REST and its corepressors mediate plasticity of neuronal gene chromatin throughout neurogenesis. *Cell* 2005;121(4):645-57.
256. Westbrook TF, Hu G, Ang XL, *et al.* SCFbeta-TRCP controls oncogenic transformation and neural differentiation through REST degradation. *Nature* 2008;452(7185):370-4.
257. Tonelli R, Purgato S, Camerin C, *et al.* Anti-gene peptide nucleic acid specifically inhibits MYCN expression in human neuroblastoma cells leading to cell growth inhibition and apoptosis. *Mol Cancer Ther* 2005;4(5):779-86.

258. Jiang R, Xue S, Jin Z. Stable knockdown of MYCN by lentivirus-based RNAi inhibits human neuroblastoma cells growth in vitro and in vivo. *Biochem Biophys Res Commun*;410(2):364-70.
259. Pession A, Tonelli R, Fronza R, *et al.* Targeted inhibition of NMYC by peptide nucleic acid in N-myc amplified human neuroblastoma cells: cell-cycle inhibition with induction of neuronal cell differentiation and apoptosis. *Int J Oncol* 2004;24(2):265-72.
260. Benard J, Raguenez G, Kauffmann A, *et al.* MYCN-non-amplified metastatic neuroblastoma with good prognosis and spontaneous regression: a molecular portrait of stage 4S. *Mol Oncol* 2008;2(3):261-71.
261. van Noesel MM, Hahlen K, Hakvoort-Cammel FG, Egeler RM. Neuroblastoma 4S: a heterogeneous disease with variable risk factors and treatment strategies. *Cancer* 1997;80(5):834-43.

---

## 8 Appendix

### 8.1 Abbreviations

A	Allele
AA	Amino Acid
ABD	Abdomen
aCGH	Array-based Comparative Genomic Hybridization
AG	Adrenal Glands
AIG	Anchorage Independent Growth
ALK	Anaplastic lymphoma kinase
ALL	Acute Lymphocytic Leukaemia
AML	Acute Myeloid Leukaemia
Ampl	Amplicon
AP	Anterior-Posterior
BMP	Bone Morphogenetic Protein
Brdu	5-bromo-2'-deoxyuridine
CCHS	Congenital Central Hypoventilation Syndrome
CD	Codon
CI	Confidence Interval
CO	Coordinate
Cod	coding
CV	Cross Validation
DAPI	2,4-diamidino-2-phenylindole
Del	Deletion
Diff	Differentiation
Dir	Direction
Dox	Doxycycline
EFS	Event-free survival
ES	Embryonic Stem
FACS	Fluorescence Activated Cell Sorting
Fav	Favorable
FCS	Fetal Calf Serum
FGF	Fibroblast Growth Factors
For	forward
Freq	Frequency

---

GN	Ganglioneuroma
GNB	Ganglioneuroblastoma
GO	Gene Ontology
GOTM	Gene Ontology Tree Machine
HR	High-Risk
HRE	HOX Responsive Element
HRP	horseradish peroxidase
HUVEC	Human Umbilical Vein Endothelial Cell
IGV	Integrative Genomics Viewer
INRG	International Neuroblastoma Risk Group
INSS	International Neuroblastoma Staging System
Intr	Intronic
IR	Intermediate-Risk
LR	Low-Risk
NB	Neuroblastoma
NC	Neural Crest
NK/C	Neck/Chest
Norm	Normal
OS	Overall Survival
PAM	Predictive Algorithm of Microarray
PcG	Polycomb Group
PI	Propidium Iodide
qRT-PCR	Quantitative real-time reverse transcriptase-polymerase chain reaction
RA	Retinoic Acid
REG	Region
Rev	Reverse
RIN	RNA integrity number
rtTA	reverse tetracycline-controlled Transactivator
S	Special
SA	Sympathoadrenal
SD	Standard Deviation
SMC	Smooth Muscle Cells
SNS	Sympathetic Nervous System
SVM	Support Vector Machine
TALE	Three-Amino Acid-Loop-Extension
Temp	Temperature
TRITC	Tetramethylrhodamine Isothiocyanate

TrxG	Trithorax Group
TUNEL	(TdT)-mediated dUTP Nick End Labeling
Unfav	Unfavorable
WGA	Whole Genome Amp

## 8.2 List of Figures

<b>Figure 1:</b> Risk stratification according to the German Neuroblastoma Trial, NB2004.....	4
<b>Figure 2:</b> Kaplan-Meier estimates for EFS and OS for 428 neuroblastoma patients stratified according to the German neuroblastoma trial NB2004.....	4
<b>Figure 3:</b> Regulators of the sympathetic nervous system cell lineage.....	11
<b>Figure 4:</b> Homeotic gene organization and transcriptional expression.....	14
<b>Figure 5:</b> Correlation of <i>HOXD3</i> , <i>HOXD8</i> , <i>HOXD9</i> and <i>HOXD10</i> expression levels with prognostic markers in neuroblastoma.....	49
<b>Figure 6:</b> Survival of neuroblastoma patients according to expression levels of <i>HOXD3</i> , <i>HOXD8</i> , <i>HOXD9</i> and <i>HOXD10</i> .....	50
<b>Figure 7:</b> Survival curves of neuroblastoma patients.....	53
<b>Figure 8:</b> Association of <i>HOXC9</i> expression with prognostic markers and survival in neuroblastoma.....	56
<b>Figure 9:</b> Association of <i>HOXC9</i> expression with tumor localization and survival of neuroblastoma patients according to the site of primary tumor.....	58
<b>Figure 10:</b> Expression of 5' clustered <i>HOX</i> genes according to primary tumor localization.....	59
<b>Figure 11:</b> Aberrations at chromosome 12 and correlation with <i>HOXC9</i> expression.....	61
<b>Figure 12:</b> Hierarchical clustering of methylation ratios.....	63
<b>Figure 13:</b> Inducible expression of Hox-C9 in SK-N-AS, IMR-32 and CHP-212 cells and physiological Hox-C9 levels in primary neuroblastomas as determined by Western blot analysis.....	65
<b>Figure 14:</b> Inducible expression of Hox-C9 in SK-N-AS and IMR-32 cells as determined by immunohistochemistry.....	66
<b>Figure 15:</b> <i>HOXC9</i> re-expression inhibits growth of neuroblastoma cells in vitro.....	67
<b>Figure 16:</b> <i>HOXC9</i> re-expression inhibits growth of neuroblastoma cells in vivo.....	69
<b>Figure 17:</b> Histological features of neuroblastoma xenografts.....	70
<b>Figure 18:</b> Hox-C9 induces neuronal differentiation in IMR-32 cells.....	71
<b>Figure 19:</b> <i>HOXC9</i> expression up-regulates neuron-related markers in IMR-32 cells.....	72
<b>Figure 20:</b> Hox-C9 induces apoptosis in neuroblastoma cell lines.....	73
<b>Figure 21:</b> Hox-C9 induces apoptosis in neuroblastoma cell lines by activating the intrinsic apoptotic pathway.....	75
<b>Figure 22:</b> Gene Ontology (GO) annotations for significantly differentially expressed genes.....	80
<b>Figure 23:</b> <i>HOXC9</i> leads to reduced expression of <i>MYCN</i> .....	81

## 8.3 List of Tables

<b>Table 1:</b> INSS (8).	2
<b>Table 2:</b> <i>HOX</i> genes in tumorigenesis	18
<b>Table 3:</b> Neuroblastoma cell line characteristics.	28
<b>Table 4:</b> Solutions for cell cycle analyses.	30
<b>Table 5:</b> Solutions for anchorage-independent growth analyses.	31
<b>Table 6:</b> Solutions for TUNEL analyses.	32
<b>Table 7:</b> Nicoletti staining solution for hypoploidy analyses.	33
<b>Table 8:</b> cDNA synthesis.	36
<b>Table 9:</b> qRT-PCR reaction.	37
<b>Table 10:</b> qRT-PCR primers.	38
<b>Table 11:</b> Primers for methylation analysis.	39
<b>Table 12:</b> Primers for Amplification.	40
<b>Table 13:</b> Sanger sequencing reaction.	41
<b>Table 14:</b> Retroviral plasmids.	42
<b>Table 15:</b> Cell lysis buffer.	43
<b>Table 16:</b> Solutions for immunoblotting.	44
<b>Table 17:</b> Antibodies for immunoblotting.	44
<b>Table 18:</b> Solutions for immunofluorescence ( <i>Hox-C9</i> staining).	45
<b>Table 20:</b> Solutions for immunofluorescence (F-Actin staining).	46
<b>Table 21:</b> <i>HOX</i> gene expression and association with prognostic markers and patient outcome in neuroblastoma.	48
<b>Table 22:</b> <i>HOX</i> classifier probes.	52
<b>Table 23:</b> Classification performance of the <i>HOX</i> classifier in the training set.	53
<b>Table 24:</b> Classification performance of the <i>HOX</i> classifier in the test set matching the criteria of the training set.	53
<b>Table 25:</b> Multivariate Cox regression models for the complete test set based on EFS and OS considering single prognostic markers and the <i>HOX</i> classifier.	54
<b>Table 26:</b> Multivariate Cox regression models based on EFS and OS considering single prognostic markers and <i>HOXC9</i> expression.	57
<b>Table 27:</b> Aberrations on chromosome 12 as determined by aCGH.	60
<b>Table 28:</b> Sequence variations in the genomic region of <i>HOXC9</i> .	62
<b>Table 29:</b> <i>HOXC9</i> promoter methylation analyses.	63

## 9 Erklärung

Ich versichere, dass ich die von mir vorgelegte Dissertation selbständig angefertigt, die benutzten Quellen und Hilfsmittel vollständig angegeben und die Stellen der Arbeit - einschließlich Tabellen, Karten, und Abbildungen - , die anderen Werken im Wortlaut oder dem Sinn nach entnommen sind, in jedem Einzelfall als Entlehnung kenntlich gemacht habe; dass diese Dissertation noch keiner anderen Fakultät oder Universität zur Prüfung vorgelegen hat; dass sie – abgesehen von unten angegebenen Teilpublikationen – noch nicht veröffentlicht worden ist sowie, dass ich eine solche Veröffentlichung vor Abschluss des Promotionsverfahrens nicht vornehmen werde.

Die Bestimmungen dieser Promotionsordnung sind mir bekannt. Die von mir vorgelegte Dissertation ist von Prof. Dr. Matthias Fischer betreut worden.

### Teilpublikationen

**Kocak H**, Ackermann S, Hero B, Kahlert Y, Oberthuer A, Juraeva D, Roels F, Theissen J, Westermann F, Deubzer H, Ehemann V, Brors B, Odenthal M, Berthold F, Fischer M. Hox-C9 activates the intrinsic pathway of apoptosis and is associated with spontaneous regression in neuroblastoma. *Cell Death Dis.* 2013 Apr 11;4:e586. doi: 10.1038/cddis.2013.84. PMID: 23579273

### Teile dieser Arbeit wurden auf folgenden Kongressen vorgestellt:

#### Vorträge

1. XXIII. Jahrestagung der Kind-Philipp-Stiftung für Leukämieforschung, 2010 Wilsede, Germany. The Homeobox Transcription Factor Hox-C9, a Key Regulator of Development, Suppresses Tumorigenicity of Neuroblastoma. **Kocak H**, Ackermann S, Hero B, Kahlert Y, Theissen J, Ehemann V, Westermann F, Odenthal M, Oberthuer A, Berthold F, Fischer M. Abstract published in *Klin Padiatr* 2010; 222 - A24, DOI: 10.1055/s-0030-1254475.
2. ANR 2010, Advances in Neuroblastoma Research, Stockholm, Sweden. The Homeobox Transcription Factor Hox-C9, a Key Regulator of Development, Suppresses Tumorigenicity of Neuroblastoma. **Kocak H**, Ackermann S, Hero B, Kahlert Y, Theissen J, Ehemann V, Westermann F, Odenthal M, Oberthuer A, Berthold F, Fischer M.
3. XXII. Jahrestagung der Kind-Philipp-Stiftung für Leukämieforschung, 2009 Wilsede, Germany. The Homeobox Transcription Factor Hox-C9 Induces Growth Suppression and Differentiation in Neuroblastoma Cell Lines. **Kocak H**, Nowacki S, Oberthuer A, Hero B, Kahlert Y, Berthold F, Fischer M. Abstract published in *Klin Padiatr* 2009; 221 - A30, DOI: 10.1055/s-0029-1222651.

4. XXI. Jahrestagung der Kind-Philipp-Stiftung für Leukämieforschung, 2008 Wilsede, Germany. Characterization of Regulatory Functions of *HOXC9* in Neuroblastoma Cells. **Kocak H**, Nowacki S, Oberthuer A, Hero B, Kahlert Y, Berthold F, Fischer M.

### **Posterpräsentationen**

1. ANR 2012, Advances in Neuroblastoma Research, Toronto, Canada. Hox-C9 activates the intrinsic pathway of apoptosis and is associated with spontaneous regression in neuroblastoma. **Kocak H**, Ackermann S, Hero B, Kahlert Y, Oberthuer A, Juraeva D, Roels F, Theissen J, Westermann F, Deubzer H, Ehemann V, Brors B, Odenthal M, Berthold F, Fischer M.

Ich versichere, dass ich alle Angaben wahrheitsgemäß nach bestem Wissen und Gewissen gemacht habe und verpflichte mich, jedmögliche, die obigen Angaben betreffenden Veränderungen, dem Promotionsausschuss unverzüglich mitzuteilen.

Köln, den .....

.....

Hayriye Kocak

## 10 Danksagung

Mein erster Dank gilt Herrn Prof. Dr. Matthias Fischer für die außerordentlich gute, fachliche und langjährige Betreuung meiner Doktorarbeit, sein Vertrauen, seine Geduld und Unterstützung, vielfältigen Anregungen, Ideen und konstruktive Kritik sowie die Überlassung dieses interessanten und spannenden Themas. Seine wertvollen Ratschläge, stete Diskussionsbereitschaft, Erfahrung, Hilfsbereitschaft und vor allem seine Begeisterung an der Forschung haben maßgeblich zum Gelingen dieser Arbeit beigetragen.

Für die Möglichkeit, diese Arbeit an der Klinik pediatriische Onkologie und Hematology der Universität zu Köln durchführen zu können, danke ich unserem Klinikleiter Herrn Prof. Dr. Frank Berthold ganz herzlich.

Meinen Tutoren aus dem MD-/PhD-Programm, Herrn Prof. Dr. Roman Thomas und Herrn Prof. Dr. Matthias Hammerschmidt, danke ich für die Betreuung, die netten und aufschlussreichen Treffen und die Begutachtung meiner Arbeit.

Unsere Kooperationspartnern Herrn Prof. Dr. Frank Westermann, Frau Dr. Hedwig Deubzer, Frau Prof. Dr. Margarethe Odenthal, Herrn Prof. Dr. Benedikt Brors danke ich für die freundliche Zusammenarbeit.

Ganz besonders möchte ich mich herzlich bei allen meinen Kollegen – Sandra, Yvonne, Anne, Falk, Barbara, André, Carolina, Andrea, Fakhera, Ruth, Nadine, Heike und Jessica - für den fachlichen und wissenschaftlichen Austausch, hilfreiche Anregungen und Ratschläge, arbeitsfördernde Diskussionen, ganz viel Geduld, Hilfsbereitschaft und Unterstützung sowie einen stets heiteren Laboralltag bedanken.

Insbesondere danke ich Yvonne, Anne und Nadine für eine besondere Freundschaft!

Ganz lieben Dank an Falk und Sandra für die gute Durchsicht meiner Doktorarbeit.

Mein Dank gilt auch allen anderen Mitarbeitern der Klinik für pediatriische Onkologie und Hematologie.

Von ganzem Herzen danke ich meinen liebevollen Eltern Cafer und Sevim Altuntas sowie meinen Brüdern Bülent und Ömer, die mich in allen meinen Taten uneingeschränkt unterstützt, an mich geglaubt und mir vertraut haben.

Ein ganz besonderer Dank gilt zuletzt meinem Ehemann. Ferdai hat mich stets aufgebaut und mir den Rücken freigehalten. Ich danke für seine unendliche Geduld, Fürsorge, sein Verständnis, aber auch Motivation und Unterstützung während der ganzen Zeit meiner Doktorarbeit.